5-5-2017

# Application of Compound Specific Stable Isotope Analysis to Spatial and Temporal Tracing of Organic Molecular Biomarkers through the Environment

Abigail M. Oakes
abigail.oakes@uconn.edu

# Application of Compound Specific Stable Isotope Analysis to Spatial and Temporal Tracing of Organic Molecular Biomarkers through the Environment

Abigail Marie Oakes, PhD

University of Connecticut, 2017

## ABSTRACT

One of the critical challenges facing modern environmental chemistry is how to identify sources, process of formation, and transport of organic compounds and pollutants in the environment. In recent decades, molecular and stable isotopic analysis of individual organic biomarkers, produced by living organisms, has emerged as a novel tool for identifying sources and processes associated with the synthesis of biological compounds. Specifically, this thesis focused on the questions related to processes controlling the production and movement of *n*-alkanes produced in plant leaf waxes and PAHs produced through the partial combustion of organic material. The aims of this thesis were to use compound-specific isotope analysis of these organic molecular biomarkers to understand how environmental changes are recorded, determine source materials, and evaluate potential methods of transport through the environment. Chapters 3 and 4 used stable hydrogen (δD) and carbon ($\delta^{13}C$) isotopes of *n*-alkanes produced by leaf waxes to determine how differences in taxonomic class are recorded and how these biomarkers are preserved in fluvial sediments. This study found that *n*-alkanes from individual plants record plant specific differences in photosynthetic processes and physiology whereas *n*-alkanes preserved in fluvial sediments can identify large scale ecosystem changes. In Chapter 5, the concentrations, δD and $\delta^{13}C$ of 16 EPA priority PAHs were measured from samples collected from around the states of Connecticut and Rhode Island. Using a multivariate approach to source identification, this study found that PAHs extracted from

sediments and soils in Connecticut were sourced from a complex mixture of vehicular exhaust, coal burning exhaust, and industrial emissions. These projects represent a significant contribution to the understanding of carbon mobility over the earth surface with broad applications to environmental pollution tracing and paleoenvironmental reconstructions.

# Application of Compound-Specific Stable Isotope Analysis to Spatial and Temporal Tracing of Organic Molecular Biomarkers through the Environment

by

Abigail Marie Oakes

B.S., Binghamton University, 2012

A dissertation submitted in partial fulfillment of the
requirements for the degree of Doctor of Philosophy at the
University of Connecticut

April 14th, 2017

2017

APPROVAL PAGE

Doctor of Philosophy Dissertation

Application of Compound Specific Stable Isotope Analysis to Spatial and Temporal Tracing of Organic Molecular Biomarkers through the Environment

Presented by

Abigail Marie Oakes

Major Advisor _____
Michael T. Hren, Ph.D.

Associate Advisor _____
Xudong Yao, Ph.D.

Associate Advisor _____
Alfredo Angeles-Boza, Ph.D.

Associate Advisor _____
Douglas Adamson, PhD.

Associate Advisor _____
Craig Tobias, Ph.D.

University of Connecticut

2017

# ACKNOWLEDGEMENTS

First a foremost I would like to thank my family and friends who have supported me throughout this long five-year process. In particular, I would like to thank my lab mates Chaoran, Jaci, Katherine, Greg, and Kellyn who have been a great support system throughout my time at UConn. I know our lab wouldn't be the place it is today without each one of us, and it has been an absolute privilege working with you. In addition, I would like to thank Emilie Hogrebe in the Chemistry main office. Not only has Emilie been an OUTSTANDING resource on any Graduate Student question, she has been a tremendous friend and I will miss helping her with new graduate student orientation.

I would like to thank my research advisor Dr. Michael Hren for his guidance into the world of geochemistry. Working with him has been a worthwhile experience and I feel I have gained valuable life skills working in his laboratory. A special thank you to my advisory committee Drs. Xudong Yao, Alfredo Angeles-Boza, Douglas Adamson, and Craig Tobais for the time and effort they have put in on my behalf. I would like to give a general thank you to the Chemistry Department for funding me throughout my time here at UConn and to the Center for Integrative Geosciences who included myself and the other Chemistry Graduate students in our lab as honorary members.

Finally, I would like to thank my parents who have been an enormous support for me through undergraduate and graduate school. They have always believed in me and never pressured me to succeed. Because of them, I learned the value of hard work and self-motivation at a young age which gave me the drive to see this through to the end. Thank you.

TABLE OF CONTENTS

TABLE OF FIGURES

# CHAPTER 1

# Applications of Stable Isotope analysis to Analytical Environmental Chemistry

Abigail M. Oakes

University of Connecticut

Department of Chemistry

Division of Analytical Chemistry

### 1.1.0 IMPORTANCE OF BIOMARKERS IN TRACING ENVIRONMENTAL CHANGES

Large scale environmental changes, often associated with anthropogenic influences, create global hazards to human health and well-being [1] as a result of pollutants released in the environment. One of the fundamental challenges of modern environmental chemistry is how to identify sources, formation processes, and movement of organically bound carbon through the environmental system. Three hundred years of industrialization in Connecticut has left a history of anthropogenic contamination in rivers [2] and floodplains [3]. Development of railroads, factories, coal, and charcoal combustion mobilized heavy metals, organic pollutants, ash, and soot across the landscape. Active development of industrial activity along coastal wetlands contributed to accumulation of persistent pollutant within a host of wetland systems. This thesis addresses how to identify sources and trace the movement of pollutant, and their precursor organic compounds through a landscape when sources are varied over space and time.

In recent decades, attempts to source organic materials have focused on analysis of organic molecular biomarkers. In environmental systems, biomarkers from living organisms are typically found in a variety of contexts (sediment, rock, crude oils, etc.) and display minimal structural alterations from their parent molecules [4,5]. This approach has been successfully used in a variety of fields including food authenticity [6], paleovegetation reconstruction [7], identification of source contaminants [8], and evaluation of the success of biodegradation and contaminant removal in aquifers [9]. Using a suite of novel modern experimental molecular and isotopic data, this thesis explores the application of stable isotopes and molecular distributions of organic molecular biomarkers as a tool to trace flow of organic carbon in the environment. Ultimately, this work used the stable isotopic

compositions and molecular distributions of organic biomarkers as novel tools for understanding the controls of production and movement of carbon through the earth surface environment.

### 1.2.0 THESIS STRUCTURE

This thesis contains six chapters. Chapter 2 presents an overview of stable isotope ratio mass spectrometry and introduces the biological and abiological processes that can drive isotope fractionation in natural ecosystems. Chapters 3 and 4 present the stable carbon ($\delta^{13}C$) and hydrogen ($\delta D$) isotope ratios of plant wax *n*-alkanes collected from modern leaves and sediments to assess 1) how plants of various taxonomic classes grown under identical conditions vary in isotopic composition over time, and 2) how this isotopic variation is recorded in fluvial sediments. Establishing this "source to sink" scenario has implications for a range of investigations using leaf wax biomarkers. In particular, results evaluate the applicability of leaf wax *n*-alkane $\delta D$ as a hydrological tracer in modern plant ecology, and has broad applications to past environmental and climatic change.

Building on this, Chapter 5 explores how stable isotope measurements of individual PAHs can be used to determine source materials. Since PAHs are typically formed from the partial combustion of organic materials, there are numerous natural and anthropogenic sources in the environment that may be differentiated through the use of compound specific $\delta D$ and $\delta^{13}C$ PAH values. Once source has been determined, tracing spatial trends in PAH deposition will lead to further understanding of carbon movement through a system. Together, this compilation of data represents a significant contribution to the future of analytical environmental monitoring with broad scale applications to the study of environmental pollutants, investigation of environmental crime, and even

paleoenvironmental reconstruction. The following sections will provide further details on these two main areas of experimental data.

## 1.3.0 TRACING BIOMARKERS FROM MODERN PLANTS: FENTON RIVER PROJECT

This project focuses on two main areas. Firstly, the effect of temporal environmental variation over a growing season on the δD (Chapter 3) and $\delta^{13}C$ (Chapter 4) *n*-alkane biomarkers produced by leaves and how they are preserved in the river sediments. Plant leaf waxes consist of a complex mixture of compounds that include hydrocarbons, ketones, esters, aldehydes, and acids [32-37]. Many of these compounds are diagnostic of plant origin and environmental changes, and are therefore useful as tracers of organic carbon in the environment. Normal alkanes (*n*-alkanes) are one of the most abundant classes in plant leaf waxes and are readily preserved in sedimentary archives, allowing for straightforward organic carbon tracing. These records are then applied to current geochemical studies of *n*-alkanes employed as paleoclimate proxies [16–20]. Since *n*-alkanes experience minimal alteration or degradation, they are believed to record processes associated with $CO_2$ and $H_2O$ uptake, thus making them highly useful in paleoenvironmental tracers [21–25].

### *1.3.1 Temporal variations in the δD of leaf n-alkanes from four riparian plant species*

While the relative abundance of hydrogen isotopes in the environment has been related to changes in the hydrological cycle, [24] understanding how changes in precipitation δD are recorded by plants is essential for studies seeking to link plants and plant products back to the location where they grew. Plant leaf wax *n*-alkanes are particularly useful as

tracers and have numerous applications in pollution bioremediation studies [26], tracing mobilized organic content to its source [27], and paleoclimate studies [24].

Hydrogen isotopes of water vary greatly with changes in elevation and latitude across a continent (Figure 1.1) [24]. Since precipitation water is the primary source of hydrogen for photosynthetic processes, it is theorized that organic matter produced during photosynthesis and preserved in sediments will function as a hydrological tracer [24]. However, organic matter preserved in sediments is complex in nature and can differ significantly in isotopic composition based on biosynthetic pathway, variations in source organism, and secondary hydrogen exchange with environmental water [24,28]. This results in difficulties interpreting biomarker source through bulk sedimentary organic matter analysis [24]. The direct analysis of individual plant derived compounds circumvents the problems associated with complex bulk mixtures. In particular, research on this focuses on lipids produced in the cuticular wax layer of terrestrial plant leaves such as *n*-alkanes [24] because they persist in the environment, hydrogens are covalently bonded with carbon atoms and therefore do not readily exchange at temperatures below 100 °C [5], and δD values are highly correlate with source water, although offset by several factors (Figure 1.2) [24].

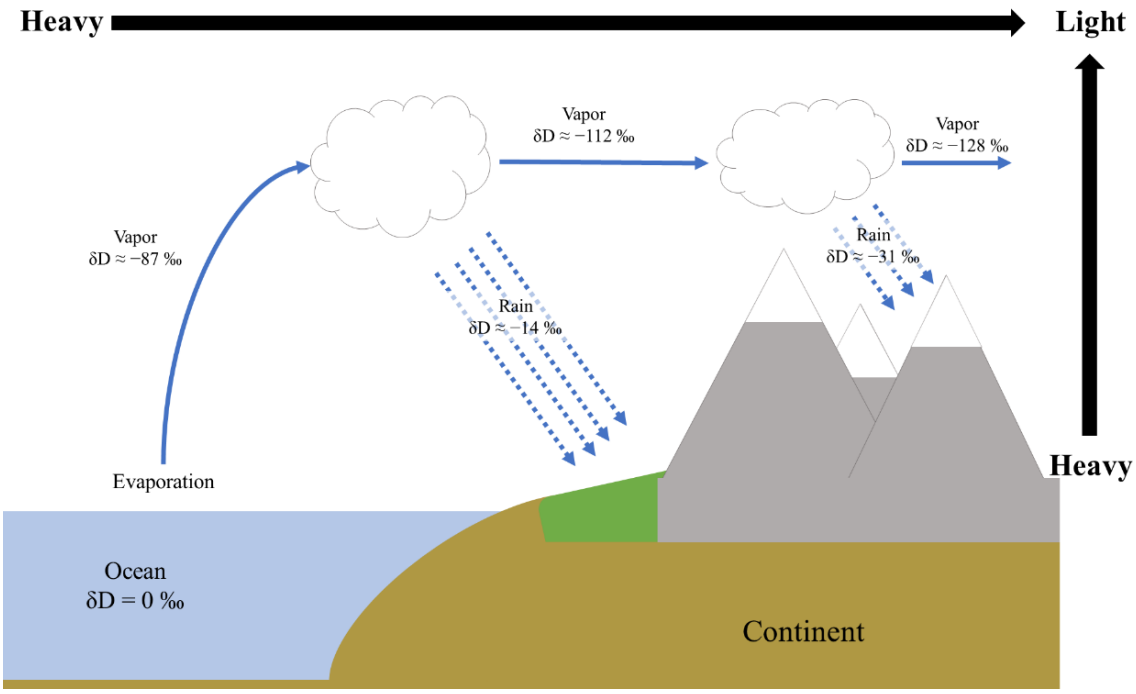


Figure 1.1 Rainout effect on δD values of water [79,80]

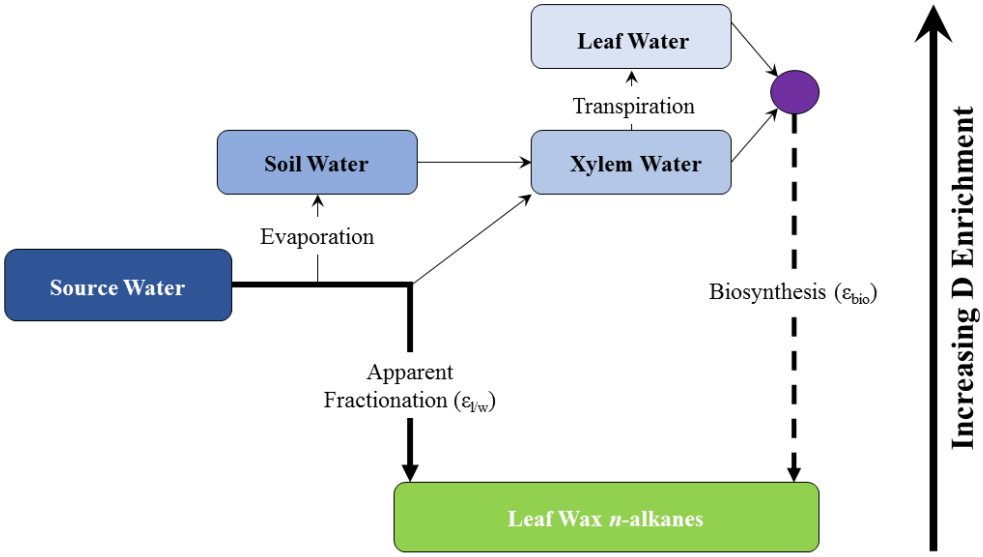


Figure 1.2 A conceptual diagram of hydrogen isotopic relationships between source water (typically precipitation or ground water) and leaf wax *n*-alkanes. The purple dot illustrates the "pool" of biosynthetically available water from potentially mixed sources. Abbreviations: $\varepsilon_{bio}$, the apparent fractionation from biosynthetic means; $\varepsilon_{l/w}$, isotopic apparent fractionation between lipids and source water [24,36,78]

Studies have postulated that the source of *n*-alkanes in sediments may be inferred by their average chain lengths. Short to mid-length *n*-alkanes ($C_{n16\text{-}25}$) are associated with predominantly submerged aquatic plants, with a few exceptions [14,29–32]. Longer chain length *n*-alkanes are then associated with terrestrial higher plants, however there have been some recent studies that have indicated that terrestrial plants may produce mid-length *n*-alkanes while aquatic plants may also contribute longer chain length *n*-alkanes [30,33–35]. As a source tracer, these inconsistencies are problematic.

To reliably use *n*-alkanes as an environmental tracer, it is critical to relate plant wax *n*-alkane geochemistry to seasonal or annual environmental signals [36–39]. In chapter 3, the stable hydrogen isotopic compositions of *n*-alkanes from four $C_3$ plants (*Pinus strobus*, *Tsuga canadensis*, *Phalaris arundinacea*, and *Corylus americana*) within the Fenton River watershed (Storrs, CT) were examined. This approach was tailored to examine how the hydrogen isotopic composition of *n*-alkanes from plants with different patterns of stomatal regulation (angiosperm, gymnosperm, grass, and shrub), plant growth, and timescales of wax synthesis changed throughout the growing season and how these changes were recorded in fluvial sediments. The project focused on streamside vegetation with roots positioned visibly in the river water to minimize potential external differences in water stress and determine how resultant stomatal regulation is reflected in *n*-alkane isotopic composition.

### *1.3.2 Seasonal variations in leaf wax n-alkane δD and $\delta^{13}C$ of four riparian plants*

Chapter 4 builds on Chapter 3 by examining the changes in $\delta^{13}C$ associated with plant wax *n*-alkanes over the growing season to evaluate how stomatal regulation of

different riparian plants during leaf flush and seasonal growth affected the fixation of carbon, water loss through transpiration, and resultant δD and $\delta^{13}C$ of *n*-alkanes produced on leaf surfaces. Stable carbon isotopes of plants have strong relationships with environmental factors including temperature [40], water availability [41,42], and atmospheric $CO_2$ concentration [43], and provide valuable insight into the growth environment of the plant that synthesized the biomarker. Plant wax *n*-alkanes reflect various carbon sources and their isotopic composition in addition to biosynthetic pathways of the *n*-alkane producers. For example, aquatic plants reflect the availability of dissolved $CO_2$ and $HCO_3^-$ in lakes [30] whereas $\delta^{13}C$ of terrestrial plants distinguishes organic matter contributions by $C_3$ and $C_4$ plants where both plants exist simultaneously [44]. In an area where $C_3$ and $C_4$ plants do not mix, changed in $\delta^{13}C$ ratios of *n*-alkanes are likely the result of changes in water stress of these plants [45]. Modern data show large variations in δD and $\delta^{13}C$ of *n*-alkanes produced by plants under similar environmental conditions [32,42,46–48]. This variability within a single ecosystem leads to complications in tracing organic carbon to its source.

While plant *n*-alkanes are believed to record environmental factors during wax production, recent studies indicate that physiological differences between plants species grown under identical environmental conditions may also be important determinants of their carbon isotope composition [32,41,42,46]. In order to use leaf wax lipids as biomarkers in environmental investigations, it is essential to understand how variability in plant physiology and function are recorded in individual biomarkers. The $\delta^{13}C$ of bulk plant materials have been shown to record intrinsic plant WUE [41,43,49,50]. Recent studies suggest, however, that it may not be possible to interpret the carbon isotope composition of

individual plant biomarkers (i.e. *n*-alkanes) in the same way as bulk tissue due to uncertainties in plant-specific responses to environmental changes [46,47,51,52]. Chapter 4 therefore uses both δD and $\delta^{13}C$ of plant leaf wax *n*-alkanes from plants exposed to the same environmental conditions to determine how variability in plant physiology and function are recorded by these biomarkers. To do this, the $\delta^{13}C$ composition of *n*-alkanes from the riparian ecosystem introduced in Chapter 2 were measured. These data were used to calculate carbon fixation, water loss through transpiration, and various other plant specific functions. Isotopic values are presented in conjunction with stomatal morphometric parameters, such as stomatal size and density. These parameters were used to calculate the WUE and $CO_2$ assimilation rate throughout the growing season to assess seasonal trends in addition to determining difference between various taxonomic classes. These values were then compared to a BIOME-BGC modelling scenario using real climate data to assess difference in plant function over time.

## 1.4.0 POLLUTANT BIOMARKER TRACING: POLYCYLIC AROMATIC HYDROCARBON (PAH) PROJECT

### *1.4.1 A multivariate approach to polycyclic aromatic hydrocarbon (PAH) source apportionment*

Polycyclic aromatic hydrocarbons (PAHs) are ubiquitous in the environment, having not only been detected in the inhabited regions of the world, but in uninhabited regions of the Antarctic [53]. Some PAHs are well known carcinogens, mutagens and teratogens, and have attracted much attention in recent years due to concerns over the effect they have on human health [54,55]. Due to their physiochemical properties, PAHs are highly mobile, persistent in the environment, and prone to bioaccumulation [54,56–59]. As a result,

the United States Environmental Protection Agency (EPA) has named 16 PAHs of particular concern (Table 1.1) for human health.

Table 1.1 EPA 16 priority PAHs and structure guide

| Substance | Structure | Substance | Structure |
|---|---|---|---|
| Naphthalene | 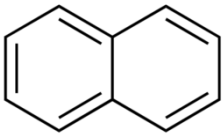 | Benz (a) anthracene | 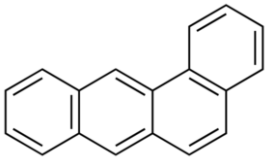 |
| Acenaphthylene | 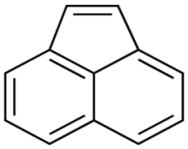 | Chrysene | 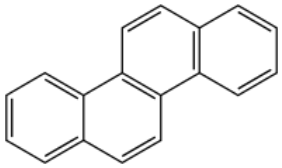 |
| Acenaphthene | 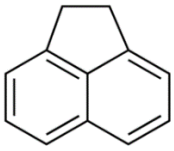 | Benzo(b) fluoranthene | 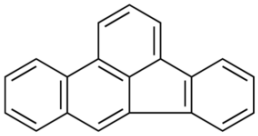 |
| Fluorene | 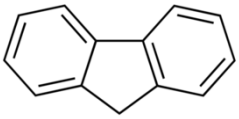 | Benzo (k) fluoranthene | 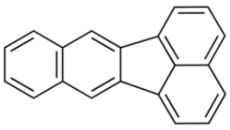 |
| Anthracene | 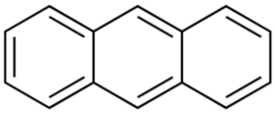 | Benzo (g,h,i) perylene | 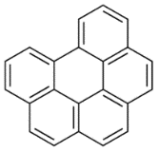 |
| Phenanthrene | 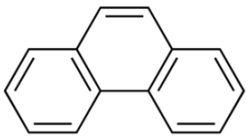 | Benzo (a) pyrene | 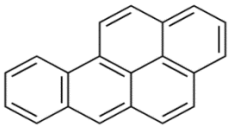 |
| Pyrene | 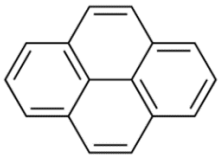 | Indeno (1,2,3-cd) pyrene | 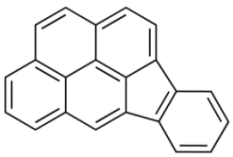 |

Polycyclic aromatic hydrocarbons are introduced to the environment through a variety of natural and anthropogenic processes [54,60]. The ubiquitous distribution of PAHs in the environment is due to PAH production that occurs during the combustion of nearly all organic material [54]. PAHs are typically divided into two categories: low molecular weight consisting of PAHs containing less than four rings and high molecular weight consisting PAHs with four rings or more [54]. In general, low molecular weight (LMW) PAHs are formed at relatively low temperatures and are considered petrogenic in nature [60]. High molecular weight (HMW) PAHs are formed at high temperatures and low oxygen conditions and are considered pyrogenic in nature [60].

Southern New England has an extensive history of industrial manufacturing, industrial-scale charcoal production, and forest clearing and burning for agriculture [3,61,62]. As a result, there are high concentrations of PAHs found in sediments along coastal environments, upland areas, urban city centers, and pristine forests [56]. In chapter 4, a multivariate approach used to identify PAH source is established. Specifically, molecular distributions and stable isotopes of PAHs are used to link composition to source and potential movement through surface ecosystems.

Organic materials extracted from sediments and soils in New England contain a complex mixture of pyrogenic and petrogenic PAHs. Various techniques are used to establish PAH source including diagnostic ratios and stable hydrogen and carbon isotope measurements of extracted PAHs. Diagnostic ratios are an identification technique for PAHs, calculated from the concentration of several pairs of PAHs (often structural isomers [63–65]). These ratios decrease analytical variability within a diverse sample set and are used to determine broad source labels, such as pyrogenic and petrogenic [63,65,66]. While

informative, these diagnostic ratios lack the specificity necessary to identify intrasource variability [66]. To account for the lack of specificity associated with diagnostic ratios, the δD and $\delta^{13}C$ of individual PAHs were measured to determine the source materials.

Numerous studies have measured variations in $\delta^{13}C$ of individual PAHs as a tool for source identification [65,67,68], however the carbon isotopic composition of compounds from different sources often vary by only a few ‰ [65,67,69–71]. To increase differentiation of source materials, recent research into hydrogen isotopic variations of PAHs have shown vast differences among PAHs produced from a range of starting materials, often on a magnitude of 100 ‰ or greater [68,72,73]. Chapter 5 therefore uses a multi-variate approach to source apportionment, combining diagnostic ratios, $\delta^{13}C$, and δD values of individual PAHs to assess how successful these techniques are for identifying region-specific trends throughout an area with widely varied land use strategies, population densities, and industrial activity. Understanding source and distribution of PAHs is key to reducing environmental pollution and creating a safer and healthier world. This complex data set establishes spatial trends in PAH distribution and sheds new light onto the use of stable isotopes for source identification.

### 1.5.0 OVERALL AIMS OF THESIS AND INDIVIDUAL PROJECTS

The primary goal of this thesis is to generate new data to further the use of biomarkers in studies tracing organic carbon through environments from sources to sinks. The Fenton River Project (Chapters 3 and 4) enhances current understandings of how environmental and physiological information is recorded in leaf wax *n*-alkanes from a diverse range of plant functional types in a riparian ecosystem. Chapter 3 focuses on the uses of δD and apparent fractionation (ε) of *n*-alkanes of individual plants as indicators of

hydrological change to shed further light on what hydrogen isotope composition of leaf wax lipids are recording and how they can be used to enhance biomarker tracing. Specific aims of this chapter include: 1) quantifying the extent that various species record hydrological change *n*-alkanes, 2) determining how the timescales of leaf wax synthesis affect the δD composition of *n*-alkanes, and 3) assessing how fluvial sediments integrate individual plant *n*-alkanes from species along a river bank.

The Fenton River project is continued in Chapter 4, where the focus switches to mechanisms influencing carbon isotope composition of plant tissues. Here, various physiological (stomata size and density) and chemical variables ($\delta^{13}C$ and δD) are measured and to assess how well carbon isotope signatures record detailed information about plant function. Several plant specific functions were calculated, including intrinsic plant water use efficiency (WUE), carbon dioxide assimilation rate, and other physiological factors. These factors were then compared to modeled plant simulations through BIOME-BGC [74–77]. The specific aims of this chapter include to 1) determining whether $\delta^{13}C_{n\text{-alkane}}$ was a reasonable substitute for $\delta^{13}C_{bulk}$ when calculating WUE using the universal equation for leaf gas exchange, 2) evaluating whether consideration of both δD and $\delta^{13}C$ signatures improve our ability to reconstruct plant assemblages and dominant environmental conditions, using *n*-alkanes from plants and sediments, and 3) quantifying the extent that differences between plant species are reflected in physical and chemical measurements, and assess their usefulness in studies seeking to trace the movement of organic carbon from plants through the environment.

The final chapter of this thesis uses the techniques outlined in Chapters 3 and 4 and applies them to the pollution biomarkers, polycyclic aromatic hydrocarbons (PAHs).

Previous studies have shown that PAHs can be used to track the extent of industrialization or measure forest fire frequency throughout history. However, these studies focus on the bulk characterization of PAHs into two widely varied categories: Pyrogenic and petrogenic. Chapter 5 focuses on modern PAHs and uses a multivariate approach to refine source apportionment of PAHs collected from environmental samples. The specific aims of this chapter include: 1) characterizing concentrations and stable isotopic ratios of PAHs in environmental samples to determine spatial variations throughout the state of Connecticut, and 2) evaluating the use of stable isotope measurements of PAHs to refine approaches to source identification based on an extensive compilation of existing and new PAH source data.

## 1.6.0 REFERENCES


(1) World Health Organization. Global environmental change http://www.who.int/globalchange/environment/en/ (accessed Jan 1, 2017).

(2) Stant, J. **2010**, 1–270.

(3) McManimon, C. **2016**, *23*, 1–7.

(4) Martinez-Frias, J.; Lazaro, E.; Esteve-Nunez, A. *Ambio* **2007**, *36* (5), 425–426.

(5) Schimmelmann, A.; Lewan, M. D.; Wintsch, R. P. *Geochim. Cosmochim. Acta* **1999**, *63* (22), 3751–3766.

(6) Budge, S. M.; Wooller, M. J.; Springer, A. M.; Iverson, S. J.; McRoy, C. P.; Divoky, G. J. *Oecologia* **2008**, *157* (1), 117–129.

(7) Tareq, S. M.; Ohta, K. *Asian J. Water, Environ. Pollut.* **2015**, *12* (1), 1–9.

(8) Kaown, D.; Shouakar-Stash, O.; Yang, J.; Hyun, Y.; Lee, K. K. *Groundwater* **2014**, *52* (6), 875–885.

(9) Bashir, S.; Hitzfeld, K. L.; Gehre, M.; Richnow, H. H.; Fischer, A. *Water Res.* **2015**, *71* (September), 187–196.

(10) Grice, K.; Lu, H.; Zhou, Y.; Stuart-Williams, H.; Farquhar, G. D. *Phytochemistry* **2008**, *69* (16), 2807–2814.

(11) Zhou, Y.; Grice, K.; Stuart-Williams, H.; Farquhar, G. D.; Hocart, C. H.; Lu, H.; Liu, W. *Phytochemistry* **2010**, *71* (4), 388–403.

(12) Zhou, Y.; Grice, K.; Chikaraishi, Y.; Stuart-Williams, H.; Farquhar, G. D.; Ohkouchi, N. *Phytochemistry* **2011**, *72* (2–3), 207–213.

(13) Diefendorf, A. F.; Freeman, K. H.; Wing, S. L.; Graham, H. V. *Geochim. Cosmochim. Acta* **2011**, *75* (23), 7472–7485.

(14) Bush, R. T.; McInerney, F. A. *Geochim. Cosmochim. Acta* **2013**, *117*, 161–179.

(15) Li, R.; Fan, J.; Xue, J.; Meyers, P. A. *Org. Geochem.* **2017**, *104*, 8–18.

(16) Zhou, W.; Zheng, Y.; Meyers, P. A.; Jull, A. J. T.; Xie, S. *Earth Planet. Sci. Lett.* **2010**, *294* (1–2), 37–46.

(17) Grice, K.; Audino, M.; Boreham, C. J.; Alexander, R.; Kagi, R. I. *Org. Geochem.* **2001**, *32* (10), 1195–1210.

(18) Xie, S.; Yi, Y.; Liu, Y.; Gu, Y.; Ma, Z.; Lin, W.; Wang, X.; Liu, G.; Liang, B.; Zhu, Z. *Sci. China Ser. D Earth Sci.* **2003**, *46* (11), 1113–1120.

(19) Zhang, Z.; Zhao, M.; Eglinton, G.; Lu, H.; Huang, C. Y. *Quat. Sci. Rev.* **2006**, *25* (5–6), 575–594.

(20) Tulipani, S.; Grice, K.; Krull, E.; Greenwood, P.; Revill, A. T. *Org. Geochem.* **2014**, *75*, 74–86.

(21) Sessions, A. L.; Burgoyne, T.; Schimmelmann, A.; Hayes, J. M. *Org. Geochem.* **1999**, *30*, 1193–1200.

(22) Tipple, B. J.; Pagani, M. *Earth Planet. Sci. Lett.* **2010**, *299* (1–2), 250–262.

(23) Tipple, B. J.; Pagani, M.; Krishnan, S.; Dirghangi, S. S.; Galeotti, S.; Agnini, C.; Giusberti, L.; Rio, D. *Earth Planet. Sci. Lett.* **2011**, *311* (1–2), 82–92.

(24) Sachse, D.; Billault, I.; Bowen, G. J.; Chikaraishi, Y.; Dawson, T. E.; Feakins, S. J.; Freeman, K. H.; Magill, C. R.; McInerney, F. A.; van der Meer, M. T. J.; Polissar, P.; Robins, R. J.; Sachs, J. P.; Schmidt, H.-L.; Sessions, A. L.; White, J. W. C.; West, J. B.; Kahmen, A. *Annu. Rev. Earth Planet. Sci.* **2012**, *40*, 221–249.

(25) Zhuang, G.; Brandon, M. T.; Pagani, M.; Krishnan, S. *Earth Planet. Sci. Lett.* **2014**, *390*, 186–198.

(26) Pond, K. L.; Huang, Y.; Wang, Y.; Kulpa, C. F. *Environ. Sci. Technol.* **2002**, *36* (4), 724–728.

(27) Seki, O.; Yoshikawa, C.; Nakatsuka, T.; Kawamura, K.; Wakatsuchi, M. *Deep Sea Res. Part I Oceanogr. Res. Pap.* **2006**.

(28) Schimmelmann, A.; Sessions, A. L.; Mastalerz, M. *Annu. Rev. Earth Planet. Sci.* **2006**, *34* (1), 501–533.

(29) Hockun, K.; Mollenhauer, G.; Ho, S. L.; Hefter, J.; Ohlendorf, C.; Zolitschka, B.; Mayr, C.; Lücke, A.; Schefuß, E. *Org. Geochem.* **2016**, *102*, 110–119.

(30) Ficken, K. J.; Li, B.; Swain, D. L.; Eglinton, G. *Org. Geochem.* **2000**, *31* (7–8), 745–749.

(31) Baas, M.; Pancost, R.; Van Geel, B.; Sinninghe Damsté, J. S. *Org. Geochem.* **2000**, *31* (6), 535–541.

(32) Oakes, A. M.; Hren, M. T. *Org. Geochem.* **2016**, *97*, 122–130.

(33) Gao, L.; Hou, J.; Toney, J.; MacDonald, D.; Huang, Y. *Geochim. Cosmochim. Acta* **2011**, *75* (13), 3781–3791.

(34) Liu, W.; Yang, H.; Wang, H.; An, Z.; Wang, Z.; Leng, Q. *Org. Geochem.* **2015**, *83–84*, 190–201.

(35) Aichner, B.; Herzschuh, U.; Wilkes, H. *Org. Geochem.* **2010**, *41* (7), 706–718.

(36) Smith, F. A.; Freeman, K. H. *Geochim. Cosmochim. Acta* **2006**, *70* (5), 1172–1187.

(37) Sachse, D.; Gleixner, G.; Wilkes, H.; Kahmen, A. *Geochim. Cosmochim. Acta* **2010**, *74* (23), 6741–6750.

(38) Douglas, P. M. J.; Pagani, M.; Brenner, M.; Hodell, D. A.; Curtis, J. H. *Geochim. Cosmochim. Acta* **2012**, *97*, 24–45.

(39) Gao, L.; Zheng, M.; Fraser, M.; Huang, Y. *Geochemistry, Geophys. Geosystems* **2014**, *15* (2), 361–373.

(40) Hall, S. A.; Penner, W. L. *Palaeogeogr. Palaeoclimatol. Palaeoecol.* **2013**, *369*, 272–281.

(41) Hou, J.; D'Andrea, W. J.; MacDonald, D.; Huang, Y. *Org. Geochem.* **2007**, *38* (8), 1251–1255.

(42) Pedentchouk, N.; Sumner, W.; Tipple, B.; Pagani, M. *Org. Geochem.* **2008**, *39* (8), 1066–1071.

(43) Franks, P. J.; Royer, D. L.; Beerling, D. J.; Van de Water, P. K.; Cantrill, D. J.; Barbour, M. M.; Berry, J. A. *Geophys Res Lerr* **2014**, *41*, 4685–4694.

(44) Magill, C. R.; Ashley, G. M.; Freeman, K. H. *Proc. Natl. Acad. Sci. U. S. A.* **2013**, *110* (4), 1175–1180.

(45) Dawson, T. D.; Mambelli, S.; Plamboek, A. H.; Templer, P. H.; Tu, K. P. *Annu. Rev. Ecol. Syst.* **2002**, *33* (2002), 507–559.

(46) Hou, J.; D'Andrea, W. J.; MacDonald, D.; Huang, Y. *Org. Geochem.* **2007**, *38* (6), 977–984.

(47) Eley, Y.; Dawson, L.; Black, S.; Andrews, J.; Pedentchouk, N. *Geochim. Cosmochim. Acta* **2014**, *128*, 13–28.

(48) Eley, Y.; Dawson, L.; Pedentchouk, N. *Org. Geochem.* **2016**, *96*, 28–42.

(49) Farquhar, G. D.; O'Leary, M. H.; Berry, J. A. *Aust. J. Plant Physiol.* **1982**, *9* (2), 121.

(50) Farquhar, G. D.; Ehleringer, J. R.; Hubick, K. T. *Annu. Rev. Plant Physiol. Plant Mol. Biol.* **1989**, *40* (1), 503–537.

(51) Lockheart, M. J.; Van Bergen, P. F.; Evershed, R. P. *Org. Geochem.* **1997**, *26* (1–2), 137–153.

(52) Hou, J.; D'Andrea, W. J.; Huang, Y. *Geochim. Cosmochim. Acta* **2008**, *72* (14), 3503–3517.

(53) Mazzera, D.; Hayes, T.; Lowenthal, D.; Zielinska, B. *Sci. Total Environ.* **1999**, *229*, 65–71.

(54) Kim, K.-H.; Jahan, S. A.; Kabir, E.; Brown, R. J. C. *Environ. Int.* **2013**, *60* (February 2017), 71–80.

(55) Boström, C.-E.; Gerde, P.; Hanberg, A.; Jernström, B.; Johansson, C.; Kyrklund, T.; Rannug, A.; Törnqvist, M.; Victorin, K.; Westerholm, R. *Environ. Health Perspect.* **2002**, *110* (Suppl 3), 451–488.

(56) Foan, L.; Leblond, S.; Thöni, L.; Raynaud, C.; Santamaría, J. M.; Sebilo, M.; Simon, V. *Environ. Pollut.* **2014**, *184*, 113–122.

(57) Baklanov, A. **2007**, 855–874.

(58) Latimer, J.; Zheng, J. In *PAHs: An ecotoxicological perspective*; Douben, P., Ed.; John Wiley & Sons Ltd., 2003.

(59) Sverdrup, L. E.; Nielsen, T.; Krogh, P. H. *Environ. Sci. Technol.* **2002**, *36* (11), 2429–2435.

(60) *Examination of the Sources of Polycyclic Aromatic Hydrocarbon (PAH) in Urban Background Soil*; Palo Alto, CA, 2008.

(61) Gordon, R. B. *Technol. Cult.* **1983**, *24* (4), 602–634.

(62) Jeon, S. B.; Olofsson, P.; Woodcock, C. E. *J. Land Use Sci.* **2014**, *9* (1), 105–130.

(63) Brown, J. N.; Peake, B. M. *Sci. Total Environ.* **2006**, *359* (1–3), 145–155.

(64) Baumard, P.; Budzinski, H.; Michon, Q.; Garrigues, P.; Burgeot, T.; Bellocq, J. *Estuar. Coast. Shelf Sci.* **1998**, *47*, 77–90.

(65) Bakhtiari, A. R.; Zakaria, M. P.; Yaziz, M. I.; Lajia, M. N. H.; Bi, X. *Environ. Asia* **2009**, *2*, 1–10.

(66) Galarneau, E. *Atmos. Environ.* **2008**, *42* (35), 8139–8149.

(67) Dvorská, A.; Lammel, G.; Klánová, J. *Atmos. Environ.* **2011**, *45* (2), 420–427.

(68) Bosch, C.; Andersson, A.; Kruså, M.; Bandh, C.; Hovorková, I.; Klánová, J.; Knowles, T. D. J.; Pancost, R. D.; Evershed, R. P.; Gustafsson, Ö. *Environ. Sci. Technol.* **2015**, *49* (13), 7657–7665.

(69) Reddy, C. M.; Pearson, A.; Xu, L.; McNichol, A. P.; Benner, B. A.; Wise, S. A.; Klouda, G. A.; Currie, L. A.; Eglinton, T. I. *Environ. Sci. Technol.* **2002**, *36* (8), 1774–1782.

(70) Bumpus, J. *Appl. Environ. Microbiol.* **1989**, *55* (1), 154–158.

(71) Dua, M.; Singh, A.; Sethunathan, N.; Johri, A. *Appl. Microbiol. Biotechnol.* **2002**, *59* (2–3), 143–152.

(72) Sun, C.; Cooper, M.; Snape, C. E. *Prepr. Pap-Am. Chem. Soc., Div Fuel Chem* **2003**, *48* (2), 760–761.

(73) Vitzthum von Eckstaedt, C.; Grice, K.; Ioppolo-Armanios, M.; Jones, M. *Atmos. Environ.* **2011**, *45* (31), 5477–5483.

(74) White, J. D.; Running, S. W.; Thornton, P. E.; Keane, R. E.; Ryan, K. C.; Fagre, D. B.; Key, C. H. *Ecol. Appl.* **1998**, *8* (3), 805–823.

(75) Di Vittorio, A. V.; Anderson, R. S.; White, J. D.; Miller, N. L.; Running, S. W. *Ecol. Modell.* **2010**, *221* (17), 2038–2053.

(76) Running, S. W.; Hunt, E. J. R. In *Scaling Physiological processes: leaf to globe*; Ehleringer, J. R., Field, C. B., Eds.; Academic: San Diego, 1993; pp 141–158.

(77) Cienciala, E.; Tatarinov, F. A. *For. Ecol. Manage.* **2006**, *237* (1–3), 252–266.

(78) Sachse, D.; Radke, J.; Gleixner, G. *Org. Geochem.* **2006**, *37* (4), 469–483.

(79) Hoefs, J. *Stable Isotope Geochemistry*; Springer-Verlag: Heidelberg, Germany, 1980.

(80) Coplen, T. B.; Herczeg, A. L.; Barnes, C. In *Environmental Tracers in Subsurface Hydrology*; Cook, P. G., Herczeg, A. L., Eds.; Kluwer Academic Publishers: Boston, 2000.

# CHAPTER TWO

# Stable Isotope Ratio Mass Spectrometry: Isotopic Fractionation and Analysis

**Abigail M. Oakes**

University of Connecticut

Department of Chemistry

Division of Analytical Chemistry

## 2.1.0 STABLE ISOTOPE PRINCIPLES

An isotope is an atom whose nuclei contains the same number of protons, but different numbers of neutrons. Almost all naturally occurring chemical elements have multiple isotopic forms, the majority of which are stable isotopes. As their name suggests, stable isotopes have a stable atomic nucleus and do not undergo radioactive decay-the loss of energy through radiation emission. While isotopes of an element are different in mass, their overall chemical properties, which are determined by the number of electrons, remain constant [1]. However, the differences in mass may have subtle chemical effects such as slightly different equilibrium constants for a particular reaction leading to enrichment or depletion of specific isotopes in different molecules in the reaction, causing isotope fractionation to occur. Isotope fractionation is the process by which the relative abundances of isotopes are altered in a chemical or physical process. The two main forms of isotopic fractionation, kinetic and equilibrium, are both mass-dependent functions, however the laws describing the partitioning of isotopes differ between the two [2].

## 2.2.0 EQUILIBRIUM STABLE ISOTOPE FRACTIONATION

Equilibrium stable isotope fractionation is typically driven by the differences in vibrational, translational, and rotational energies of molecules containing different isotopes of the same element [3,4]. In terms of energy, when a heavier isotope is exchanged for a lighter isotope the total nuclear charge and electronic distributions remain constant, thus leaving the potential energy curve unchanged. However, molecules containing heavier isotopes have higher binding energies (i.e. are more stable) leading to differences in the zero-point energy (ZPE) of isotopically different molecules (Figure 2.3). Equilibrium

fractionation distributes isotopes in a system in such a way that the total energy of the system is minimized [5].

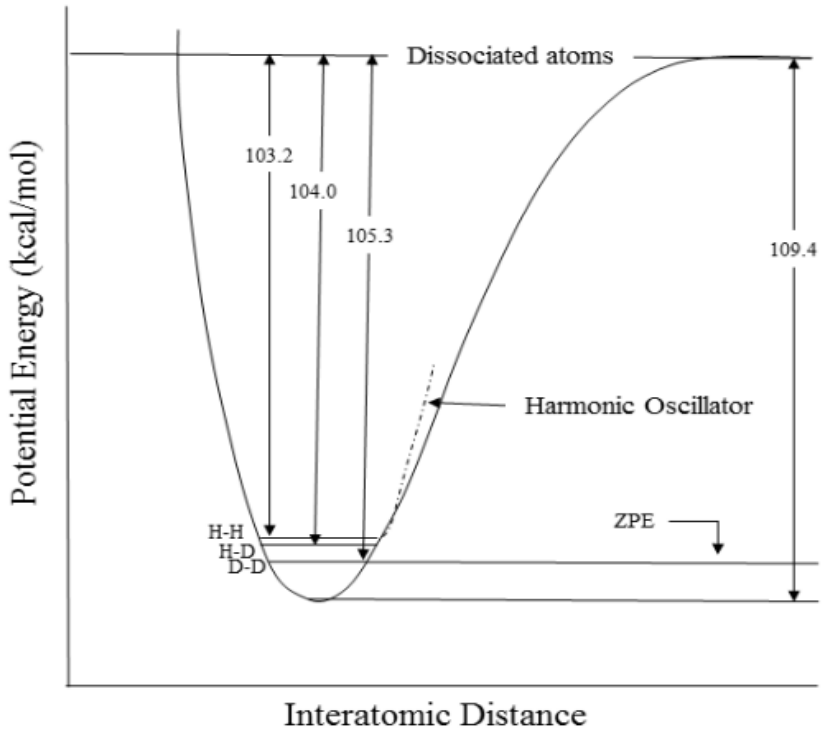


Figure 2.3 Potential energy diagram for the hydrogen molecule showing the zero-point energies and molecular dissociation energies of $H_2$, HD, and $D_2$

## 2.3.0 KINETIC STABLE ISOTOPE FRACTIONATION

Kinetic isotope fractionation occurs due to the differences in reaction rates of isotopic molecules. The kinetic energy equation

$$KE = \frac{1}{2}mv^2 \qquad (2.1)$$

states that, given identical kinetic energy, molecules with a higher mass (i.e. molecules containing the heavier isotope) move slower and therefore react slower [6]. Since equilibrium fractionation occurs in reversible reactions, kinetic fractionation is common in unidirectional reactions where the products are separated from the reactants as well as

diffusion and differential bond breaking scenarios. This indicates that the products for a unidirectional reaction are typically depleted in the heavy isotope (Figure 2.4) [6]. Biological processes are typically unidirectional as organisms will preferentially use the molecule containing the lighted isotope because it requires less energy to break and form bonds [7].

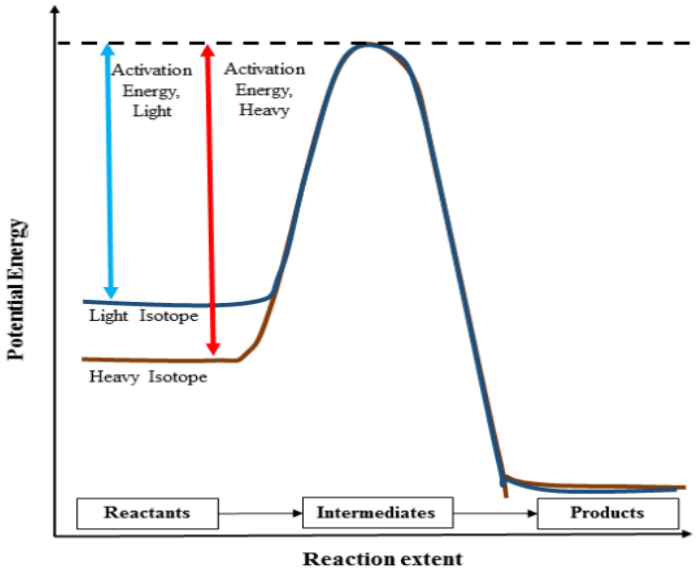


Figure 2.4 Schematic diagram of the potential energy trajectory involved in a molecular reaction. The product containing the heavier isotope is more stable, and therefore requires more energy to complete the reaction than the reactant containing the lighter isotope.

### 2.4.0 STABLE ISOTOPE ANALYSIS

Analytical methods of tracing the source of organic compounds often establish commonality between two substances by identifying their constituent elements, functional groups, and determining their chemical structures. However, this is not always a straightforward process. For example, two samples of common table sugar will contain identical elements, functional groups, etc. and all the previously mentioned data will conclude that they are chemically indistinguishable [8]. However, isotopic variations occur in a variety of materials and the isotopic profile of a given material is unique to that materials origin and history [9]. Difference in photosynthetic pathways of carbon and hydrogen fixation

for individual plants causes differences in isotopic signatures of the molecules they produce, as do variations in the isotopic composition of source water. This means that sugar derived from sugar cane will have a different isotopic signature than sugar derived from beets, and plants harvested from Europe will have a different signature than those harvested from South America [8].

Establishing an isotopic profile or signature is accomplished by measuring the ratios of stable isotopes of a variety of elements such as $^{2}H/^{1}H$, $^{13}C/^{12}C$, $^{15}N/^{14}N$, etc. While variations on a global scale are minute, there are subtle variations in the isotopic composition of compounds that contain these elements that are introduced during biological, chemical, and physical processes. These variations in the natural abundances of stable isotopes are expressed using delta (δ) notation as shown in equations 2.2 and 2.3:

$$\text{ratio } (R) = \frac{\text{abundance heavy isotope}}{\text{abundance light isotope}} \tag{2.2}$$

$$\delta = \left(\frac{R_{samp}}{R_{std}} - 1\right) * 1000 \tag{2.3}$$

samples δ-values are expressed in parts per thousand or 'per mil' (‰) notation, and are relative to an international standard ($R_{std}$) [9].

## 2.5.0 STABLE ISOTOPE RATIO INSTRUMENTATION

### *2.5.1 Compound-Specific Isotope Ratio Mass Spectrometry*

While there are many methods of stable isotope analysis including liquid chromatography-isotope ratio mass spectrometry (LC-IRMS), and bulk characterization of isotopes with elemental analysis-IRMS and high temperature conversion (IRMS), this work focuses on the use of gas chromatography-IRMS (GC-IRMS) for compound specific

analysis. In compound-specific isotope ratio mass spectrometry (CS-IRMS), an unknown mixture is eluted through a gas chromatography column and separated into its constituent compounds. When measuring carbon, the gaseous compounds are sent to a combustion reactor where they are heated to approximately 1000 °C in the presence of oxygen. The molecules are oxidatively combusted into $CO_2$ and water, and the $CO_2$ is sent to the IRMS for analysis. For compound-specific hydrogen, the gaseous molecules are passed through a pyrolysis reactor where they decompose in the absence of oxygen into solid carbon and $H_2$ gas before being sent for isotope analysis (Figure 2.5).

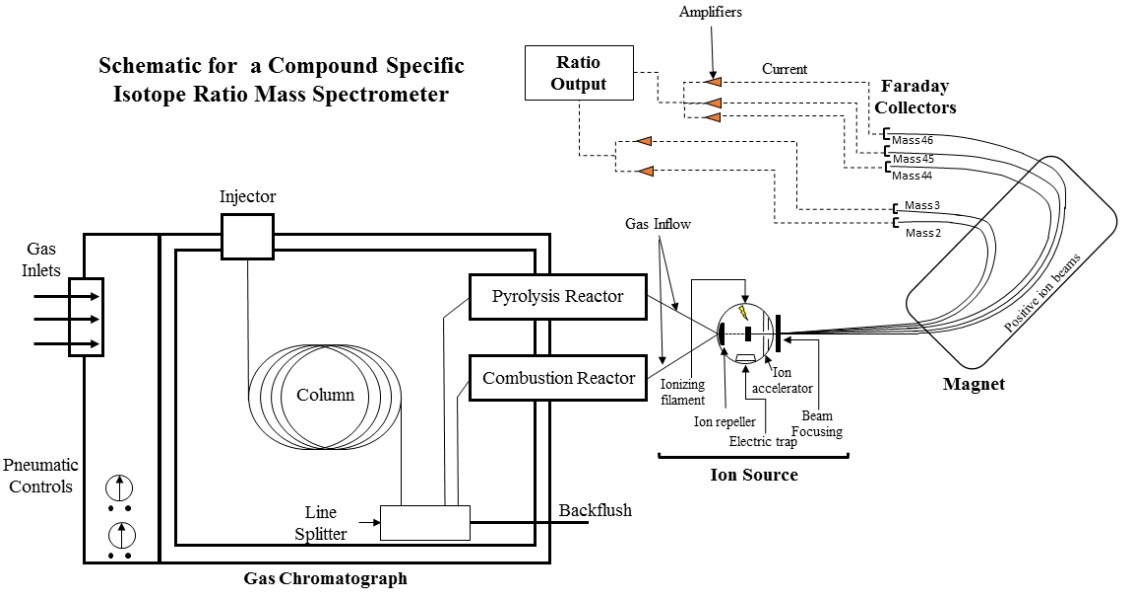


Figure 2.5 General schematic for a Gas chromatograph coupled with and Isotope ratio mass spectrometer (GC-IRMS) capable of measuring compound specific H/D ratios and $^{13}C/^{12}C$ ratios

The IRMS is a specialized instrument that uses a magnetic sector to separate ions based on their mass and contains multiple collectors [10,15]. Equation 2.4 tells us the radius of the curvature of the path taken by an ion with mass *m* and charge *z* [16]:

$$\frac{m}{z} = \frac{eB^2r^2}{2V} \tag{2.4}$$

Ions are selected for detection by adjusting the magnetic field (B) or accelerating the voltage (V) [16].

Once passed through the magnetic sector, ions are detected by an array of Faraday cups. Faraday cups (FC) are conductive metal cups that are placed in a vacuum to intercept a beam of charged particles (Figure 2.6) [17]. The cup is one part of a larger circuit where current is accurately measured and is directly proportional to the number of ions hitting the cup. FC detectors are useful for compound specific stable isotope measurements because they exhibit no mass discrimination. The detection is based solely on charge, leading to higher precision than other mass analysis detectors [17].

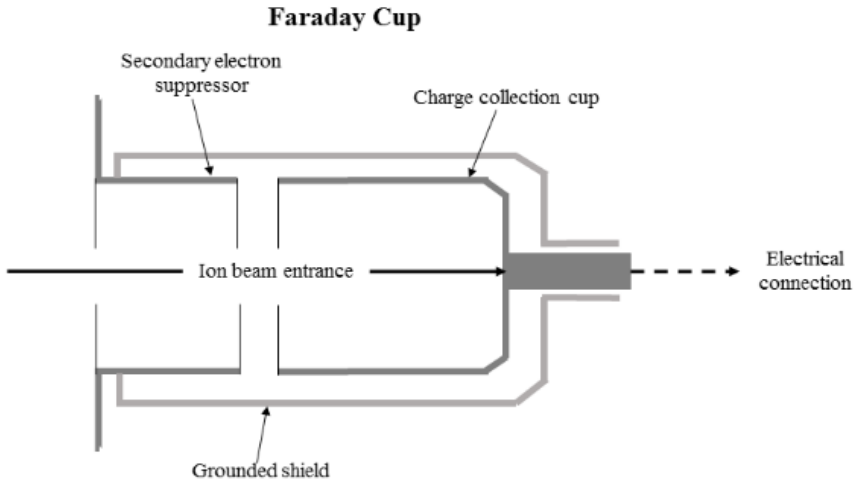


Figure 2.6 General schematic for a Faraday cup ion collector use in IRMS

All stable isotope measurements are made relative to a standard reference material of known isotopic composition. Primary isotope standards are internationally recognized materials that can be used for the purpose of comparing samples measured in different laboratories (Table 2.2). The international standards for carbon and hydrogen stable

isotopes are Pee Dee Belemnite (PDB) and Vienna Standard Mean Ocean Water (VSMOW), respectively [10].

Table 2.2 Internationally accepted stable isotope standards for hydrogen, carbon, nitrogen, oxygen, and sulfur [18]

| Element | Standard | Abbreviation |
|---|---|---|
| H | Vienna Standard Mean Ocean Water | VSMOW |
| C | *Belemnitella americana* from Cretaceous Peedee formation, SC USA | PDB |
| N | Atmospheric $N_2$ | -- |
| O | Vienna Standard Mean Ocean Water | VSMOW |
| | *Belemnitella americana* from Cretaceous Peedee formation, SC USA | PDB |
| S | Troilite (FeS) from Canyon Diablo iron meteorite | CD |

### *2.5.2 Bulk Hydrogen Isotope Ratio Mass Spectrometry*

Hydrogen isotopes of water samples are measured using a Thermo Scientific Temperature Conversion Elemental Analyzer (TC/EA) connected to a Themo Delta V isotope ratio mass spectrometer. TC/EA is a pyrolysis technique that allows for the direct analysis of $\delta^{18}O$ and $\delta D$ in bulk organic materials or inorganic samples. The instrument consists of an injection port capable of introducing both liquids and solids into a reactor where they are completely converted into gases (either CO or $H_2$). From the reactor, the gases are passed into a short isothermal gas chromatography column that is attached to the TC/EA before being introduced to the IRMS for isotope analysis (Figure 2.7).

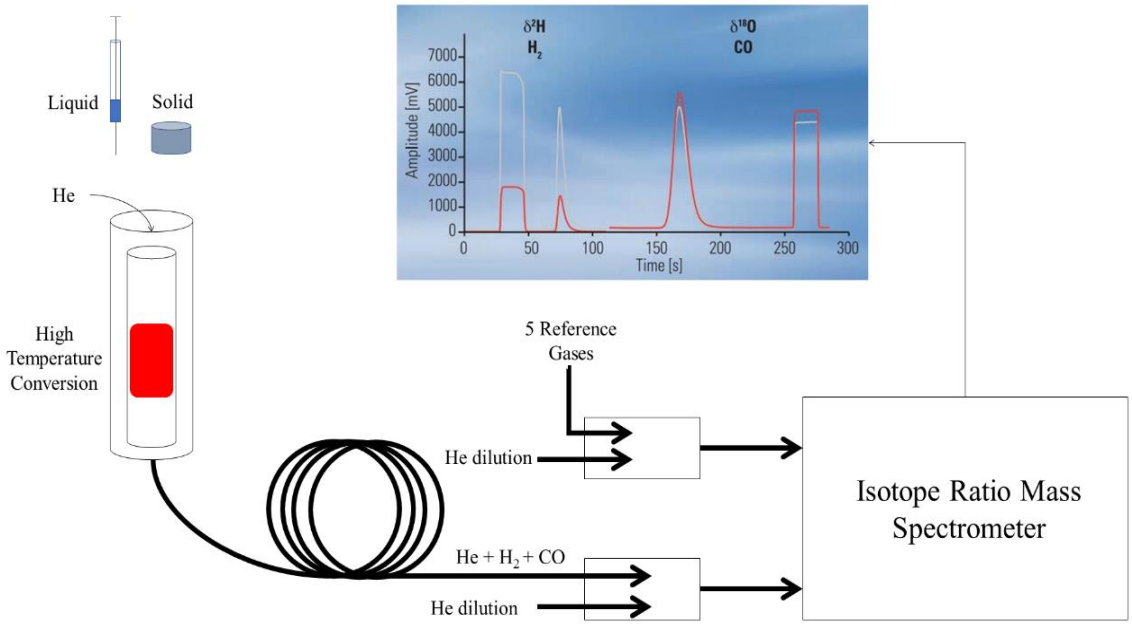


Figure 2.7 General Schematic for a TC/EA IRMS

The reactor is housed in a fused alumina tube and consists of a glassy carbon tube containing glass carbon filling and silver wool. These fillings are intended to keep the sample, as well as any reaction gases, from coming in contact with any oxygen containing surfaces (e.g. $Al_2O_3$) and remove any unintended halogen atoms prior to introduction to the packed GC column [9,18]. The evolved gases are then separated using the isothermal packed GC-column (e.g. molecular sieves). This is particularly important because $N_2$ is isobaric with CO (m/z 28) and is known to have an ionization effect with $H_2$ [9]. Once through the GC column, the sample gas is sent through to the IRMS where its isotopic ratios are analyzed (Figure 2.7).

## 2.6.0 REFERENCES


(1) *Encyclopedia Britannica*; Encyclopedia Britannica, Inc, 2006.

(2) Young, E. D.; Galy, A.; Nagahara, H. *Geochim. Cosmochim. Acta* **2002**, *66* (6), 1095–1104.

(3) Urey, H. C. *J. Chem. Soc.* **1946**, 562–581.

(4) Schauble, E. *Rev. Mineral. Geochemistry* **2004**, *55* (1), 65.

(5) Hayes, J. M. *Org. geochemistry Contemp. Anc. Sediments* **1983**, *5* (August), e5.

(6) Kendall, C.; Caldwell, E. A. *Isotope Tracers in Catchment Hydrology*; Kendall, C., McDonnell, J. J., Eds.; Elsevier Science B.V.: Amsterdam, 1998.

(7) Clark, I.; Fritz, P. *Environmental Isotopes in Geochemistry*; Dtein, J., Starkweather, A. W., Eds.; CRC Press LLC: New York, 1997.

(8) Meier-Augenstein, W. *Stable Isotope Forensics: An Introduction to the Forensic Application of Stable Isotope Analysis*; John Wiley & Sons Ltd., 2010.

(9) Carter, J.; Barwick, V. *Good practice guide for isotope ratio mass spectrometry*; 2011.

(10) Muccio, Z.; Jackson, G. *Analyst* **2009**, No. 134, 213–222.

(11) Wong, W. W.; Hachey, D. L.; Zhang, S.; Clarke, L. L. *Rapid Commun. mass Spectrom.* **1995**, *9* (11), 1007–1011.

(12) Nygren, U.; Ramebäck, H.; Berglund, M.; Baxter, D. C. *Int. J. Mass Spectrom.* **2006**, *257* (1–3), 12–15.

(13) Jochmann, M. A.; Blessing, M.; Haderlein, S. B.; Schmidt, T. C. *Rapid Commun. Mass Spectrom.* **2006**, *20*, 3639–3648.

(14) Nelson, S. T. *Rapid Commun. Mass Spectrom.* **2000**, *14* (4), 293–297.

(15) Gross, J. *Mass Spectrometry*, 2nd ed.; Springer-Verlag: Berlin, 2011.

(16) Harris, D. C. *Quantitative Chemical Analysis*, 7th ed.; Macmillan, 2010.

(17) Busch, K. L. *Spectroscopy* **2011**, *26* (11).

(18) *High Temperature Conversion Elemental Analyzer*; 2010.

(19) Hoefs, J. *Stable Isotope Geochemistry*; Springer-Verlag: Heidelberg, Germany, 1980.

# CHAPTER THREE

# Temporal variations in the δD of leaf *n*-alkanes from four riparian plant species

**Abigail M. Oakes** [1]

Michael T. Hren [1,2]

[1] University of Connecticut, Department of Chemistry

[2] University of Connecticut, Center for Integrative Geosciences

Published in: *Organic Geochemistry*, (**2016**) 97:122−130

### 3.1.0 ABSTRACT

The hydrogen isotopic composition of terrestrial plant leaf waxes is widely used as a proxy for the isotopic composition of ambient water at the time of plant growth, yet there is considerable uncertainty about how environmental or plant-specific factors impact apparent hydrogen isotope fractionation. We sampled leaves from four riparian plant species (*Pinus strobus*, *Tsuga canadensis*, *Phalaris arundinacea* and *Corylus americana*) during the 2013 growing season (April to October) to evaluate the controls of hydrogen isotope fractionation in plant-derived *n*-alkanes. Our data show that plants from different taxonomic classes produce distinct seasonal patterns of isotopic change that could reflect differences in stomatal regulation, soil versus groundwater uptake, and timescales of wax synthesis. These patterns are distinct even for plants from the same functional group (i.e. angiosperms versus gymnosperms). *P. strobus* (gymnosperm tree) and *P. arundinacea* (angiosperm grass) are characterized by a significant increase in apparent fractionation during the growing season (> 50 ‰ change). In contrast, *n*-alkanes from *C. americana* (angiosperm) show a decrease in ε value from –145 ± 8 ‰ during early season growth to –111 ± 6 ‰ late in the season. *T. canadensis* (gymnosperm) exhibits a constant ε of –123 ± 10 ‰ throughout the growing season with minimal temporal change. Sedimentary *n*-alkanes collected from the stream channel adjacent our plant sample locality show minor changes over the sampling period with a mean ε value of –130 ± 6 ‰. Apparent fractionation differences between plant species greatly exceed variations in stream composition throughout the growing season, indicating that differences in the timing of wax production or groundwater δD cannot alone explain the variation in ε between different plant types. In contrast to individual plant leaves, fluvial sediments represent a

time-integrated ecosystem average of *n*-alkane δD that yields a more consistent isotopic record of changes in ambient ecosystem water than individual plants.

## 3.2.0 INTRODUCTION

Higher plants produce a range of organic molecules within, and on the surface of, leaves to provide protection from predation, minimize water loss, and add structural support for leaf architecture [1–6]. One of the most abundant classes of plant-derived wax compounds is straight chain normal alkanes (*n*-alkanes). These compounds are produced on the surface of leaves and are preserved in sedimentary archives with minimal degradation or isotopic alteration at low temperatures (~150 °C) over geologic time [7–11]. As a result, *n*-alkanes constitute a valuable record of past environmental conditions.

Numerous studies have employed the stable hydrogen isotopes of plant-derived *n*-alkanes preserved in ancient sediments to interpret changes in paleoelevation [12,13], isotope hydrology [14–16], ecosystem change [17,18] and paleoenvironment [19,20]. However, complications in reconstructing paleoenvironments result from uncertainty in the timing of wax production, sedimentary deposition and integration, and how isotopes of individual *n*-alkanes relate to ambient environmental conditions (i.e. temperature, precipitation, precipitation isotopes, moisture availability and ecosystem type).

Hydrogen ($\delta D_{n\text{-alkane}}$) stable isotopes of terrestrial plant *n*-alkanes reflect the isotopic composition of ambient water modified by environmental parameters such as temperature, precipitation, stomatal regulation, water use efficiency and plant functional types [8–10,15,21–25]. Varied environmental factors affect ambient precipitation isotopes, such as the degree of soil or leaf-water evaporation or the magnitude of biosynthetic fractionation, and alter the leaf water composition and thus, final *n*-alkane δD [10,26–29]. A

number of studies have examined apparent fractionation between plant *n*-alkane and leaf or xylem water [5,29,30]. While this is informative of biological functions of plants, it does not fully address how plant *n*-alkane isotopes relate to ambient precipitation or groundwater. In order to reliably utilize δD of individual leaf wax *n*-alkanes as a proxy for isotope hydrology, it is critical to relate plant wax *n*-alkane geochemistry to seasonal or annual environmental signals [17,31–33].

We examined the stable hydrogen isotopic compositions of *n*-alkanes from four $C_3$ plants (*Pinus strobus*, *Tsuga canadensis*, *Phalaris arundinacea*, and *Corylus americana*) within the Fenton River watershed (Storrs, CT). This approach was tailored to examine how the hydrogen isotopic composition of *n*-alkanes from plants with different patterns of stomatal regulation (angiosperm, gymnosperm, grass, and shrub), plant growth, and timescales of wax synthesis changes throughout the growing season. We focused on streamside vegetation with roots positioned visibly in the river water to minimize potential external differences in water stress and determine how resultant stomatal regulation is reflected in *n*-alkane isotopic composition. Our data indicates the possibility that differences in stomatal regulation and/or function rather than the timescale of synthesis account for the large differences in *n*-alkane hydrogen isotopic composition throughout the growing season. Temporal variations in plant δD during the growing season greatly exceed seasonal variation in groundwater δD and most likely reflect biologic differences in stomatal regulation of transpiration and $CO_2$ fixation. In contrast to individual plant leaves, river sediments are temporal integrators that minimize heterogeneity in an ecosystem. Thus, we argue that soils or sediments provide the best ecosystem level record of the isotopic composition of ambient water during plant growth.

## 3.3.0 SAMPLE COLLECTION AND METHODS

### *3.3.1 Study catchment and sample collection*

The Fenton River is a minimally-altered ~89 $km^2$ drainage located in northeastern Connecticut and covered by a mixed deciduous forest. The climate is moist-temperate and receives ~120 cm/yr precipitation. Temperature ranges from a mean of –6 °C in January to 21 °C in July, with a mean annual temperature of 15.7 °C (Supplementary Table 3.3) and $\delta D_{precipitation}$ varies from ~ –30 ‰ to –100 ‰ throughout the year [34,35].

We sampled modern leaves from four plants along the banks of the Fenton River (41°50'01" N, 72°15'02" W; Supplementary Figure 3.15) on a weekly to biweekly basis initiated in April 2013, prior to the period of leaf-out of deciduous trees, through the period of leaf senescence in October 2013. Targeted species included (a) White Pine (*Pinus strobus*); (b) Eastern Hemlock (*Tsuga canadensis*); (c) Reed canary-grass (*Phalaris arundinacea*); and (d) American Hazelnut (*Corylus americana*). In order to reduce heterogeneity in sampling, the same four trees were sampled from each sample period. Furthermore, during each sampling period, several leaves/needles/blades were sampled from various locations on each plant to get an average per plant, per week. All plants were situated immediately adjacent the river channel (< 1 m from bank full channel) and had roots visible in the stream channel below base-flow groundwater level. These species were chosen because they make up much of the young growth found along the river banks and, as such, are major contributors to sediment *n*-alkane concentrations. For conifers and grass, early season collection of leaves/needles contained mostly old growth, as that was all that was available. As the season progressed, we specifically targeted new growth for *P. strobus*, *T. canadensis*, and *P. arundinacea*. In addition to leaf samples, we collected

sediment adjacent the plants in the stream channel and stream water for each period of leaf sample collection.

Sediments were collected from the streambed located on the northwest side of the small outcropping that the *P. arundinacea* was grown on. Samples were taken from here due to the accumulation of organic matter flowing through the catchment as a result of base flow deposition. A sample was collected concurrently with the plant samples throughout the growing season and heterogeneity was minimized by collecting from the same location and no deeper than 2–4 cm from the surface of the deposited materials. Samples were collected in ashed glassware and immediately frozen to minimize post-sampling alteration. The water was collected from the center of the stream in a PTFE bottle with a screw cap and sealed underwater in order to remove all headspace.

### *3.3.2 Extraction, separation, and analytical methods*

Leaves and sediments were frozen following sampling and then freeze-dried (Labconco Freezone 4.5) prior to *n*-alkane extraction. A minimum of 3–5 leaves were extracted via sonication using a 9:1 (v/v) dichloromethane-methanol (DCM: MeOH) solution. Sediments were freeze-dried and extracted using Soxhlet extraction. A minimum of 100 g of sediment was weighed and extracted using a 2:1 DCM: MeOH mixture for 24 hours. TLE's were saponified with ~5 ml of 1 M KOH in MeOH and heated for 2 hours at 85 °C. The reaction was quenched using 5 ml of 5 % NaCl. The neutral fraction was separated via liquid/liquid extraction for *n*-alkane separation.

*n*-Alkanes were separated by silica gel column chromatography and analyzed on a Thermo-Scientific Trace GC Ultra fitted with a split-splitless (SSL) injector and flame ionization detector (FID) using a BP-1 column (60 m × 0.25 mm i.d., 0.25 µm film

thickness) with He as the carrier (1.5 ml/min). We calculated carbon preference indices (CPI) (Eq. 3.1) and Average Chain Length (ACL) (Eq. 3.2), and Average Higher Plant Chain Length (Eq. 3.3) to evaluate temporal changes in the distribution of alkanes. These equations are:

$$CPI = \frac{(C_{23}+C_{25}+C_{27}+C_{29}+C_{31}+C_{33})+(C_{25}+C_{27}+C_{29}+C_{31}+C_{33}+C_{35})}{2(C_{24}+C_{26}+C_{28}+C_{30}+C_{32}+C_{34})} \quad (3.1)$$

$$ACL = \frac{(C_{25}(25)+C_{27}(27)+C_{29}(29)+C_{31}(31)+C_{33}(33))}{(C_{25}+C_{27}+C_{29}+C_{31}+C_{33})} \quad (3.2)$$

$$AHPCL = \frac{(C_{27}(27)+C_{29}(29)+C_{31}(31))}{C_{27}+C_{29}+C_{31}} \quad (3.3)$$

where $C_x$ corresponds to the area of the individual *n*-alkane peak from the gas chromatogram.

### *3.3.3 Stable hydrogen isotope analyses*

Hydrogen isotopes of individual *n*-alkanes were measured using a Thermo GC-Isolink attached to a Thermo Scientific Delta V Plus isotope ratio mass spectrometer with a 30 m × 0.25 μm ID, 0.25 μm film thickness BP-5 fused silica column with a helium carrier at a flow of 1.5 ml/min. The initial GC oven temperature was held at 50 °C for 1 min then warmed to 180 °C at 12 °C/min, followed by a ramp to 320 °C at 6 °C/min and held at 320 °C for 4 min. We measured the $H_3^+$ factor daily prior to standard calibration and sample analysis. This averaged 6.4 over the duration of analysis.

The isotopic compositions of individual *n*-alkanes were determined using an in-house laboratory gas reference and a suite of *n*-alkanes of known isotopic composition that were measured multiple times at a range of concentrations (Mix A5 prepared by

A. Schimmelmann). Typical standard deviation for repeated analysis of A. Schimmelann's Mix A5 *n*-alkane isotope standard was less than 4 ‰.

Hydrogen isotopes of stream waters were analyzed using a Thermo Scientific Temperature Conversion Elemental Analyzer (TC/EA) coupled to a Thermo Delta V Plus. Water samples were measured in triplicate the mean values are presented. Samples are expressed relative to VSMOW by comparison with a suite of International and laboratory standards (e.g., SMOW, SLAP, GISP). Repeat analyses of water standards yield a precision of ±3 ‰.

The calculated enrichment factor (ε) is used to characterize the hydrogen isotopic fractionation between source and product. This may be defined by Eq. 3.4:

$$\varepsilon = \left[\left(\frac{\delta D_{n-alkanes}+1}{\delta D_{water}+1}\right) - 1\right] \quad (3.4)$$

and includes a variety of fractionations associated with physical and biochemical processes. In the above formulation [36], the δ equation excludes the commonly utilized multiplier of 1000 for delta calculations and is defined by Eq. 3.5 for the calculation of epsilon values:

$$\delta D_{n-alkane} = \left[\left(\frac{R_{sample}}{R_{standard}}\right) - 1\right] \quad (3.5)$$

## 3.4.0 RESULTS AND DISCUSSION

### *3.4.1 Abundance, Carbon Preference Index (CPI), and chain length distribution of n-alkyl lipids*

We normalized the abundances and distribution of *n*-alkanes in plant extracts relative to the total mass of the extracted leaves (Figure 3.8, Supplementary Table 3.4). The *n*-alkane concentrations in *P. strobus* and *T. canadensis* are characterized most

prominently by large spikes in *n*-alkane concentration mid-season (days 200–250) (Figure 3.8). The angiosperms *P. arundinacea* and *C. americana* peak early in the season (days 100 – 150) and remain fairly constant throughout the growing season (Figure 3.8).

Increases in *n*-alkane concentration during the period of growth (*P. strobus, T. canadensis*) suggest continued wax production throughout the growing season. The spikes seen in both species occur immediately after a period of heavy rain, which could possibly indicate increased production of *n*-alkanes after they have been physically removed by natural processes. Thus, changes in *n*-alkane $\delta D_{nC27\text{-}33}$ of *P. strobus* and *T. canadensis* likely reflect changes in internal leaf water throughout the growing season. The relative stability of *n*-alkane concentrations after leaf flush (*P. arundinacea, C. americana*) indicates that for these angiosperm plants, the bulk of leaf waxes are formed early in the growing season. For *P. arundinacea,* peak *n*-alkane production occurs during late April as the weather warms and daylight hours increase, while for *C. americana,* waxes are produced with the bud and decrease with expansion of leaf mass during leaf flush. For

these two angiosperms, a temporally-biased period of formation indicates that *n*-alkanes from these two plants should reflect early season water δD.

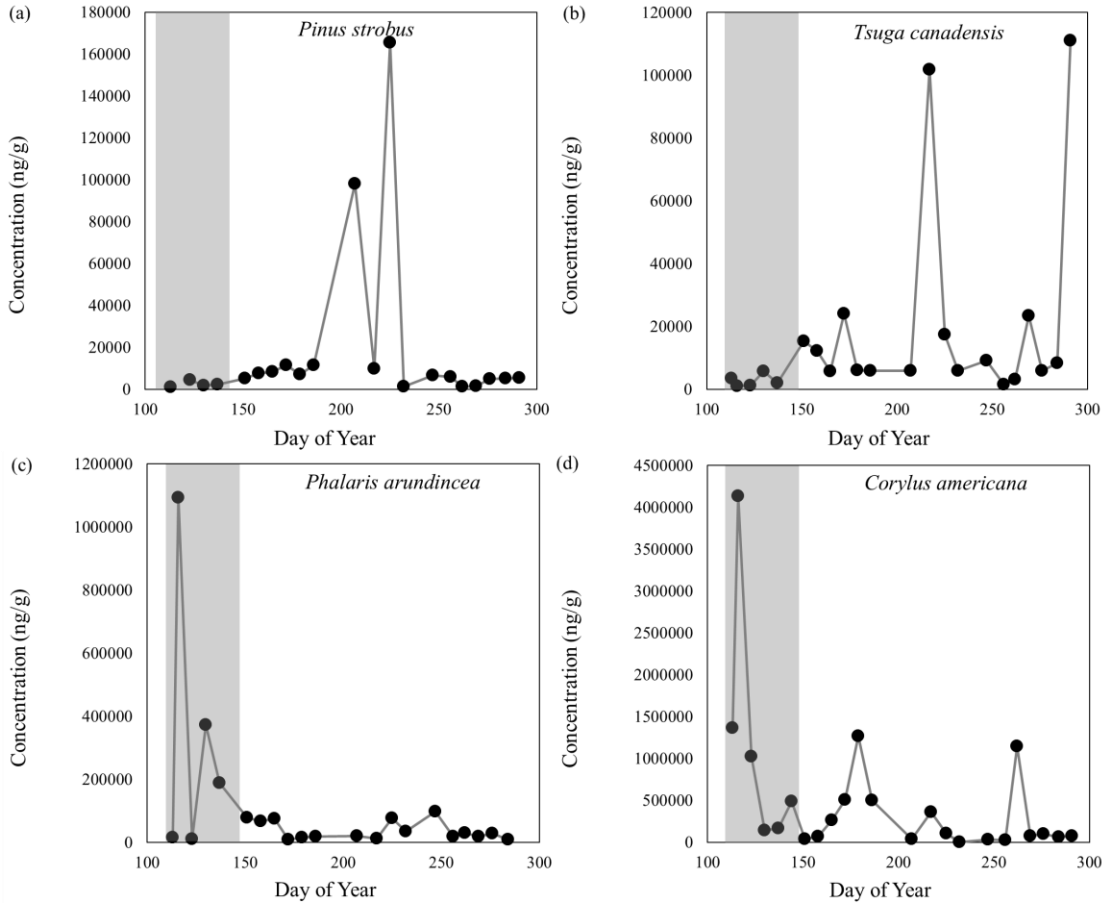


Figure 3.8 Leaf *n*-alkane concentrations for (a) *P. strobus*, (b) *T. canadensis*, (c) *P. arundinacea*, and (d) *C. americana* throughout the growing season. Concentrations represent the total *n*-alkane concentration relative to leaf dry weight (ng/g). For *C. americana* (d) leaf flush occurred during days 113 to 137, as indicated by the gray box

The distribution of sedimentary *n*-alkanes mirrors those of the plants, with maximum abundances of *n*-$C_{29}$ to *n*-$C_{33}$, and the most abundant *n*-alkane being *n*-$C_{29}$ (Figure 3.9). Angiosperms exhibit far higher concentrations of long-carbon chain *n*-alkanes than the gymnosperm samples (317 µg/g and 3.6 µg/g for $C_{29}$ for *C. americana* and *P. strobus* respectively) and may bias the sedimentary pool (Figure 3.9). Indeed,

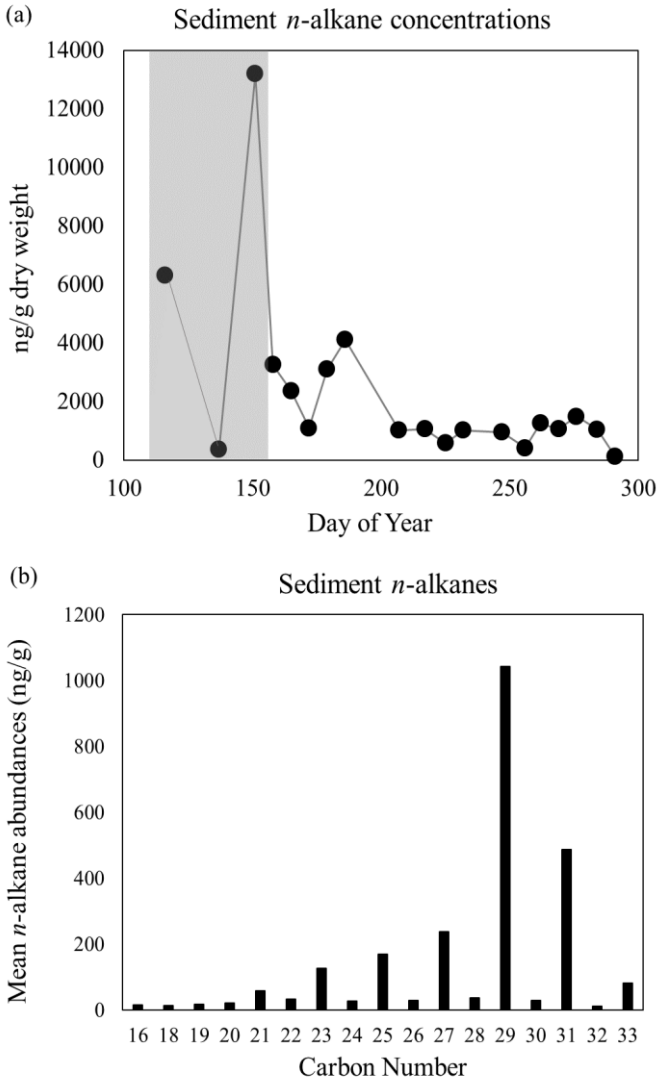


Figure 3.9 (a) Total *n*-alkane abundances from collected sediments throughout the growing season in ng/g of dry material. Since sediments are assumed to incorporate the organic matter from the surrounding environment, (b) shows the weighted abundances of each *n*-alkane of all sampled plant species combined throughout the growing season in ng/g of dry material. Similar abundance patterns are seen in both graphs ($C_{29}$ has the largest abundance

sedimentary *n*-alkanes mirror the distribution in *C. americana* and other similar angiosperm vegetation. Soil *n*-alkane abundances show an almost identical pattern to *C. americana* (Figure 3.9 and Figure 3.10). This could be due to the fact that *C. americana*, and other deciduous trees shed alkane-rich leaf material each Autumn, adding more sedimentary *n*-alkanes than conifers with smaller leaf areas and lower normal alkane abundances. However, the overall concentration and distribution of *n*-alkanes preserved in fluvial sediments will vary as a function of both leaf-wax concentration and overall representation within an ecosystem.

The CPI of plant *n*-alkanes is a measure of the distribution of odd and even carbon chain compounds and reflects variations in production and loss of different *n*-alkanes. *T. canadensis* shows modest

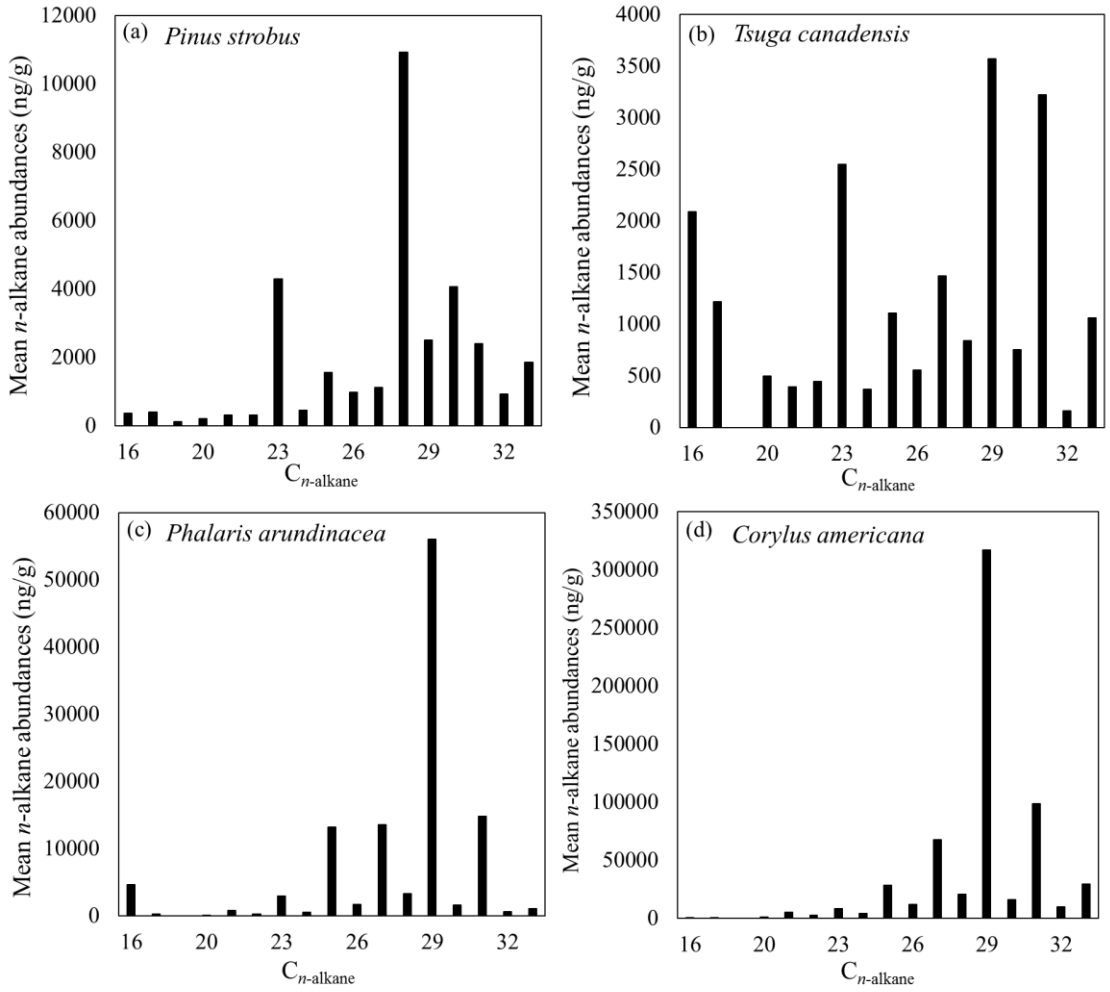


Figure 3.10 Individual *n*-alkane abundances collected from (a) *P.strobus*, (b) *T. canadensis*, (c) *P. arundinacea* and (d) *C. americana* combined throughout the growing season.

change in CPI over the growing season (5 to 10), while CPI for *P. strobus* increases steadily (5 to 20) and *P. arundinacea* decreases (25 to 10) (Figure 3.11; Supplementary Table 3.4). *C. americana* is unique because it shows a sharp increase from below 10 on day 113 to above 50 on day 116, followed by a steep drop to approximately 10 on day 144, corresponding to leaf flush (Figure 3.11). These data point to variations in the timing of wax synthesis and/or degradation for each of the sampled species.

Previous studies of *n*-alkanes indicate a relationship between ACL or AHPCL and extreme climate conditions [37,38]. For *P. strobus*, *T. canadensis*, and *P. arundinacea*, there are only minute changes throughout the growing season. The AHPCL for each of these range from 29.1 to 30.3, 28.9 to 30.0, and 28.8 to 30.1 respectively (Figure 3.11; Supplementary Table 3.4). *C. americana* experiences an increase in AHPCL over the first 6 weeks from 28.1 to 29.9 where it remained stable for the duration of the season (Figure 3.11).

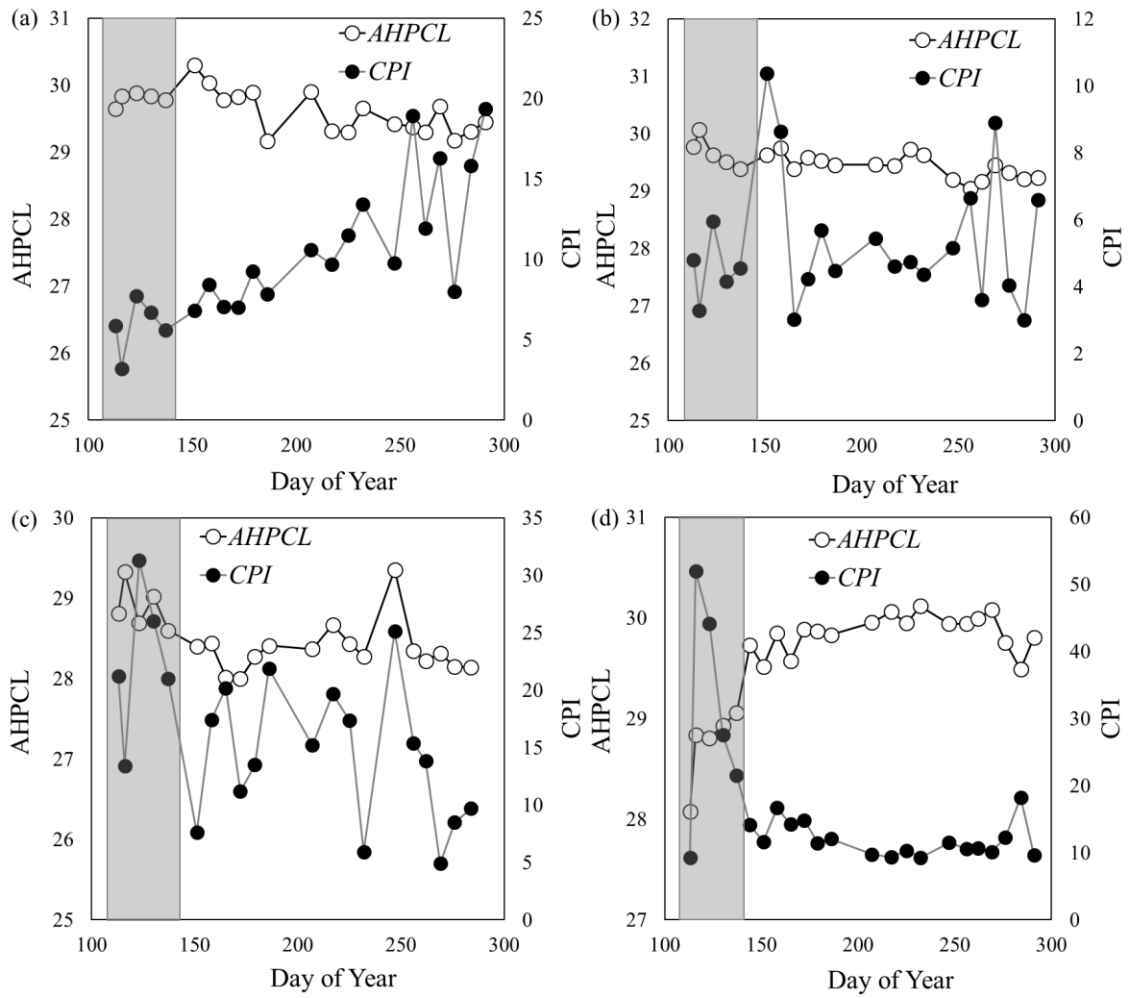


Figure 3.11 The carbon preference index (CPI) and average higher plant chain length (AHPCL) for (a) *P. strobus*, (b) *T. canadensis*, (c) *P. arundinacea*, and (d) *C. americana* throughout the growing season. Leaf flush occurred during days 113 to 137, as indicated by the gray box.

The chain length range observed for our *P. strobus* is slightly larger than reported by Tipple and Pagani in their 2013 study of plants along a North American transect. These differences may stem from differences in climate, summer precipitation and ambient relative humidity. Since our plants have roots directly in the water system, we suspect that our specimens have reduced water stress compared to upland plant growth or vegetation in more arid environments. Reduced water stress and/or higher relative humidity may minimize the need to produce longer chain lengths, which have lower vapor pressure and higher melting point, during peak summer conditions. AHPCL in *C. americana* increases from 28.1 to 29.7 from day 113 to 144 (during leaf flush) where it stabilizes for the remainder of the growing season. This trend is similar to other broadleaf angiosperms reported by Tipple et al. (2013) [29] of ~27.5 to 28.9. This indicates that the composition of *n*-alkanes changes most substantially during leaf bud and leaf flush. Coupled with concentration and CPI data, this suggests there is little to no leaf wax production after leaf flush and all the long chain *n*-alkanes are formed at that time [29].

### *3.4.2 Seasonal trends in δD and ε values*

Plants utilize water from a range of depths within the critical zone [39]. We measured the hydrogen isotopic composition of stream water during the sampling period to constrain changes in composition of ambient water available to plant roots below the water table. All sampled plants had visible roots below base-flow groundwater level (less than 1 m below the surface), providing direct access to the stream and a means of minimizing potential water stress. Stream δD varied little over the period of sampling, ranging from –48 ± 1.7 ‰ in the early spring (days 100–150) to –42 ± 2.5 ‰ in peak summer (days 200–300). Water δD varied most during days 150–200 to approximately –57 ‰, a 10 ‰ difference from

previous weeks (Figure 3.12). This drop followed three weeks of intense rainfall and flooding.

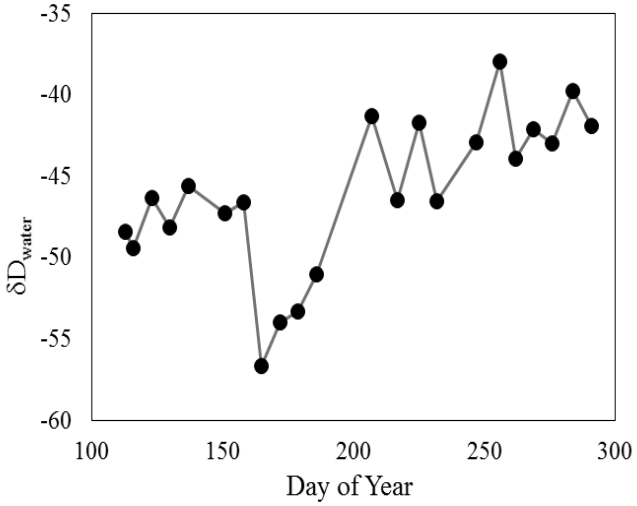


Figure 3.12 δD of stream water throughout collection period. Water was collected from the center of the stream and measured in triplicate with standard precision ±3 ‰.

Environmental water is the primary hydrogen source for *n*-alkanes synthesized within the leaves [10,40]. Greenhouse and field-based studies show no isotopic change during water uptake in roots [41]. As a result, changes in the δD of plant source water should be evident in changes in the composition of *n*-alkanes [5,6,18]. Our data show dramatically larger isotopic changes in *n*-alkanes than in source water. This can only result from fractionation after uptake of groundwater due to evaporative loss during transpiration, which would yield isotopically-enriched leaf water relative to groundwater, or storage of cold season soil water that is used in biosynthesis early in the growing season. We believe that the latter is unlikely because early season *n*-alkanes show the most enriched δD values, when winter water should be the most depleted.

Weighted $\delta D_{nC27\text{-}33}$ of *P. strobus* and *P. arundinacea* both decrease throughout the growing season. *P. strobus* shows fairly constant $\delta D_{nC27\text{-}33}$ (~ –194 ± 5 ‰) until early July, when values decrease to –215 ± 11 ‰, while *P. arundinacea* decreases early in the season from –196 ± 16 ‰ to a steady value of ~ –218 ± 5 ‰ (Figure 3.13). In contrast, *T. canadensis* $\delta D_{nC27\text{-}33}$ remains constant at ~ –160 ‰ (Figure 3.13). For *C. americana*,

$\delta D_{nC27\text{-}33}$ is initially depleted (~ –186 ± 7 ‰), followed by an increase in δD value throughout leaf flush (days 113–144) to a stable ~ –152 ± 8 ‰ (Figure 3.13).

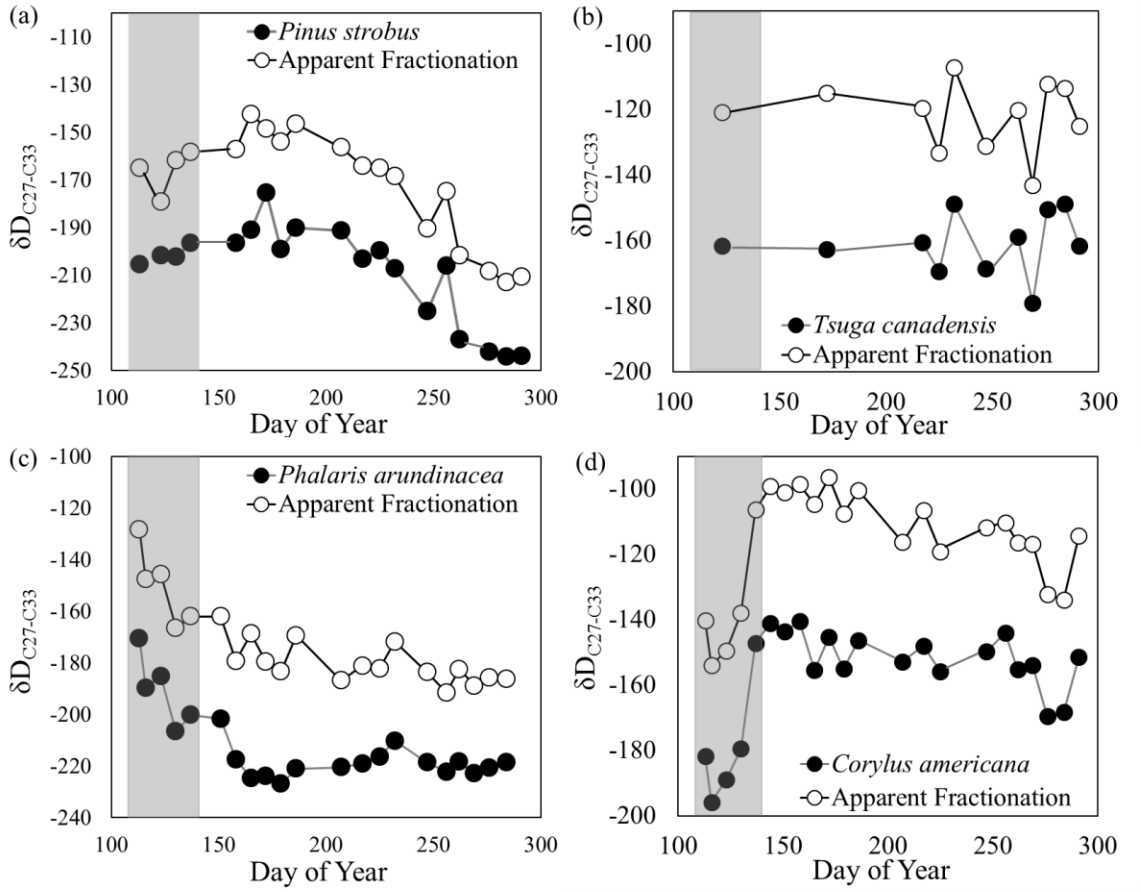


Figure 3.13 Isotopic composition ($\delta D_{nC27–C33}$) and apparent fractionation (ε) of (a) *P. strobus*, (b) *T. canadensis*, (c) *P. arundinacea*, and (d) *C. americana* throughout the growing season. Leaf flush occurred during days 113 to 137, as indicated by the gray box

For *P. strobus*, peak 2013 summer temperatures coincided with the transition to more isotopically-depleted *n*-$C_{25}$–*n*-$C_{33}$ values (days 178 to 248). Previous work shows that conifers have difficulty maintaining open stomata in the daytime during periods of high temperature and low precipitation, but open their stomata at night to allow $CO_2$ diffusion to the sites of $CO_2$ fixation [42]. This could lead to a decrease in leaf-water evaporation due to a change in transpiration. However, since the roots of the pine are directly in the water source, the plant may experience reduced water stress, allowing the plant to maximize $CO_2$

diffusion into the stomata rather than minimizing water loss, which can be confirmed through a growth chamber study. For *C. americana* and *P. arundinacea*, the most significant changes in *n*-alkane δD occur during days 113 to 144 of plant growth during leaf flush and peak wax synthesis.

Noise in isotope data from individual plants may result from a mixture of old growth and new growth, however recent high-resolution temporal studies also show strong seasonal variations and heterogeneity within an individual plant [29,43]. This heterogeneity may derive from variability in the source of water used in biosynthesis, the leaf life cycle and timescale of wax synthesis, and plant-specific factors that influence stomatal regulation and transpiration of leaf water [22,31,42,44–53].

We measured the δD of individual *n*-alkanes preserved in fluvial sediments collected adjacent to plant sample locality. The mean seasonal abundance-weighted $n$-$C_{27}$-$n$-$C_{33}$ δD was –170 ± 4 ‰ (Figure 3.14, Supplementary Table 3.5). The integration of multiple plants over time leads to a more stable isotopic signature than individual plants, which vary greatly over a single growing season. Several studies have observed a spatial correlation between sediment *n*-alkane δD values and climate variables [17,51,54,55]. Our sediments are less affected by short-term changes in isotopic values than plants, yielding a better record of general paleoenvironmental conditions than data from individual leaves. Figure 3.14 shows a comparison of the δD values of the sediments with the weighted δD values of the four sampled plants.

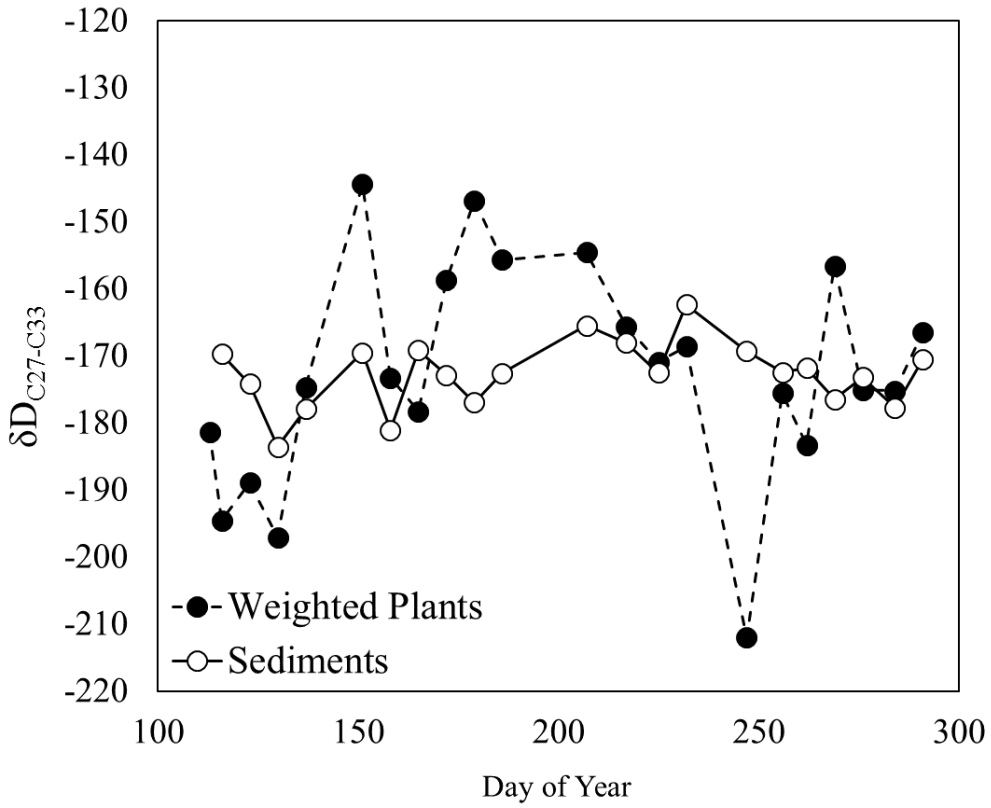


Figure 3.14 Abundance weighted $\delta D_{nC27\text{-}C33}$ for sediments throughout the growing season compared with abundance weighted $\delta D_{nC27\text{-}C33}$ for all plant species measured.

Sediments appear to show a muted temporal change over the period of sampling and smaller variations than those observed in the weighted average of the sampled plants. We calculated the abundance weighted δD of *n*-alkanes for the four sampled plants to assess how well this compares with sediment *n*-alkane δD. Sedimentary organic matter is derived from both terrestrially sourced plant matter as well as microbially cycled organic matter. However, we focused on long-carbon chain normal alkanes that are dominantly produced by plants and integrated into the sedimentary flux within the small Fenton catchment. The mean *n*-alkane δD calculated from weekly individual *n*-alkane δD (weighted for δD values and *n*-alkane abundances for each plant) varies throughout the sampling period. This pattern is similar to the δD of *n*-alkanes extracted from the sediment

samples, however the magnitude of change is reduced in sediments compared to the abundance weighted calculated value derived from our four plants (Figure 3.14). It should be noted that the sediment *n*-alkane δD values are an accumulation of a broader area with more plants. This may explain the slight differences in the patterns and the muted changes expressed in the sediments. These data suggest that sediments are biased by short timescale variability, but it is a second order effect relative to the long-term (multi-year) integration of *n*-alkanes from a variety of plants across a catchment.

Plants with different photosynthetic pathways exhibit distinct apparent fractionation ($\varepsilon_{n\text{-alkane}}$) due to differences in timing of water synthesis or water use strategies, with $C_3$ grasses averaging ~ –170 ‰, $C_4$ grasses ~ –145 ‰, and $C_3$ trees and shrubs averaging ~ –120 ‰ [5,22,29,31,47,56–58]. The variability and magnitude of leaf water enrichment can be attributed to various environmental parameters and plant physiological processes [59]. One of the primary goals of this experiment was to create a modern-day proxy that compared $\delta D_{n\text{-alkane}}$ to $\delta D_{water}$ in order to better understand how they are related, for use in reconstructing paleohydrology.

The ε value for *P. strobus* is relatively constant at –152 ± 11 ‰ throughout the early growing season, then decreased steadily to –174 ± 9 ‰ in early fall (Figure 3.13). *P. arundinacea* shows a decrease in ε early in the growing season with an average of –156 ± 16 ‰ over weeks 1 through 9 and achieves a constant value of –182 ± 6 ‰ (Figure 3.13). These fractionations are larger than nearly all previously published data for similar plant classes ($\varepsilon_{Pinus\ strobus}$ = –128 ± 12 ‰, $\varepsilon_{grass}$ ~ –145 ‰; Tipple and Pagani 2013 and references therein). In contrast, ε values for *T. canadensis* remain constant at –123 ± 10 ‰ with respect to stream water, while for *C. americana* they increase from

~ –145 ‰ during leaf flush to –111 ± 6 ‰, after which it remains stable (Figure 3.13). Both *T. canadensis* and *C. americana* have ε values similar to those published previously.

Eley et al. (2014) [18] suggest that for a constant water source, apparent fractionation should remain constant throughout a growing season since source water is the only hydrogen source. However, the only specimen in our study with effectively constant ε is *T. canadensis*. *P. strobus, C. americana,* and *P. arundinacea* all show a large change in ε throughout the growing season despite all accessing the same potential water pool. *C. americana* is the first to attain steady state values (~day 130), followed by *P. arundinacea* (day 158) and by *P. strobus* (day 256). We cannot exclude uptake of shallow soil water by individual plants, however the temporal patterns observed in our *n*-alkane data are not easily explained by temporal shifts in precipitation δD during the growing season. Our data suggest that the major difference in the hydrogen isotopic composition of higher plant *n*-alkanes is not strictly a difference in the timing of wax synthesis, but rather regulation of stomata in response to environmental stressors.

Tipple et al. (2013) [29] observed that for deciduous $C_3$ species such as *C. americana,* the δD of *n*-alkanes will only reflect the environment at the time of wax synthesis. This interpretation was supported by *n*-alkane concentration, ACL, and δD data. Our data for angiosperms shows that during leaf flush, *n*-alkane concentrations peak, indicating maximum production. After several weeks, concentrations decrease to a stable value. ACL and δD of the *n*-alkanes follow a similar pattern. However, distinct trends in *n*-alkane δD for different plant species and approximately constant groundwater δD show that plants from the same functional group may be located adjacent each other yet show distinct temporal patterns. These data are most plausibly explained by differences in individual

plant stomatal regulation in response to environmental variability throughout the growing season. Such variability requires records that integrate heterogeneity between plants in order to properly constrain the ecosystem-level geochemical signals, which can be provided by fluvial sediments.

## 3.5.0 CONCLUSIONS

We sampled leaves from four co-occurring plant species in the Fenton River catchment in Storrs, CT throughout the 2013 growing season to evaluate controls on the δD of individual plant *n*-alkanes for different plant functional types (*P. strobus, T. canadensis, P. arundinacea,* and *C. americana*). We specifically selected plants that were closely associated in space and had roots directly in the river water to evaluate how well these organic proxies reflect ambient water in the environment. River water and sediment samples were collected concurrently with the plant specimens. Our data show distinct timescales of wax synthesis and growth, and temporal shifts in $\varepsilon_{n\text{-alkane}}$. The deciduous angiosperm *C. americana* appears to show dominant wax production during leaf flush, followed by minimal change throughout the remainder of the growing season. *P. strobus, T. canadensis,* and *P. arundinacea* all show signs of continual leaf wax synthesis but distinct patterns of hydrogen isotopes.

The ε values for our plants change significantly throughout the season, with the exception of *T. canadensis*. Observed changes are far larger than the change in river/groundwater δD and indicate strong control of factors such as stomatal regulation, biosynthesis, or timescales of wax synthesis. Proximity to groundwater source may also impact apparent fractionation, as measured ε values in this study are larger than studies from upland sites (with the exception of *T. canadensis*) [5,22,29,31,47,56–58]. Sediments integrate

biomass from different plant types and possibly represent a weighted ecosystem average of *n*-alkanes. Given the heterogeneity between plants in our study that share a close proximity to the stream edge, our data indicates that the temporal and spatial integration provided by fluvial sediments produces the best organic molecular archive of ecosystem level paleoenvironment and paleohydrology, though this is likely biased by differences in wax production and timescales of integration.

## 3.6.0 ACKNOWLEDGMENTS

We thank Kellyn Patros and Jaclyn White for their help collecting and processing samples. In addition, we thank Robert Capers for his assistance with plant identification. Financial support for this project was provided by NSF-EAR-1338256. The authors thank C. Ponton, A. Sessions, and two anonymous reviewers for their helpful feedback throughout the review process.

## 3.7.0 REFERENCES


(1) Barthlott, W.; Neinhuis, C. *Planta* **1997**, *202* (1), 1–8.

(2) Barbour, M. M.; Schurr, U.; Henry, B. K.; Wong, S. C.; Farquhar, G. D. *Plant Physiol.* **2000**, *123* (2), 671–680.

(3) Barbour, M. M.; Roden, J. S.; Farquhar, G. D.; Ehleringer, J. R. *Oecologia* **2004**, *138* (3), 426–435.

(4) Jetter, R.; Kunst, L.; Samuels, A. L. *Annu. Plant Rev.* **2007**, *23*, 145–181.

(5) Sachse, D.; Radke, J.; Gleixner, G. *Org. Geochem.* **2006**, *37* (4), 469–483.

(6) Nichols, J.; Booth, R. K.; Jackson, S. T.; Pendall, E. G.; Huang, Y. *Geochim. Cosmochim. Acta* **2010**, *74* (4), 1407–1416.

(7) Schimmelmann, A.; Lewan, M. D.; Wintsch, R. P. *Geochim. Cosmochim. Acta* **1999**, *63* (22), 3751–3766.

(8) Tipple, B. J.; Pagani, M. *Earth Planet. Sci. Lett.* **2010**, *299* (1–2), 250–262.

(9) Tipple, B. J.; Pagani, M.; Krishnan, S.; Dirghangi, S. S.; Galeotti, S.; Agnini, C.; Giusberti, L.; Rio, D. *Earth Planet. Sci. Lett.* **2011**, *311* (1–2), 82–92.

(10) Sachse, D.; Billault, I.; Bowen, G. J.; Chikaraishi, Y.; Dawson, T. E.; Feakins, S. J.; Freeman, K. H.; Magill, C. R.; McInerney, F. A.; van der Meer, M. T. J.; Polissar, P.; Robins, R. J.; Sachs, J. P.; Schmidt, H.-L.; Sessions, A. L.; White, J. W. C.; West, J. B.; Kahmen, A. *Annu. Rev. Earth Planet. Sci.* **2012**, *40*, 221–249.

(11) Zhuang, G.; Brandon, M. T.; Pagani, M.; Krishnan, S. *Earth Planet. Sci. Lett.* **2014**, *390*, 186–198.

(12) Polissar, P. J.; Freeman, K. H.; Rowley, D. B.; McInerney, F. A.; Currie, B. S. *Earth Planet. Sci. Lett.* **2009**, *287* (1–2), 64–76.

(13) Hren, M. T.; Pagani, M.; Erwin, D. M.; Brandon, M. *Geology* **2010**, *38* (1), 7–10.

(14) Schefuß, E.; Schouten, S.; Schneider, R. R. *Nature* **2005**, *437* (7061), 1003–1006.

(15) Pagani, M.; Pedentchouk, N.; Huber, M.; Sluijs, A.; Schouten, S.; Brinkhuis, H.; Damsté, J. S. S.; Dickens, G. R. *Nature* **2006**, *442* (7103), 671–675.

(16) Jacob, J.; Huang, Y.; Disnar, J. R.; Sifeddine, A.; Boussafir, M.; Spadano Albuquerque, A. L.; Turcq, B. *Quat. Sci. Rev.* **2007**, *26* (7–8), 1004–1015.

(17) Douglas, P. M. J.; Pagani, M.; Brenner, M.; Hodell, D. A.; Curtis, J. H. *Geochim. Cosmochim. Acta* **2012**, *97*, 24–45.

(18) Eley, Y.; Dawson, L.; Black, S.; Andrews, J.; Pedentchouk, N. *Geochim. Cosmochim. Acta* **2014**, *128*, 13–28.

(19) Sauer, P. E.; Eglinton, T. I.; Hayes, J. M.; Schimmelmann, A.; Sessions, A. L. *Geochim. Cosmochim. Acta* **2001**, *65* (2), 213–222.

(20) Voelker, S. L.; Meinzer, F. C.; Lachenbruch, B.; Brooks, J. R.; Guyette, R. P. *Plant, Cell Environ.* **2014**, *37* (3), 766–779.

(21) Lockheart, M. J.; Poole, I.; Van Bergen, P. F.; Evershed, R. P. *Org. Geochem.* **1998**, *29* (4), 1003–1008.

(22) Chikaraishi, Y.; Naraoka, H. *Phytochemistry* **2003**, *63* (3), 361–371.

(23) Chikaraishi, Y.; Naraoka, H.; Poulson, S. R. *Phytochemistry* **2004**, *65* (10), 1369–1381.

(24) Hou, J.; D'Andrea, W. J.; Huang, Y. *Geochim. Cosmochim. Acta* **2008**, *72* (14), 3503–3517.

(25) Yang, H.; Liu, W. G.; Leng, Q.; Hren, M. T.; Pagani, M. *Org. Geochem.* **2011**, *42*, 283–288.

(26) Sessions, A. L.; Burgoyne, T.; Schimmelmann, A.; Hayes, J. M. *Org. Geochem.* **1999**, *30*, 1193–1200.

(27) Feakins, S. J.; Sessions, A. L. *Org. Geochem.* **2010**, *41* (12), 1269–1276.

(28) Kahmen, A.; Hoffmann, B.; Schefuß, E.; Arndt, S. K.; Cernusak, L. A.; West, J. B.; Sachse, D. *Geochim. Cosmochim. Acta* **2013**, *111*, 50–63.

(29) Tipple, B. J.; Berke, M. A; Doman, C. E.; Khachaturyan, S.; Ehleringer, J. R. *Proc. Natl. Acad. Sci. U. S. A.* **2013**, *110* (7), 2659–2664.

(30) Gao, L.; Edwards, E. J.; Zeng, Y.; Huang, Y. *PLoS One* **2014**, *9* (11).

(31) Smith, F. A.; Freeman, K. H. *Geochim. Cosmochim. Acta* **2006**, *70* (5), 1172–1187.

(32) Sachse, D.; Gleixner, G.; Wilkes, H.; Kahmen, A. *Geochim. Cosmochim. Acta* **2010**, *74* (23), 6741–6750.

(33) Gao, L.; Zheng, M.; Fraser, M.; Huang, Y. *Geochemistry, Geophys. Geosystems* **2014**, *15* (2), 361–373.

(34) Bowen, G. J.; Revenaugh, J. *Water Resour. Res.* **2003**, *39* (10), 1–13.

(35) Bowen, G. J. The Online Isotopes in Precipitation Calculator.

(36) Coplen, T. B. *Rapid Commun. Mass Spectrom.* **2011**, *25*, 2538–2560.

(37) Dodd, R.; Proveda, M. *Biochem. Syst. Ecol.* **2003**, No. 31, 1257–1270.

(38) Rommerskirchen, F.; Eglinton, G.; Dupont, L.; Guntner, U.; Wenzel, C.; Rullkotter, J. *Geochemistry, Geophys. Geosystems* **2003**, *4*.

(39) Dawson, T. E.; Ehleringer, J. R. *Nature*. 1991, 335–337.

(40) Yao, Y.; Liu, W. *J. Arid Land* **2014**, *6* (5), 592–600.

(41) Ellsworth, P. Z.; Williams, D. G. *Plant Soil* **2007**, *291* (1–2), 93–107.

(42) Zweifel, R.; Steppe, K.; Sterck, F. J. *J. Exp. Bot.* **2007**, *58* (8), 2113–2131.

(43) Kahmen, A.; Dawson, T. E.; Vieth, A.; Sachse, D. *Plant, Cell Environ.* **2011**, *34* (10), 1639–1651.

(44) Guenther, F.; Aichner, B.; Siegwolf, R.; Xu, B.; Yao, T.; Gleixner, G. *Quat. Int.* **2013**, *313–314*, 3–16.

(45) Hou, J.; D'Andrea, W. J.; MacDonald, D.; Huang, Y. *Org. Geochem.* **2007**, *38* (8), 1251–1255.

(46) Liu, W.; Yang, H. *Glob. Chang. Biol.* **2008**, *14*, 2166–2177.

(47) Pedentchouk, N.; Sumner, W.; Tipple, B.; Pagani, M. *Org. Geochem.* **2008**, *39* (8), 1066–1071.

(48) Diefendorf, A. F.; Freeman, K. H.; Wing, S. L.; Graham, H. V. *Geochim. Cosmochim. Acta* **2011**, *75* (23), 7472–7485.

(49) Gao, L.; Burnier, A.; Huang, Y. *Rapid Commun. Mass Spectrom.* **2012**, *26* (2), 115–122.

(50) McInerney, F. A.; Helliker, B. R.; Freeman, K. H. *Geochim. Cosmochim. Acta* **2011**, *75*, 541–554.

(51) Garcin, Y.; Schefuß, E.; Schwab, V. F.; Garreta, V.; Gleixner, G.; Vincens, A.; Todou, G.; Séné, O.; Onana, J. M.; Achoundong, G.; Sachse, D. *Geochim. Cosmochim. Acta* **2014**, *142*, 482–500.

(52) Rosado, B. H. P.; de Mattos, E. A.; Sternberg, L. da S. L. *An. Acad. Bras. Cienc.* **2013**, *85* (3), 1035–1045.

(53) Wang, Y. V.; Larsen, T.; Leduc, G.; Andersen, N.; Blanz, T.; Schneider, R. R. *Geochim. Cosmochim. Acta* **2013**, *111*, 128–139.

(54) Sachse, D.; Radke, J.; Gleixner, G. *Geochim. Cosmochim. Acta* **2004**, *68* (23), 4877–4889.

(55) Polissar, P. J.; Freeman, K. H. *Geochim. Cosmochim. Acta* **2010**, No. 74, 5785–5797.

(56) Bi, X.; Sheng, G.; Liu, X.; Li, C.; Fu, J. *Org. Geochem.* **2005**, *36* (10), 1405–1417.

(57) Liu, W.; Yang, H.; Li, L. *Oecologia* **2006**, *150*, 330–338.

(58) Hou, J.; D'Andrea, W. J.; MacDonald, D.; Huang, Y. *Org. Geochem.* **2007**, *38* (6), 977–984.

(59) Sachse, D.; Kahmen, A.; Gleixner, G. *Org. Geochem.* **2009**, *40* (6), 732–742.

## 3.8.0 SUPPLEMENTARY DATA

The Fenton River catchment is a sub-regional basin of the greater Thames River basin in the eastern portion of Connecticut. The sampling site is located Mansfield Connecticut, but the river itself crosses through Mansfield, Chaplin, Willington, Ashford and Union CT [1]. The Fenton River was chosen for this project because it is contained in a minimally altered landscape, since existing land use can affect water quality. The term "minimally altered" means that the majority of the land located within the watershed is undeveloped woodlands (Supplementary Figure 3.15). According to the Connecticut Department of Energy and Environmental Protection [1], 74 % of the Fenton River Watershed is forested, with only 14% urban land use [1].

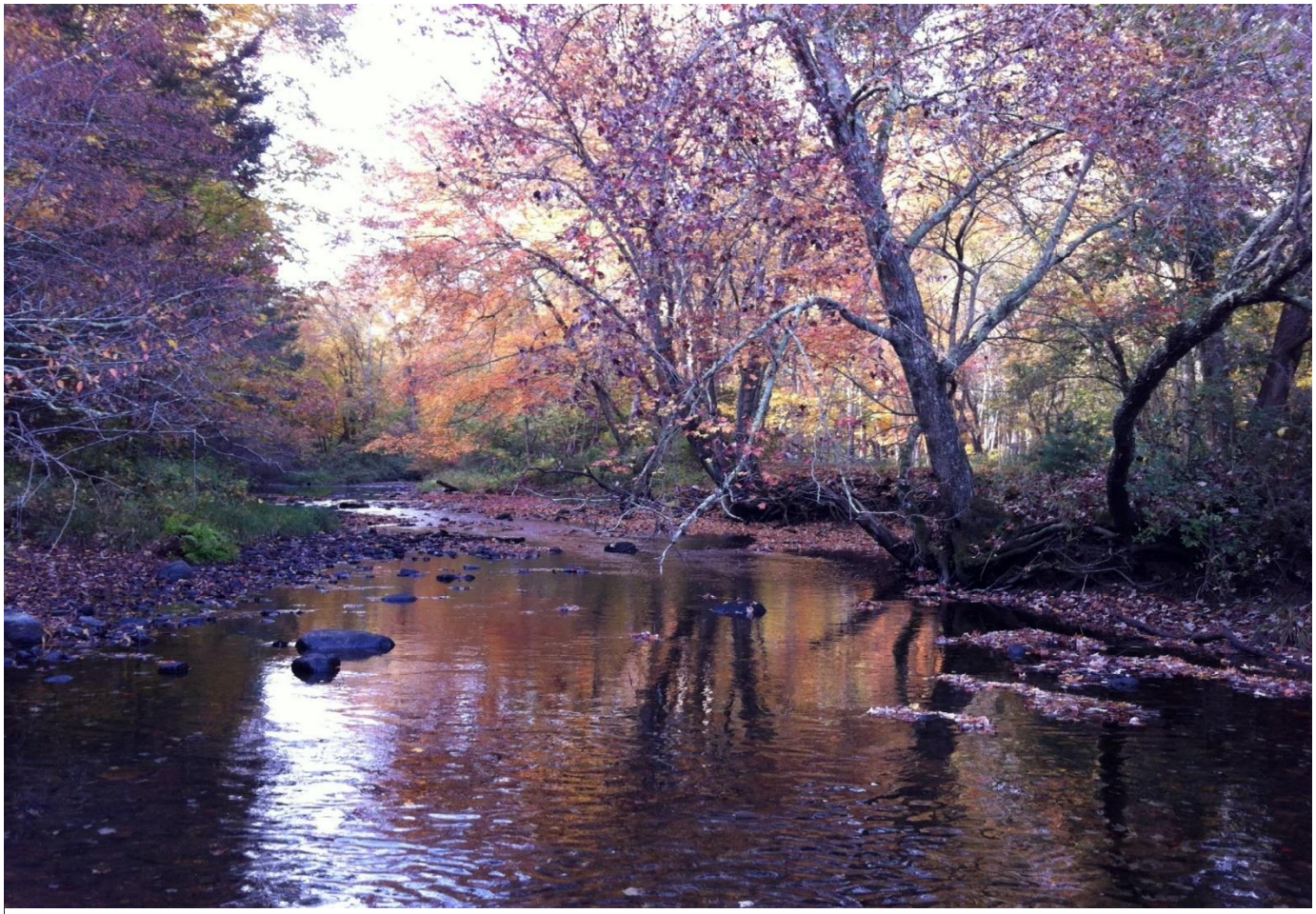

Supplementary Figure 3.15 Image of the Fenton River sampling site 41° 49.537 N, 72° 14.222 W

Supplementary Table 3.3 Climate data from April 2013 to October 2013 at the Fenton River sampling location

Temperature, precipitation, and humidity are weekly averages of local climate measurements

| Day # | Ave. Temp. ($^0$C)[a] | Ave. Precip. (cm)[a] | Ave. Humid. (%)[a] | Day # | Evapotrans. (cm)[b] |
|---|---|---|---|---|---|
| 60 | 2.7 | 0.10 | 58.7 | 15 | 0.99 |
| 67 | 4.7 | 7.29 | 58.4 | 44 | 1.55 |
| 74 | 0.6 | 0.00 | 42.0 | 74 | 3.33 |
| 81 | 3.2 | 0.00 | 51.0 | 105 | 5.79 |
| 88 | 5.8 | 2.62 | 57.6 | 135 | 9.04 |
| 95 | 11.1 | 0.76 | 59.0 | 165 | 10.21 |
| 102 | 9.3 | 1.52 | 48.7 | 195 | 11.30 |
| 109 | 10.4 | 0.81 | 54.3 | 225 | 9.50 |
| 116 | 11.1 | 0.00 | 46.4 | 255 | 6.40 |
| 122 | 11.1 | 0.56 | 52.4 | 285 | 3.91 |
| 129 | 13.8 | 0.56 | 52.4 | 315 | 1.83 |
| 136 | 13.3 | 1.32 | 61.9 | 345 | 1.04 |
| 143 | 18.2 | 1.70 | 65.9 | | |
| 150 | 14.4 | 5.44 | 59.0 | | |
| 157 | 21.2 | 2.03 | 59.3 | | |
| 164 | 18.6 | 15.67 | 64.4 | | |
| 171 | 19.4 | 7.85 | 59.7 | | |
| 178 | 23.5 | 0.46 | 59.1 | | |
| 185 | 24.4 | 2.01 | 72.4 | | |
| 192 | 26.8 | 2.49 | 67.0 | | |
| 199 | 26.1 | 0.94 | 65.3 | | |
| 206 | 27.7 | 3.66 | 63.1 | | |
| 213 | 21.7 | 1.35 | 70.9 | | |
| 220 | 20.7 | 2.08 | 63.3 | | |
| 227 | 21.2 | 3.28 | 60.6 | | |
| 234 | 21.1 | 0.03 | 67.4 | | |
| 241 | 22.2 | 4.75 | 63.6 | | |
| 248 | 22.4 | 0.69 | 69.7 | | |
| 255 | 19.8 | 0.69 | 60.0 | | |
| 262 | 15.6 | 1.70 | 68.4 | | |
| 269 | 16.2 | 3.12 | 67.7 | | |
| 276 | 15.8 | 0.00 | 69.7 | | |
| 283 | 17.7 | 1.96 | 70.6 | | |
| 290 | 13.7 | 0.00 | 67.6 | | |
| 297 | 11.5 | 0.15 | 72.1 | | |
| 304 | 7.1 | 0.00 | 52.4 | | |

[a] http://www.ct.gov/caes/cwp/view.asp?a=2831&q=520212

[b] Monthly average of evapotranspiration measured from 1975 to 2004 in the city of Hartford.

Supplementary Table 3.4 Calculated concentrations, CPI, ACL, and AHPCL of *n*-alkanes $C_{23}$ to $C_{33}$ for *P. strobus*, *T. canadensis*, *P. arundinacea*, *C. americana*, and collected sediment samples.

| ng/g dry material | | | | | | | | | | | | | | | | |
|---|---|---|---|---|---|---|---|---|---|---|---|---|---|---|---|---|
| Day | Sample | $C_{n\,23}$ | $C_{n\,24}$ | $C_{n\,25}$ | $C_{n\,26}$ | $C_{n\,27}$ | $C_{n\,28}$ | $C_{n\,29}$ | $C_{n\,30}$ | $C_{n\,31}$ | $C_{n\,32}$ | $C_{n\,33}$ | CPI | ACL | AHPCL | $C_{n\,23\text{-}33}$ |
| *Pinus strobus* | | | | | | | | | | | | | | | | |
| 113 | fen-1-a13 | 353 | - | 61 | - | - | - | 278 | - | 282 | - | 65 | 5.9 | 29.5 | 29.6 | 1037 |
| 116 | fen-2-a13 | - | - | - | - | - | - | - | - | - | - | - | 3.2 | 29.1 | 29.8 | |
| 123 | fen-3-a13 | 364 | | 94 | - | 42 | - | 840 | 14 | 1120 | - | 1009 | 7.7 | 30.5 | 29.9 | 4416 |
| 130 | fen-4-a13 | - | 91 | - | 1 | - | 420 | - | 580 | - | 303 | - | 6.7 | 30.0 | 29.8 | 1799 |
| 137 | fen-5-a13 | 223 | - | 22 | - | - | - | 185 | - | 294 | - | 106 | 5.6 | 29.8 | 29.8 | 2297 |
| 151 | fen-7-a13 | 188 | - | - | - | - | - | 581 | - | 1773 | 34 | 1728 | 6.8 | 31.2 | 30.3 | 5055 |
| 158 | fen-8-a13 | 1393 | - | 274 | - | 79 | - | 1071 | 47 | 2107 | 42 | 1804 | 8.4 | 30.6 | 30.0 | 7635 |
| 165 | fen-9-a13 | 3226 | 43 | 544 | - | 178 | - | 1062 | 36 | 1510 | - | 1058 | 7.1 | 29.9 | 29.8 | 8202 |
| 172 | fen-10-a13 | 3700 | 52 | 704 | - | 411 | - | 1553 | 189 | 2523 | 93 | 1692 | 7.0 | 30.0 | 29.8 | 11535 |
| 179 | fen-11-a13 | 1995 | - | 363 | - | 161 | - | 1099 | 35 | 1760 | 12 | 1421 | 9.3 | 30.3 | 29.9 | 7153 |
| 186 | fen-12-a13 | 6991 | - | 1325 | - | 494 | - | 1905 | - | 808 | - | - | 7.9 | 28.0 | 29.1 | 11522 |
| 207 | fen-13-a13 | - | 81 | - | 2072 | 478 | 42201 | 3996 | 41743 | 2177 | 4783 | - | 10.6 | 30.0 | 29.9 | 97999 |
| 217 | fen-14-a13 | 4314 | 115 | 1396 | - | 756 | - | 1376 | 23 | 1121 | - | 374 | 9.7 | 28.8 | 29.3 | 9715 |
| 225 | fen-15-a13 | 48330 | 3455 | 18527 | 845 | 13197 | 1094 | 29300 | 1913 | 26911 | 1160 | 12753 | 11.5 | 29.0 | 29.3 | 165523 |
| 232 | fen-16-a13 | 459 | - | 99 | - | 27 | - | 244 | - | 337 | - | - | 13.4 | 28.8 | 29.7 | 1166 |
| 247 | fen-17-a13 | 2175 | 90 | 782 | - | 516 | - | 1280 | 41 | 1240 | - | - | 9.8 | 28.5 | 29.4 | 6518 |
| 256 | fen-18-a13 | 1885 | - | 428 | - | 129 | - | 1289 | - | 911 | - | 180 | 18.9 | 29.1 | 29.4 | 5942 |
| 262 | fen-19-a13 | 616 | - | 142 | - | 55 | - | 303 | - | 198 | - | 2 | 11.9 | 28.8 | 29.3 | 1315 |
| 269 | fen-20-a13 | 616 | - | - | - | | - | 454 | - | 345 | - | - | 16.3 | 29.0 | 29.7 | 1420 |
| 276 | fen-21-a13 | 1505 | 54 | 620 | - | 603 | 3 | 959 | 27 | 854 | - | - | 8.0 | 28.3 | 29.2 | 4981 |
| 284 | fen-22-a13 | 1715 | 28 | 582 | - | 349 | - | 1080 | - | 787 | - | - | 15.8 | 28.4 | 29.3 | 5093 |
| 291 | fen-23-a13 | 1527 | - | 473 | - | 320 | - | 1098 | - | 960 | - | - | 19.4 | 28.6 | 29.5 | 5342 |
| *Tsuga canadensis* | | | | | | | | | | | | | | | | |
| 113 | fen-1-b13 | 60 | - | - | - | 1 | - | 560 | - | 795 | - | - | 4.8 | 29.4 | 29.8 | 3489 |
| 116 | fen-2-b13 | 102 | - | 96 | - | 78 | 75 | 355 | - | 247 | - | - | 3.3 | 28.9 | 30.1 | 953 |
| 123 | fen-3-b13 | 200 | - | 61 | - | 92 | 8 | 389 | 14 | 431 | - | - | 6.0 | 29.2 | 29.6 | 1214 |
| 130 | fen-4-b13 | 526 | 34 | 367 | 94 | 493 | 283 | 1404 | 253 | 1423 | - | 168 | 4.2 | 29.2 | 29.5 | 5684 |
| 137 | fen-5-b13 | 205 | 9 | 474 | 20 | 195 | 78 | 472 | 74 | 443 | - | 30 | 4.5 | 28.3 | 29.4 | 2000 |
| 151 | fen-7-b13 | 10407 | 12 | 1148 | - | 66 | - | 709 | - | 880 | - | 10 | 10.4 | 28.3 | 29.6 | 15253 |
| 158 | fen-8-b13 | 8242 | - | 936 | - | - | - | 498 | - | 880 | - | - | 8.6 | 28.5 | 29.7 | 12219 |
| 165 | fen-9-b13 | 1903 | - | 218 | 747 | - | - | 1792 | - | 570 | - | - | 3.0 | 28.8 | 29.4 | 5664 |
| 172 | fen-10-b13 | 2188 | 130 | 2102 | 412 | 1977 | 1451 | 5914 | 1282 | 6360 | 36 | 941 | 4.2 | 29.2 | 29.6 | 24026 |
| 179 | fen-11-b13 | 281 | - | 166 | - | 269 | - | 1554 | 54 | 1855 | - | 209 | 5.7 | 28.8 | 29.5 | 5950 |
| 186 | fen-12-b13 | 882 | - | 394 | - | 406 | 96 | 1382 | 97 | 1315 | - | - | 4.5 | 29.0 | 29.5 | 5900 |
| 207 | fen-13-b13 | 794 | - | 270 | - | 535 | 188 | 1574 | 163 | 1336 | - | - | 5.4 | 29.4 | 29.5 | 5903 |
| 217 | fen-14-b13 | 6823 | 1526 | 6163 | 1462 | 8332 | 4656 | 22011 | 4670 | 19381 | 271 | 1442 | 4.6 | 29.1 | 29.4 | 101761 |
| 225 | fen-15-b13 | 867 | 49 | 595 | 178 | 1178 | 787 | 4447 | 987 | 5382 | 46 | 886 | 4.7 | 28.3 | 29.7 | 17457 |
| 232 | fen-16-b13 | 563 | - | 97 | - | 373 | - | 1727 | 52 | 1830 | - | 139 | 4.4 | 29.3 | 30.0 | 5856 |
| 247 | fen-17-b13 | 1269 | 15 | 760 | 36 | 1211 | 360 | 2756 | 254 | 1857 | - | - | 5.2 | 28.6 | 29.2 | 9058 |
| 262 | fen-19-b13 | 927 | - | 291 | - | 296 | 48 | 914 | - | 502 | - | - | 3.6 | 28.4 | 29.2 | 3125 |
| 269 | fen-20-b13 | 3893 | 196 | 1253 | - | 943 | - | 3266 | 345 | 4966 | 216 | 3919 | 8.9 | 29.1 | 29.8 | 23463 |
| 276 | fen-21-b13 | 745 | - | 265 | - | 551 | 212 | 1677 | 144 | 1213 | - | - | 4.0 | 28.9 | 29.3 | 5872 |
| 284 | fen-22-b13 | 599 | 45 | 525 | 197 | 926 | 613 | 2393 | 381 | 1526 | - | - | 3.0 | 28.7 | 29.2 | 8351 |
| 291 | fen-23-b13 | 14048 | 1665 | 6002 | 1855 | 11341 | 2899 | 22483 | 2530 | 17527 | 219 | 2849 | 6.6 | 29.0 | 29.2 | 110982 |
| *Phalaris arundinacea* | | | | | | | | | | | | | | | | |
| 113 | fen-1-d13 | - | - | 1656 | - | 3873 | - | 4864 | - | 2693 | - | - | 21.2 | 28.3 | 28.8 | 15241 |
| 116 | fen-2-d13 | 8957 | 896 | 124830 | 19006 | - | 42987 | 741486 | 8773 | 145108 | - | - | 13.4 | 28.8 | 29.3 | 1092376 |
| 123 | fen-3-d13 | - | - | 1053 | 60 | 3022 | - | 4002 | - | 1629 | - | 459 | 31.3 | 28.5 | 28.7 | 10277 |
| 130 | fen-4-d13 | 1169 | - | 13955 | - | 72991 | 8103 | 195943 | 3007 | 76778 | 124 | - | 26.0 | 28.9 | 29.0 | 372913 |
| 137 | fen-5-d13 | 284 | 153 | 12964 | 809 | 42545 | 1979 | 62117 | - | 17461 | - | - | 21.0 | 28.2 | 28.6 | 188463 |
| 151 | fen-7-d13 | 29368 | 1876 | 22456 | 709 | 15218 | 1418 | 297 | 936 | 3611 | 681 | - | 7.6 | 26.3 | 27.8 | 78533 |
| 158 | fen-8-d13 | 4772 | 649 | 22032 | 387 | 13977 | 831 | 15458 | 411 | 6846 | - | - | 17.4 | 27.0 | 28.4 | 66732 |
| 165 | fen-9-d13 | 3568 | 868 | 18915 | 1291 | 25787 | 988 | 17481 | 221 | 2917 | - | 707 | 20.2 | 27.2 | 28.0 | 74566 |
| 172 | fen-10-d13 | 352 | 141 | 2330 | 243 | 2564 | 120 | 1618 | - | 224 | - | - | 11.2 | 27.0 | 28.0 | 8474 |
| 179 | fen-11-d13 | 425 | 177 | 3250 | 396 | 4889 | 301 | 5001 | - | 849 | - | 121 | 13.5 | 27.6 | 28.3 | 15928 |
| 186 | fen-12-d13 | 709 | 77 | 2936 | 220 | 4992 | 213 | 6671 | - | 1128 | - | 185 | 21.9 | 27.9 | 28.4 | 18622 |
| 207 | fen-13-d13 | 969 | 194 | 3625 | 349 | 5232 | 364 | 6927 | - | 954 | - | - | 15.2 | 27.6 | 28.4 | 20699 |
| 217 | fen-14-d13 | 167 | - | 1216 | 104 | 2942 | 156 | 5848 | - | 1239 | - | 323 | 19.7 | 28.4 | 28.7 | 12150 |
| 225 | fen-15-d13 | 1339 | 650 | 19041 | 1451 | 17501 | 1515 | 30194 | 357 | 3049 | - | - | 17.4 | 27.5 | 28.4 | 76633 |
| 232 | fen-16-d13 | 756 | 1237 | 5166 | 2035 | 10538 | 1434 | 11309 | - | 1556 | - | - | 5.9 | 27.7 | 28.3 | 34030 |
| 247 | fen-17-d13 | 725 | - | 3418 | - | 12803 | 498 | 34230 | 292 | 39786 | - | 6224 | 25.1 | 29.3 | 29.4 | 98463 |
| 256 | fen-18-d13 | 781 | 402 | 3091 | 459 | 4794 | 344 | 5894 | - | 872 | - | - | 15.4 | 28.5 | 28.9 | 18364 |
| 262 | fen-19-d13 | 804 | 279 | 4965 | 609 | 9789 | 507 | 10517 | - | 1111 | - | - | 13.8 | 27.6 | 28.2 | 30072 |
| 269 | fen-20-d13 | 554 | 301 | 2924 | 558 | 4887 | 603 | 5433 | 60 | 909 | 1095 | 68 | 4.9 | 27.7 | 28.3 | 18425 |
| 276 | fen-21-d13 | 737 | 697 | 5321 | 1141 | 9164 | 787 | 8117 | 9 | 1094 | - | 112 | 8.5 | 27.5 | 28.1 | 28563 |
| 284 | fen-22-d13 | 282 | 167 | 2244 | 272 | 2994 | 187 | 2551 | - | 299 | - | - | 9.7 | 27.3 | 28.1 | 9625 |

| | | | | | | | | | | | | | | | |
|---|---|---|---|---|---|---|---|---|---|---|---|---|---|---|---|
| *Corylus americana* | | | | | | | | | | | | | | | |
| 113 | fen-1-f13 | 45548 | 5269 | 47454 | 37959 | 625259 | 115497 | 475525 | 10957 | - | - | - | 9.2 | 30.2 | 30.0 | 1363467 |
| 116 | fen-2-f13 | 31989 | 6853 | 245796 | 2207 | 378484 | 15210 | 3373450 | 11389 | 68917 | - | - | 51.9 | 28.6 | 28.8 | 4134295 |
| 123 | fen-3-f13 | 7894 | 1171 | 97866 | - | 113983 | 5489 | 772235 | 2208 | 23847 | - | - | 44.2 | 28.4 | 28.8 | 1024692 |
| 130 | fen-4-f13 | 5423 | 2390 | - | 2282 | 68060 | 6246 | - | 6359 | 49853 | - | - | 27.5 | 28.6 | 28.9 | 140612 |
| 137 | fen-5-f13 | 1563 | - | 26224 | - | 19200 | 171 | 95038 | - | 23277 | - | - | 21.5 | 28.4 | 29.1 | 165473 |
| 144 | fen-6-f13 | - | - | 9131 | - | 25080 | 3315 | 234130 | 13253 | 196530 | 4788 | - | 14.2 | 29.6 | 29.7 | 486226 |
| 151 | fen-7-f13 | 208 | - | 1880 | - | 2407 | 323 | 17665 | 1068 | 10601 | 147 | - | 11.6 | 29.2 | 29.5 | 34298 |
| 158 | fen-8-f13 | 334 | - | 1774 | - | 3581 | 902 | 28744 | 2380 | 30311 | - | - | 16.7 | 29.7 | 29.8 | 68025 |
| 165 | fen-9-f13 | - | 6361 | - | 15499 | 2233 | 141692 | 6877 | 87420 | 525 | - | - | 14.3 | 29.4 | 29.6 | 261171 |
| 172 | fen-10-f13 | - | - | 1962 | - | 18443 | 5043 | 225653 | 21298 | 233492 | - | - | 14.8 | 29.8 | 29.9 | 505891 |
| 179 | fen-11-f13 | - | - | 5866 | - | 40256 | 13189 | 522018 | 48813 | 506994 | 34220 | 96872 | 11.5 | 30.1 | 29.9 | 1268227 |
| 186 | fen-12-f13 | 8 | - | 1052 | - | 12193 | 5062 | 244860 | 18245 | 207065 | 11080 | - | 12.1 | 29.8 | 29.8 | 499565 |
| 207 | fen-13-f13 | 258 | - | 151 | - | 899 | 319 | 16137 | 1798 | 17717 | 1025 | - | 9.8 | 29.9 | 30.0 | 38767 |
| 217 | fen-14-f13 | - | - | 427 | - | 8133 | 3766 | 303737 | 25991 | - | 17873 | - | 9.3 | 30.3 | 30.1 | 359926 |
| 225 | fen-15-f13 | 42 | - | 155 | - | 1953 | 698 | 43010 | 4284 | 45893 | 2641 | 7835 | 10.3 | 30.2 | 29.9 | 106510 |
| 232 | fen-16-f13 | 491 | - | 20 | - | 282 | - | 481 | - | 399 | - | - | 6.1 | 28.6 | 29.1 | 1672 |
| 247 | fen-17-f13 | - | - | - | - | - | - | 14761 | - | 15910 | - | - | 11.5 | 30.0 | 29.9 | 30671 |
| 256 | fen-18-f13 | - | - | - | - | - | - | 12635 | - | 14170 | - | - | 10.6 | 30.0 | 29.9 | 26805 |
| 262 | fen-19-f13 | 8259 | 2075 | 8486 | 2232 | 22057 | 11308 | 437632 | 49144 | 501748 | 26954 | 65542 | 10.7 | 30.1 | 30.0 | 1146889 |
| 269 | fen-20-f13 | - | - | - | - | | - | 27565 | 1636 | 37878 | 535 | 3851 | 10.2 | 30.3 | 30.1 | 71466 |
| 276 | fen-21-f13 | - | - | - | - | 1436 | - | 52589 | 1707 | 39874 | 257 | 2913 | 12.3 | 29.8 | 29.8 | 98775 |
| 284 | fen-22-f13 | - | - | 3920 | - | 10957 | - | 26959 | 287 | 19760 | - | - | 18.3 | 28.9 | 29.3 | 61885 |
| 291 | fen-23-f13 | - | - | - | - | 292 | - | 38147 | 1394 | 32324 | - | 818 | 9.7 | 29.9 | 29.8 | 72975 |
| Sediments | | | | | | | | | | | | | | | | |
| 116 | Fen-2 | 239 | 59 | 420 | 50 | 560 | 86 | 3089 | 61 | 1177 | 24 | 174 | 19.3 | 29.0 | 29.3 | 6309 |
| 137 | Fen-5 | 18 | - | 18 | 33 | 30 | - | 148 | - | 67 | 26 | 17 | 3.4 | 29.2 | 29.3 | 368 |
| 151 | Fen-7 | 588 | 116 | 995 | 105 | 1053 | 136 | 6723 | 94 | 2370 | 19 | 334 | 26.6 | 29.0 | 29.3 | 13198 |
| 158 | Fen-8 | 176 | 45 | 239 | 41 | 341 | 54 | 1297 | 49 | 710 | 17 | 129 | 13.3 | 29.1 | 29.3 | 3263 |
| 165 | Fen-9 | 143 | 39 | 164 | 36 | 248 | 40 | 898 | 36 | 531 | 9 | 91 | 11.7 | 29.1 | 29.3 | 2377 |
| 172 | Fen-10 | 65 | 20 | 96 | 19 | 139 | 21 | 399 | 13 | 283 | - | - | 10.9 | 28.9 | 29.3 | 1103 |
| 179 | Fen-11 | 174 | 44 | 286 | 45 | 358 | 39 | 1253 | 29 | 585 | 12 | 92 | 14.9 | 28.9 | 29.2 | 3108 |
| 186 | Fen-12 | 217 | 45 | 248 | 44 | 458 | 63 | 1842 | 43 | 1027 | - | - | 18.5 | 29.0 | 29.3 | 4119 |
| 207 | Fen-13 | 47 | 8 | 48 | 9 | 107 | 13 | 427 | 10 | 258 | - | 65 | 16.0 | 29.4 | 29.4 | 1024 |
| 217 | Fen-14 | 112 | 0 | 146 | 26 | 259 | 40 | 231 | 33 | 89 | - | 42 | 6.5 | 28.1 | 28.4 | 1062 |
| 225 | Fen-15 | 27 | 6 | 27 | 6 | 64 | 10 | 215 | 8 | 156 | 5 | 39 | 8.4 | 29.4 | 29.4 | 588 |
| 232 | Fen-16 | 47 | 9 | 44 | 10 | 109 | 13 | 466 | 9 | 245 | - | 45 | 15.5 | 29.3 | 29.3 | 1028 |
| 247 | Fen-17 | 53 | 10 | 44 | 11 | 94 | 16 | 335 | 13 | 250 | 3 | 68 | 10.6 | 29.5 | 29.4 | 955 |
| 256 | Fen-18 | - | 6 | 40 | 8 | 79 | 11 | - | 12 | 189 | - | 49 | 5.9 | 29.7 | 29.8 | 424 |
| 262 | Fen-19 | 111 | 21 | 114 | 22 | 194 | 34 | 169 | 26 | 443 | - | 36 | 8.6 | 29.2 | 29.6 | 1269 |
| 269 | Fen-20 | 52 | 11 | 52 | 13 | 114 | 19 | 372 | 17 | 297 | - | 82 | 12.2 | 29.5 | 29.5 | 1072 |
| 276 | Fen-21 | 108 | 16 | 136 | 17 | 167 | 22 | 529 | 15 | 327 | 3 | 71 | 13.2 | 29.0 | 29.3 | 1491 |
| 284 | Fen-22 | 89 | 17 | 99 | 16 | 118 | 14 | 336 | 21 | 220 | 4 | 55 | 9.2 | 29.0 | 29.3 | 1060 |
| 291 | Fen-23 | 4 | - | 7 | - | 15 | - | 49 | - | 37 | - | 6 | 9.4 | 29.3 | 29.4 | 119 |

" - " Dash lines indicate peak was below the detection level.

Supplementary Table 3.5 Measured isotope and apparent fractionation values for individual odd numbered *n*-alkanes from $C_{25}$ to $C_{33}$ for *P. strobus*, *T. canadensis*, *P. arundinacea*, *C. americana*, and collected sediment samples

| | | | | | | | | | | |
|---|---|---|---|---|---|---|---|---|---|---|
| *Pinus strobus* | | | | | | | | | | |
| 123 | 5/3/2013 | fen-3-a13 | 1 | - | - | -184 | -183 | -196 | -187 | -147 |
| 130 | 5/10/2013 | fen-4-a13 | 1 | - | - | - | -202 | - | -202 | -162 |
| 137 | 5/17/2013 | fen-5-a13 | 1 | -165 | -150 | -199 | -201 | -202 | -196 | -157 |
| 158 | 6/7/2013 | fen-8-a13 | 1 | - | - | - | -197 | - | -197 | -157 |
| 165 | 6/14/2013 | fen-9-a13 | 2 | -173 | -166 | -194 | -194 | -196 | -191 | -142 |
| 172 | 6/21/2013 | fen-10-a13 | 2 | -157 | | -181 | -199 | -200 | -194 | -148 |
| 179 | 6/28/2013 | fen-11-a13 | 2 | -177 | -184 | -200 | -198 | -206 | -199 | -154 |
| 186 | 7/5/2013 | fen-12-a13 | 1 | -172 | - | -190 | - | - | -190 | -147 |
| 207 | 7/23/2013 | fen-13-a13 | 2 | -185 | -187 | -200 | -190 | - | -191 | -156 |
| 217 | 8/5/2013 | fen-14-a13 | 2 | -186 | -184 | -201 | -202 | -207 | -199 | -160 |
| 225 | 8/13/2013 | fen-15-a13 | 1 | -207 | - | -215 | -220 | - | -217 | -183 |
| 232 | 8/20/2013 | fen-16-a13 | 1 | -210 | -174 | -214 | -210 | -211 | -207 | -168 |
| 247 | 9/4/2013 | fen-17-a13 | 2 | -205 | -191 | -226 | -224 | -233 | -225 | -191 |
| 256 | 9/13/2013 | fen-18-a13 | 1 | -194 | -194 | -206 | -209 | -213 | -205 | -174 |
| 262 | 9/19/2013 | fen-19-a13 | 2 | -198 | -182 | -221 | -223 | -224 | -221 | -185 |
| 276 | 10/3/2013 | fen-21-a13 | 2 | -217 | -225 | -226 | -227 | -231 | -227 | -192 |
| 284 | 10/11/2013 | fen-22-a13 | 2 | -208 | -209 | -227 | -231 | -239 | -227 | -195 |
| 291 | 10/18/2013 | fen-23-a13 | 2 | -203 | -202 | -228 | -230 | -239 | -228 | -194 |
| *Tsuga canadensis* | | | | | | | | | | |
| 123 | 5/3/2013 | fen-3-b13 | 1 | - | - | -169 | -162 | - | -165 | -125 |
| 151 | 5/31/2013 | fen-7-b13 | 1 | -123 | - | - | - | - | - | - |
| 172 | 6/21/2013 | fen-10-b13 | 1 | -197 | -158 | -162 | -166 | - | -163 | -115 |
| 217 | 8/5/2013 | fen-14-b13 | 1 | -208 | -187 | -158 | -153 | -162 | -160 | -120 |
| 225 | 8/13/2013 | fen-15-b13 | 1 | -188 | -184 | -170 | -162 | -165 | -170 | -128 |
| 232 | 8/20/2013 | fen-16-b13 | 1 | -181 | -171 | -151 | -139 | -156 | -148 | -124 |
| 247 | 9/4/2013 | fen-17-b13 | 1 | -202 | -185 | -168 | -163 | -160 | -169 | -131 |
| 262 | 9/19/2013 | fen-19-b13 | 1 | -189 | -177 | -167 | -153 | - | -163 | -138 |
| 269 | 9/26/2013 | fen-20-b13 | 1 | - | - | -185 | -172 | - | -179 | -143 |
| 276 | 10/3/2013 | fen-21-b13 | 1 | -161 | -148 | -148 | -161 | - | -153 | -133 |
| 284 | 10/11/2013 | fen-22-b13 | 1 | -186 | -167 | -148 | -143 | -152 | -149 | -134 |
| 291 | 10/18/2013 | fen-23-b13 | 1 | - | -183 | -163 | -153 | - | -162 | - |

| | | | | | | | | | | |
|---|---|---|---|---|---|---|---|---|---|---|
| *Phalaris arundinacea* | | | | | | | | | | |
| 113 | 4/23/2013 | fen-1-d13 | 1 | -198 | -172 | -169 | -170 | - | -170 | -128 |
| 116 | 4/26/2013 | fen-2-d13 | 1 | -196 | -196 | -187 | -186 | - | -191 | -149 |
| 123 | 5/3/2013 | fen-3-d13 | 2 | -201 | -192 | -181 | -170 | - | -185 | -146 |
| 130 | 5/10/2013 | fen-4-d13 | 1 | -202 | -205 | -207 | -210 | - | -207 | -167 |
| 137 | 5/17/2013 | fen-5-d13 | 1 | -190 | -191 | -185 | -183 | -184 | -187 | -148 |
| 151 | 5/31/2013 | fen-7-d13 | 1 | -193 | -198 | -200 | - | - | -199 | -159 |
| 158 | 6/7/2013 | fen-8-d13 | 1 | -206 | -222 | -210 | -225 | - | -218 | -179 |
| 165 | 6/14/2013 | fen-9-d13 | 2 | -226 | -220 | -215 | -211 | -210 | -216 | -169 |
| 172 | 6/21/2013 | fen-10-d13 | 2 | -227 | -224 | -224 | -212 | -209 | -224 | -180 |
| 179 | 6/28/2013 | fen-11-d13 | 2 | -232 | -228 | -228 | -215 | -190 | -227 | -183 |
| 186 | 7/5/2013 | fen-12-d13 | 1 | -215 | -213 | -211 | -209 | - | -212 | -169 |
| 207 | 7/23/2013 | fen-13-d13 | 2 | -217 | -218 | -223 | -217 | -210 | -221 | -187 |
| 217 | 8/5/2013 | fen-14-d13 | 2 | -228 | -215 | -223 | -211 | -188 | -219 | -181 |
| 225 | 8/13/2013 | fen-15-d13 | 2 | -210 | -214 | -220 | -211 | - | -216 | -182 |
| 232 | 8/20/2013 | fen-16-d13 | 2 | -212 | -207 | -213 | -215 | - | -210 | -172 |
| 247 | 9/4/2013 | fen-17-d13 | 2 | -205 | -220 | -224 | -224 | - | -223 | -189 |
| 256 | 9/13/2013 | fen-18-d13 | 2 | -219 | -220 | -218 | -221 | -212 | -213 | -182 |
| 262 | 9/19/2013 | fen-19-d13 | 2 | -223 | -217 | -219 | -221 | -192 | -218 | -182 |
| 269 | 9/26/2013 | fen-20-d13 | 2 | -229 | -224 | -223 | -223 | - | -223 | -189 |
| 276 | 10/3/2013 | fen-21-d13 | 2 | -234 | -223 | -224 | -220 | - | -223 | -188 |
| 284 | 10/11/2013 | fen-22-d13 | 2 | -211 | -214 | -217 | -189 | - | -215 | -182 |
| *Corylus americana* | | | | | | | | | | |
| 113 | 4/23/2013 | fen-1-f13 | 2 | -184 | -172 | -193 | -208 | - | -182 | -140 |
| 116 | 4/26/2013 | fen-2-f13 | 1 | -158 | -187 | -197 | - | - | -196 | -154 |
| 123 | 5/3/2013 | fen-3-f13 | 1 | -159 | -184 | -190 | - | - | -189 | -149 |
| 130 | 5/10/2013 | fen-4-f13 | 2 | -139 | -175 | -183 | -155 | - | -179 | -138 |
| 137 | 5/17/2013 | fen-5-f13 | 2 | -123 | -145 | -153 | -126 | - | -147 | -106 |
| 144 | 5/24/2013 | fen-6-f13 | 2 | - | - | -146 | -137 | - | -141 | -99 |
| 151 | 5/31/2013 | fen-7-f13 | 2 | -160 | -154 | -144 | -141 | -150 | -144 | -101 |
| 158 | 6/7/2013 | fen-8-f13 | 2 | -161 | -144 | -146 | -144 | -140 | -144 | -103 |
| 165 | 6/14/2013 | fen-9-f13 | 2 | - | -151 | -161 | -159 | -157 | -158 | -110 |
| 172 | 6/21/2013 | fen-10-f13 | 1 | - | -138 | -146 | -143 | -154 | -145 | -96 |
| 179 | 6/28/2013 | fen-11-f13 | 1 | - | -142 | -156 | -154 | -162 | -155 | -109 |
| 186 | 7/5/2013 | fen-12-f13 | 2 | -167 | -164 | -150 | -141 | -143 | -146 | -101 |
| 207 | 7/23/2013 | fen-13-f13 | 2 | - | -159 | -152 | -152 | -157 | -153 | -116 |
| 217 | 8/5/2013 | fen-14-f13 | 2 | - | -146 | -153 | -143 | -152 | -148 | -106 |
| 225 | 8/13/2013 | fen-15-f13 | 2 | - | -151 | -156 | -156 | -157 | -156 | -119 |
| 247 | 9/4/2013 | fen-17-f13 | 2 | - | -161 | -153 | -146 | -149 | -150 | -112 |
| 256 | 9/13/2013 | fen-18-f13 | 1 | - | - | -147 | -142 | -139 | -144 | -105 |
| 262 | 9/19/2013 | fen-19-f13 | 1 | - | - | -157 | -155 | -149 | -156 | -119 |
| 269 | 9/26/2013 | fen-20-f13 | 2 | - | -166 | -160 | -151 | -148 | -154 | -117 |
| 276 | 10/3/2013 | fen-21-f13 | 2 | -193 | -193 | -179 | -157 | -160 | -170 | -133 |
| 284 | 10/11/2013 | fen-22-f13 | 2 | - | -176 | -176 | -163 | -166 | -169 | -134 |
| 291 | 10/18/2013 | fen-23-f13 | 2 | -186 | -207 | -150 | -148 | -157 | -151 | -114 |

| Sediments | | | | | | | | | |
|---|---|---|---|---|---|---|---|---|---|
| 116 | 4/26/2013 | Fen-2 | 2 | -192 | -169 | -177 | -164 | -150 | -170 | -127 |
| 123 | 5/3/2013 | Fen-3 | 1 | -181 | -177 | -181 | -168 | -167 | -174 | -134 |
| 130 | 5/10/2013 | Fen-4 | 2 | -190 | -181 | -183 | -170 | -168 | -178 | -131 |
| 137 | 5/17/2013 | Fen-5 | 2 | -182 | -181 | -183 | -161 | -169 | -174 | -130 |
| 151 | 5/31/2013 | Fen-7 | 2 | -143 | -167 | -177 | -160 | -156 | -168 | -126 |
| 158 | 6/7/2013 | Fen-8 | 2 | -178 | -173 | -178 | -172 | -158 | -174 | -126 |
| 165 | 6/14/2013 | Fen-9 | 3 | - | -160 | -174 | -164 | -146 | -168 | -116 |
| 172 | 6/21/2013 | Fen-10 | 2 | - | -150 | -175 | -152 | -179 | -166 | -111 |
| 179 | 6/28/2013 | Fen-11 | 2 | -190 | -167 | -178 | -165 | -159 | -171 | -118 |
| 186 | 7/5/2013 | Fen-12 | 2 | -215 | -176 | -168 | -158 | -145 | -168 | -119 |
| 207 | 7/23/2013 | Fen-13 | 2 | -147 | -159 | -173 | -155 | -148 | -165 | -128 |
| 217 | 8/5/2013 | Fen-14 | 2 | -162 | -169 | -175 | -162 | -155 | -169 | -130 |
| 225 | 8/13/2013 | Fen-15 | 2 | -172 | -166 | -172 | -160 | -156 | -166 | -124 |
| 232 | 8/20/2013 | Fen-16 | 2 | -144 | -143 | -175 | -157 | -145 | -163 | -124 |
| 247 | 9/4/2013 | Fen-17 | 2 | -164 | -164 | -178 | -165 | -157 | -170 | -134 |
| 256 | 9/13/2013 | Fen-18 | 2 | -178 | -175 | -174 | -162 | -161 | -169 | -134 |
| 262 | 9/19/2013 | Fen-19 | 2 | -178 | -167 | -176 | -162 | -148 | -169 | -128 |
| 269 | 9/26/2013 | Fen-20 | 1 | -170 | -177 | -183 | -167 | -168 | -170 | -127 |
| 276 | 10/3/2013 | Fen-21 | 1 | -192 | -176 | -178 | -162 | - | -173 | -136 |
| 284 | 10/11/2013 | Fen-22 | 1 | -131 | -187 | -177 | -173 | -140 | -178 | -144 |
| 291 | 10/18/2013 | Fen-23 | 1 | -172 | -175 | -176 | -162 | -177 | -170 | -134 |

" - " Dash lines indicate peak was below the detection level.

## 3.9.0 SUPPLEMENTARY REFERENCES

(1) State of Connecticut Department of Energy & Environmental Protection (DEEP) http://www.ct.gov/deep/site/default.asp; Accessed 2/27/2017

# CHAPTER FOUR

# Seasonal variations in leaf wax *n*-alkane δD and $\delta^{13}C$ of four riparian plants: The effect of environmental and physiological factors on measured and modeled plant WUE and isotopic composition

Abigail M. Oakes[a]

Chaoran Wang[a], Joseph D. White[b], Michael T. Hren[a,c,*]

[a] *Department of Chemistry, 55 N. Eagleville Rd., University of Connecticut, Storrs CT 06269, USA*

[b] *Department of Biology, Baylor University, One Bear Place #97388, Waco TX 76798-7388, USA*

[c] *Center for Integrative Geosciences, 345 Mansfield Rd., University of Connecticut, Storrs CT 06269, USA*

## 4.1.0 ABSTRACT

Carbon and hydrogen isotopes of normal alkanes (*n*-alkanes) in modern plants and sediments provide a record of biochemical processes and responses to environmental factors. We analyzed leaf wax *n*-alkanes of three riparian gymnosperm trees (*Pinus strobus*, *Tsuga canadensis* in the sun, *Tsuga canadensis* in the shade) and two angiosperm plants (*Corylus americana*, *Phalaris arundinacea*) to examine the controls of C and H isotope fractionation in plant-derived *n*-alkanes over a growing season. Weighted *n*-alkane $\delta^{13}C$ of gymnosperm species are generally isotopically-enriched ($\delta^{13}C_{nC27\text{-}33} > -35$ ‰) compared to angiosperms ($\delta^{13}C_{nC27\text{-}33} < -35$ ‰), but all plants show significant isotopic variability throughout a growing season. Temporal variations in *n*-alkane $\delta^{13}C$ for all four species are associated with distinct mean summer *n*-alkane δD (*P. strobus* ~ –210 ‰, *T. canadensis* ~ –160 ‰, and –170 to –220 ‰ for *C. americana* and *P. arundinacea,* respectively). To evaluate controls of C and H isotope variability, we measured stomatal parameters to quantify $CO_2$ assimilation rates and water use efficiency (WUE). These are coupled with simulated leaf $\delta^{13}C_{nC27\text{-}33}$ and WUE for each species using stomatal morphological parameters, daily season climate information from a nearby climate station, and the BIOME-BGC model. Our data show: 1) clear differences in $CO_2$ assimilation rates of gymnosperms (above 1.5 $\mu mol*m^{-2}s^{-1}$) and angiosperms (below 1.5 $\mu mol*m^{-2}s^{-1}$); 2) plants grown in the sun have higher WUE than leaves from the same plant grown in the shade, but minimal difference in abundance-weighted $\delta D_{nC27\text{-}33}$; 3) measured and modeled (WUE) show good agreement for all species with the exception of *C. americana*, which only shows agreement for early season. In total our data show that inter-species variations

in leaf *n*-alkane δD and $\delta^{13}C$ reflect biophysical differences between individual plant species such as stomatal density and size, whereas temporal shifts in these data reflect a combination of biochemical (stomatal conductance and WUE) and physical responses to changing environmental conditions as well as species-specific differences in timescales of wax synthesis. Thus, paired model and isotopic data from fossil leaves may yield climate and/or environmental information for different seasons or timescales of integration. Application of BIOME-BGC models with fossil leaf biomarkers may provide information on plant and climate data for distinct temporal intervals of the past.

## 4.2.0 INTRODUCTION

Vascular plants produce a range of organic molecular compounds on the surface of their leaves to provide protection, minimize water loss, and add structural support [1–6]. Saturated, aliphatic compounds within the lipid layer are generally synthesized during leaf growth and provide a chemical record of processes related to carbon and hydrogen fixation. Straight chain normal alkanes (*n*-alkanes) are one of the more abundant and ubiquitous compounds found in plant leaf waxes [7–9]. In recent years, *n*-alkanes have been increasingly utilized for paleoclimate reconstruction because they record processes associated with carbon isotope discrimination and water uptake [10–12] and are readily preserved in sedimentary archives [13–15]. In addition, *n*-alkanes show minimal isotopic alteration over long timescales and at temperatures below 150 °C, providing a potential record of conditions at the time of molecular synthesis [13–17].

Numerous studies have used plant wax *n*-alkanes preserved in sedimentary archives to interpret changes in paleoenvironment such as elevation, ecosystem, hydrology and

other environmental parameters [18–22]. These paleoenvironmental reconstructions are founded on modern datasets that evaluate the relationship between plant *n*-alkanes (i.e. $\delta^{13}C$ and $\delta D$) and environmental factors such as precipitation isotopes, temperature, water stress/use efficiency, and plant functional type [23–25]. Despite broad relationships between geochemical signals and environmental variables [15] modern studies also show large variations in $\delta D$ and $\delta^{13}C$ of leaf waxes for different plant species in similar environmental conditions [12,23,26–28]. This variability between plants within a single ecosystem complicates paleoenvironmental interpretation and highlights the challenge of relating biologically-produced signatures to external environmental variables. Specifically, it is uncertain how physical factors that regulate plant gas exchange (e.g. stomatal size, density, conductance, etc.) impact carbon isotope discrimination or hydrogen isotope fractionation over the course of a growing season or for plants with different functional strategies.

Modern studies on the effects of climate variation and water availability on individual plant biomarkers provide an opportunity to refine the use of these molecular signals for paleoenvironmental reconstruction. Hydrogen ($\delta D$) isotopes of leaf wax lipids generally reflect the $\delta D$ composition of ambient ground or source water, modified by various environmental parameters including temperature, humidity, and aridity [13–15,29–34]. However, $\delta D_{n\text{-alkanes}}$ show considerable differences between plant species from a single sampling site grown under the same environmental conditions [26–28,33,35]. These hydrogen isotopic differences have, in the past, been attributed to the Péclet effect which postulates an isotopic difference between plants with varying "effective path lengths". Contrary to Péclet effect studies, recent work shows that $\delta D_{leaf\ water}$ values are more depleted with

increasing path length [36,37]. Carbon isotopes provide an opportunity to better constrain physical and environmental drivers (stomatal density and regulation, humidity, water availability, etc.) of variability in hydrogen isotopes of plant waxes and to assess fundamental biologic responses to external conditions.

Stable carbon ($\delta^{13}C$) isotope measurements of bulk leaf materials are well established as a record of plant water use efficiency (WUE) via the extent of stomatal conductance and $CO_2$ assimilation and fixation [23,25,38,39]. Numerous studies have demonstrated that WUE and $\delta^{13}C$ are affected by various environmental factors including water stress, tree size, and light availability [40–46]. While these data show that bulk carbon isotope discrimination and WUE respond to environmental conditions, there is still considerable uncertainty over the utility of individual biomarker isotopes as a record of plant-specific differences in response to environmental variables. This is particularly important because a number of studies now demonstrate temporal differences in the timing of synthesis of different biomarker compound classes [28,47–49].

The goal of this study was to evaluate how variability in plant physiology and function impacts temporal patterns of carbon fixation, water loss through transpiration, and the resultant $\delta D$ and $\delta^{13}C$ values of *n*-alkanes produced on the leaf surfaces. We measured carbon and hydrogen isotopic compositions of *n*-alkanes from five $C_3$ plants, three trees and one grass, (*Pinus strobus*, *Tsuga canadensis* (sun and shade), *Phalaris arundinacea*, and *Corylus americana*) collected from the Fenton River watershed in Storrs, CT on a weekly to biweekly basis over the 2013 growing season. In addition, we measured stomatal morphometric parameters and density and linked isotopic data to calculations of WUE. We

specifically targeted plants grown adjacent to the stream (< 1 m distance) with roots visibly situated below the water table to minimize any potential water stress. These data were coupled with model predictions of WUE using the BIOME-BGC model and real climate data to assess temporal differences in plant function, carbon assimilation, and biomarker production.

## 4.3.0 METHODS

### *4.3.1 Study catchment and sample collection*

We collected leaves, river sediments, and river water samples on a weekly to biweekly basis from April to October 2013 along the Fenton River in the University of Connecticut Forest located in north-east Connecticut (41°49.537 N, 72°14.222 W). This area is characterized by a humid continental climate with cold winters, warm, humid summers, and average rainfall of ~120 cm $yr^{-1}$. We sampled leaves from three gymnosperms (*P. strobus*, and *T. canadensis* in the sun and shade) and two angiosperms (*C. americana* and *P. arundinacea*) over the course of the growing season [28]. These plants were in close proximity to each other (< 3m apart) with roots below the water table (visible on the stream cut-bank).

For each plant, we collected a minimum of 3 to 5 leaves weekly to biweekly from April to October. These leaves were extracted via sonication using a 9:1 dichloromethane (DCM)-MeOH mixture (15 min x3). At each sampling interval, we also sampled river sediment [28] and extracted ~ 100g via Soxhlet extraction using a 2:1 DCM-MeOH mixture. Lipid fractions were separated via silica gel column chromatography using sequential hexanes, DCM, and methanol. The hexane fraction was analyzed for *n*-alkane purity using

a Thermo-Scientific Trace GC Ultra fitted with a split-splitless (SSL) injector and flame ionization detector (FID). Samples were analyzed using a BP-1 column (60 m x 0.25mm I.D, 0.25 µm film thickness) with He as the carrier (1.5 mL/min).

### *4.3.2 Stable carbon isotope analysis*

Carbon isotopes of individual *n*-alkanes were measured using a Thermo GC-Isolink connected to a MAT 253 gas isotope ratio mass-spectrometer. Compounds were separated using a 30 m x 0.25mm x 0.25µm BP-5 fused silica column with a helium carrier flow of 1.5 mL/min. The isotopic composition of *n*-alkanes was determined relative to a suite of *n*-alkanes with known isotopic composition (Mix A5, A. Schimmelmann). Typical standard deviation for standards is less than 0.3‰ 1 σ.

### *4.3.3 $CO_2$ assimilation and Water Use Efficiency Calculations*

Stomata are microscopic pores on the surface of leaves that allow for the exchange of water vapor and $CO_2$ within a leaf. Regulation of stomata controls the diffusion of $CO_2$ into the leaf and the loss of water through this pore via transpiration. The relationship between maximum pore area and leaf gas exchange capacity must be conserved and is governed by the physics of diffusion [50–52]. The maximum diffusive conductance to water vapor or $CO_2$ can be calculated with respect to stomatal processes:

$$g_{wmax} = \frac{d}{v} * D * \frac{a_{max}}{l + \frac{\pi}{2}\sqrt{\frac{a_{max}}{\pi}}} \quad (4.1)$$

where the maximum area of the open stomatal pore ($a_{max}$) and pore depth are dependent on stomata size (S), which can be approximated by the length of the guard cell multiplied by the total width of the guard cell. Stomatal density (D) is equal to the number of stomata

relative to total leaf area ($mm^{-2}$). Maximum conductance is also dependent on d, the diffusivity of water vapor in air ($m^2s^{-1}$) and v, the molar volume of air ($m^3mol^{-1}$) [52].

To estimate $g_{wmax}$ for our leaf samples, we first measured stomatal dimensions (S and D) from sampled leaves imaged using a Macropod Pro with a microscope kit with natural and fluorescent light at 20x and 10x magnification (Macroscopic Solutions) (Figure 4.16). For S, we measured the length and width of 25 randomly selected stomatal guard cells. Stomatal density (D) was calculated by quantifying stomatal count per image field of view for ten images, to provide an approximation of total stomatal density. We quantified stomatal density for 2-3 leaf samples spanning the growing season. Since stomata are formed during leaf growth, the size and density should (and do) remain effectively constant throughout the growing season, after the leaf has reached full size. Higher counts of stomatal guard cell measurements can refine precision of mean stomatal size, however the congruence of measurements spanning the growing season indicates this is not a significant source of error to overall calculations. With these measurements, we calculated total conductance ($g_{c(tot)}$) from $g_{cmax}$ as determined from stomatal measurements:

$$g_{c(tot)} = \left(\frac{1}{g_{cb}} + \frac{1}{\zeta_{gwmax}} + \frac{1}{g_m}\right)^{-1} \quad (4.2)$$

where the leaf boundary layer conductance to $CO_2$ ($g_{cb}$) is equal to 0.11* $\sqrt{}$(u/d) where 'u' is the mean wind speed (approx. 2 m/s) and d is the dimension of the leaf (0.72*leaf width), mesophyll conductance ($g_m$) is 0.2 mol $CO_2$ $m^{-2}s^{-1}$ for deciduous angiosperms and 0.1 mol $CO_2$ $m^{-2}s^{-1}$ for evergreen gymnosperms [53], and the operational stomatal conductance ($\zeta g_{wmax}$) is $0.2*g_{cmax}$ [25,54].

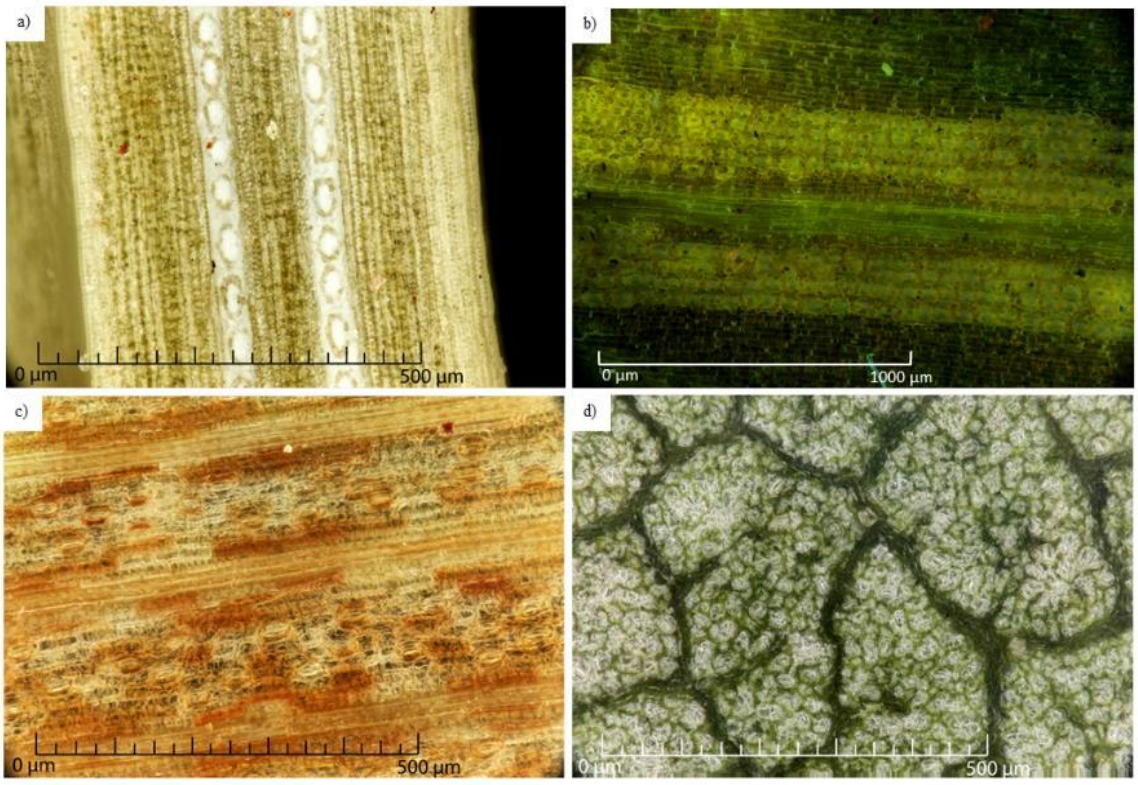


Figure 4.16 Microscopic leaf stomata images from a) *P. strobus*, b) *T. canadensis*, c) *P. arundinacea*, and d*) C. americana*

We defined water use efficiency (WUE) as the ratio of net carbon dioxide assimilation to stomatal conductance and which can be indirectly estimated through measures of the carbon isotope discrimination (intrinsic WUE) [55]. To calculate discrimination, we follow Franks et al., 2014:

$$c_a = \frac{A_n}{g_{c(tot)} * (1 - \frac{c_i}{c_a})} \quad (4.3)$$

where $g_{c(tot)}$ represents total operational conductance of $CO_2$, $A_n$ is the rate of $CO_2$ assimilation, and $c_i/c_a$ is the ratio of leaf internal $CO_2$ concentration to atmospheric $CO_2$ concentration [56–59]. This model was originally proposed to determine the atmospheric

concentration of $CO_2$ ($c_a$) for paleoclimate reconstructions, however, by rearranging (2) we can solve for WUE:

$$WUE = \frac{A_n}{g_{c(tot)}} = c_a\left(1 - \frac{c_i}{c_a}\right) \quad (4.4)$$

An estimate of $c_i/c_a$ can be determined from the bulk carbon isotope composition, $\delta^{13}C_{bulk}$, of the plant leaf. The difference between the $\delta^{13}C_{bulk}$ and $\delta^{13}C_{air}$ provides a measure of the carbon isotope discrimination of the plant, $\Delta_{leaf}$ which can be related back to $c_i/c_a$ by:

$$\frac{c_i}{c_a} = \left[\frac{\Delta_{leaf} - a}{b - a}\right] \quad (4.5)$$

where a is equal to the carbon isotope fractionation due to diffusion of $CO_2$ in air (4.4‰) [38,60] and b is the fractionation of carbon due to fixation with RuBP carboxylase (30‰) [25].

Leaf carbon discrimination ($\Delta_{leaf}$) was calculated by:

$$\Delta_{leaf} = \frac{\delta^{13}C_{air} - \delta^{13}C_{leaf}}{1 + \frac{\delta^{13}C_{leaf}}{1000}} \quad (4.6)$$

where $\delta^{13}C_{air}$ and $\delta^{13}C_{leaf}$ are expressed in ‰. On average, *n*-alkanes are depleted in $^{13}C$ by approximately 6.0±1‰ relative to total leaf $\delta^{13}C$ [61], however it is well known that this offset can vary significantly between plants and likely varies throughout a growing season. This heterogeneity is a significant source of uncertainty in estimates of $c_i/c_a$ and ultimately WUE. If we assume the relative depletion in *n*-alkanes relative to bulk is constant for each plant, and "correct" bulk leaf isotopic composition, $\delta^{13}C_{nC27\text{-}33}$ can replace $\delta^{13}C_{leaf}$ in Eq. 4.5. For discrimination calculations, a $\delta^{13}C_{air}$ value of –8.0 ‰ was used, which reflects modern $\delta^{13}C$ of atmospheric $CO_2$ at the time of plant growth [39,62].

### *4.3.4 Ecosystem Process Modeling*

The ecosystem process model BIOME-BGC ver. 4.2 (http://www.ntsg.umt.edu/project/biome-bgc) [63–65] was used to simulate WUE and non-alkane $\delta^{13}C_{leaf}$ for the four species to assess consistency between values derived from the bulk leaf $\delta^{13}C_{nC27\text{-}33}$ and assess potential underlying environmental conditions affecting these values during the observation period. The model has a long history of use and accurate projection of ecosystem processes at fine [66,67] and broad [68–70] spatial scales. Parameterization for individual species has also been shown to correspond well to annual growth and productivity [71].

From BIOME-BGC, we output daily estimated $A_n$ and $g_{c(tot)}$ values using simulations driven by 2013 meteorological data from the NOAA cooperative weather station USC #00068138 near Storrs, CT, USA. For all species, the $A_n$ and $g_{c(tot)}$ values were for the full-sun fraction of the simulated canopy. For *T. canadensis*, we also output the shaded canopy values of $A_n$ and $g_{c(tot)}$ for comparison. To estimate non-alkane $\delta^{13}C_{leaf}$ from modeled values, we first calculated $c_i$ using Equation 4, where $c_a$ was set for these simulations at 400 ppm. Next, the value of $\Delta_{leaf}$ was calculated using Equation 5 substituting the modeled value of $c_i$. Finally the non-alkane $\delta^{13}C_{leaf}$ was estimated from $\Delta_{leaf}$ based on as the difference in $\delta^{13}C_{air}$ and $\delta^{13}C_{leaf}$ assuming $\delta^{13}C_{air} = –8.0$ ‰ [39,62].

## 4.4.0 RESULTS

### *4.4.1 Carbon Isotopic measurements*

Our two-gymnosperm species (*P. strobus, T. canadensis*) showed considerably enriched $\delta^{13}C_{nC27\text{-}33}$ values with respect to the angiosperm samples, and less variability over

the course of the growing season (Supplementary Table 4.9). Specifically, abundance weighted $\delta^{13}C_{nC27\text{-}33}$ of *P. strobus* (White Pine) became more depleted throughout the growing season, with early season $\delta^{13}C_{nC27\text{-}33}$ values of –31 ‰ and ending near –33 ‰ (Figure 4.17). Similarly, we observed a decrease in $\delta^{13}C_{nC27\text{-}33}$ over the growing season for *T. canadensis* (Eastern Hemlock). This is true for samples collected in both the sun (–30.4 to –32.0 ‰; Figure 4.17) and shade (–32.2 to –36.0 ‰; Figure 4.17). The magnitude of variation for the *T. canadensis* (shaded) leaves was twice the variation of the full sunlight leaves (4 ‰ and 2 ‰ respectively; Figure 4.17). The largest variation in isotopic composition occurred between days 232 and 262 and occurred simultaneously with a large enrichment in $\delta^{13}C_{nC27\text{-}33}$ in *P. arundinacea* (Figure 4.17).

The $\delta^{13}C_{nC27\text{-}33}$ values of *P. arundinacea* ranged widely over the growing season, with a general enrichment in carbon isotopes over the growing season from approximately –39 ‰ to –38 ‰ (Figure 4.17). Throughout the growing season, *P. arundinacea* experienced two periods of carbon isotopic enrichment, once early in the season between days 130 and 158 and again towards the end of the sampling period, days 232 to 256 (Figure 4.17). The angiosperm *C. americana* (American hazelnut) shows a brief interval with more $^{13}C$-enriched values (–38 to –36 ‰) during leaf flush (days 113 to 137) followed by a gradual negative shift throughout the duration of the sampling period to values of less than – 41 ‰ (Figure 4.17).

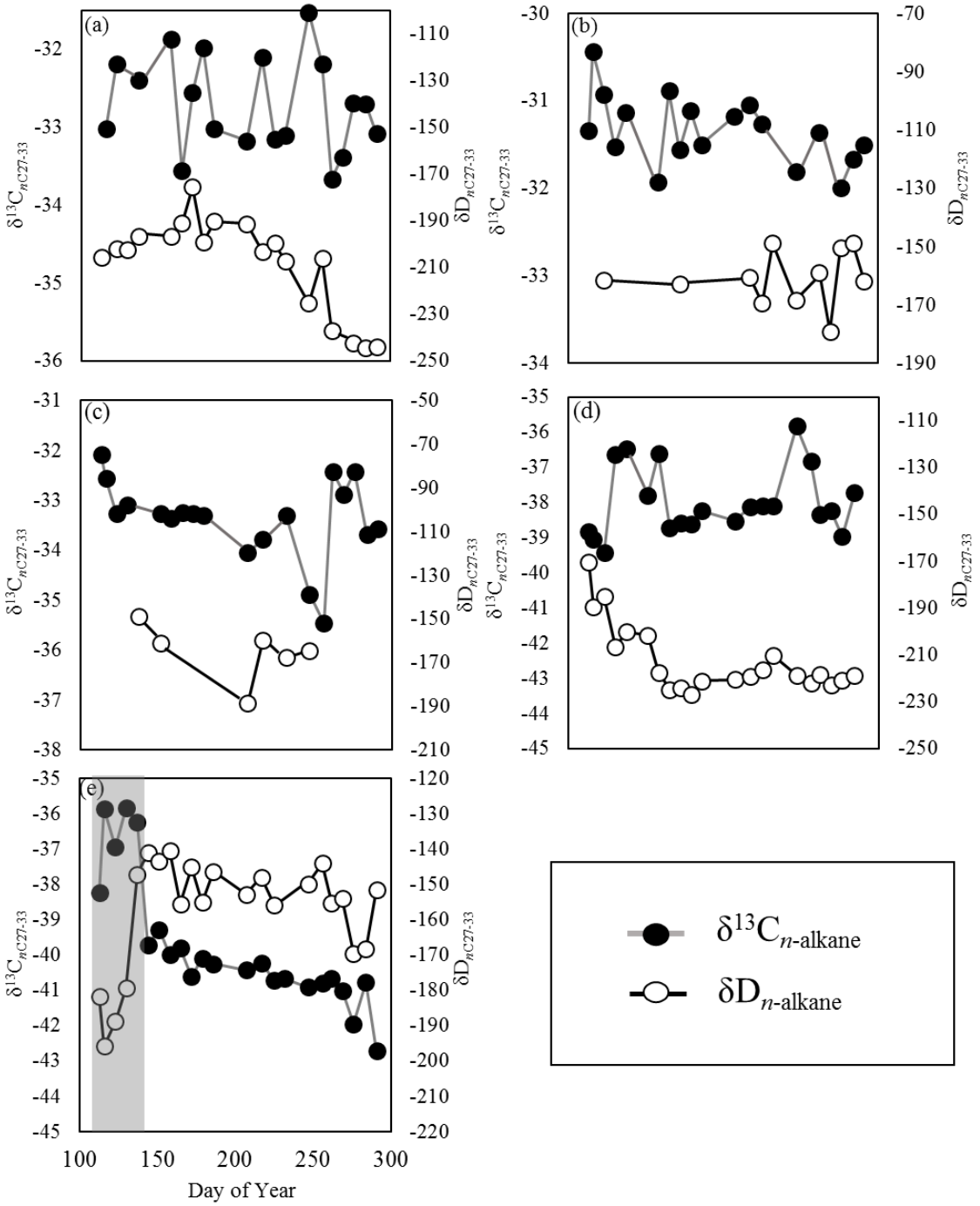


Figure 4.17 Variations in carbon (Black Circles) and hydrogen (White Circles) isotope values over time for a) *P. strobus,* b) *T. canadensis* in the sun, c) *T. canadensis* in the shade, d) *P. arundinacea*, and e) *C. americana*. Leaf flush is represented by the gray box (d)

We measured the $\delta^{13}C_{nC27\text{-}33}$ of individual *n*-alkanes preserved in fluvial sediments collected adjacent to the plant sample site. The mean seasonal abundance weighted $nC_{27\text{-}33}$ was –32.8 ± 0.4 ‰ (Figure 4.18). The $\delta D_{nC27\text{-}33}$ value for the same time periods was – 170 ± 4 ‰ [28]. The $\delta^{13}C_{nC27\text{-}33}$ of the sediments fluctuate less over time than the $\delta^{13}C_{nC27\text{-}33}$ of individual plants.

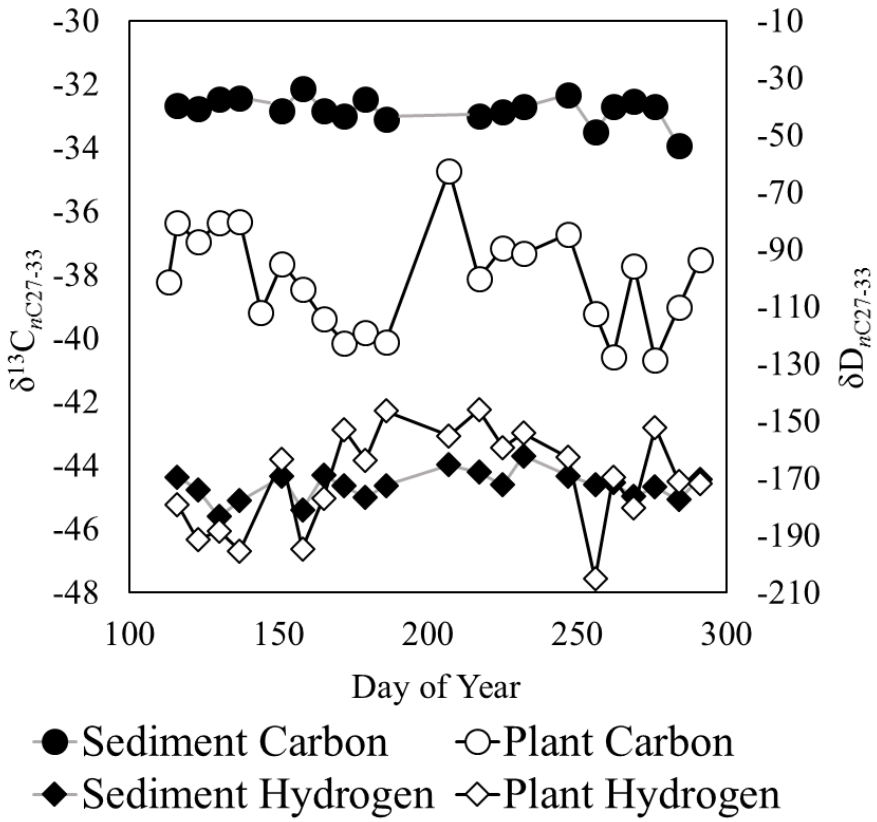


Figure 4.18 Variations in sediment $\delta^{13}C_{nC27\text{-}33}$ (black circles) and $\delta D_{nC27\text{-}33}$ (black diamonds) throughout the growing season. Plant weighted averages over time for $\delta^{13}C_{nC27\text{-}33}$ and $\delta D_{nC27\text{-}33}$ are represented by the white circles and white diamonds respectively

The species sampled exhibit moderate heterogeneity in $\delta^{13}C_{nC27\text{-}33}$ over the course of the growing season (end of April to mid-October). The magnitude of variation for *P. strobus*, *P. arundinacea*, and *C. americana* were 2.2, 3.6, and 6.9 ‰ respectively. The exception to this was *T. canadensis*, where heterogeneity appeared to be driven by exposure to differing amounts of sunlight. The magnitude of variation throughout the growing season for *T. canadensis* located in the sun and shade were 1.6 and 2.8 ‰, respectively. Angiosperms *C. americana* and *P. arundinacea* had highly depleted seasonally-averaged $\delta^{13}C_{nC27\text{-}33}$ values (–39.7 and –38.0 ‰ respectively) relative to associated gymnosperms *P. strobus* and *T. canadensis* in sun and shade (–32.7, –31.3, and –33.4 ‰ respectively). $\delta^{13}C_{nC27\text{-}33}$ values for gymnosperms grown in a temperate humid environment are enriched by up to 4.0 ‰ in $\delta^{13}C$ compared to an arid environment (*Pinus sylvestris* and *Picea pungens*) [26].

### *4.4.2 Water Use Efficiency (WUE)*

Throughout the growing season, each of our sample species showed a distinct pattern in calculated WUE (Figure 4.19). Gymnosperm samples were characterized by $WUE_{calc}$ (herein referred to as WUE) between 100 and 200 ppm and showed only modest variation throughout the growing season. *P. strobus* experienced a decrease from 190 to 160, while *T. canadensis* (sun leaves) decreased from 184 to 167 ppm (Figure 4.19). For *T. canadensis* (shade) WUE was more dynamic, averaging between 134 and 154 ppm early in the season (days 113 to 179), dropping to approximately 120 mid-season (days 207 to 247) to a season low of 99 ppm on day 256, before rising to between 149 and 128 (days 262 to 291, Figure 4.19). For *P. arundinacea* and *C. americana* the WUE fell below

100 ppm. *P. arundinacea* increases from approximately 40 to 60 (Figure 4.19) while *C. americana* decreases from 100 to below 20 in a clear, non-linear pattern. The largest decrease for *C. americana* occurs between days 113 and 150 during leaf flush, after which it levels out for the remainder of the experiment (Figure 4.19)

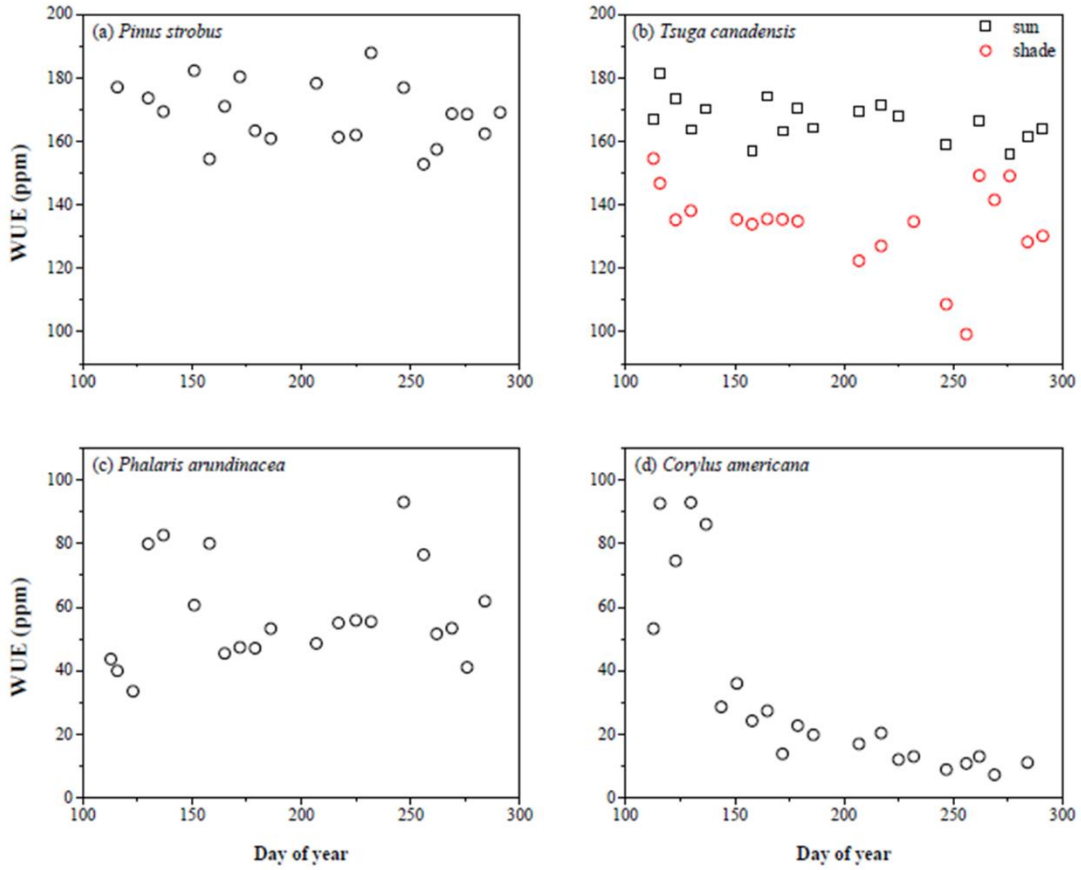


Figure 4.19 Temporal variations in water use efficiency for a) *P. strobus*, b) *T. canadensis* in the sun and shade, c) *P. arundinacea*, and d) C. *americana*

### *4.4.3 BIOME- BGC ecophysical modeling for plant species*

BIOME-BGC parameterization of the ecophysiological attributes for the individual species required a multi-step approach. Plant types are broadly represented in BIOME-BGC as functional plant types based on leaf longevity (i.e. deciduousness v. evergreen), leaf size (i.e. broad v. needle), and presence or absence of woody stems. To select appropriate modeling parameters for each species, we started with the default input tables of required ecophysiological variable values provided with the BIOME-BGC model [72] for evergreen needle-leafed forests, representing *P. strobus* and *T. canadensis*, deciduous broad-leafed forest, representing *C. americana*, and $C_3$ grass, representing *P. arundinacea*. Separate input parameter tables were created for the evergreen species *P. strobus* and *T. canadensis*. One of the most important variables, $g_{c(max)}$, was set for each species using the mean values derived from this study. Parameters were then changed based on species-specific values listed as part of the study by White et al. (2000) [72]. No specific physiological values for *P. arundinacea* were reported, therefore, this species was simulated using default values. Next, parameter values were changed for *P. strobus*, *T. canadensis*, and *C. americana* using values from literature sources. Finally, some input parameters were changed as part of the calibration by comparing the range and seasonal pattern of $\delta^{13}C_{nC27\text{-}33}$ – derived WUE values. Changes in parameter values by species were guided by only changing values within natural range of observation. All final input parameter values are listed in Table 4.6.

For the majority of the samples, the simulated BIOME-BGC WUE was relatively similar to the observed WUE of the samples. For *P. strobus* and *P. arundinacea*, simulated WUE matches the observed values with an average between 150 and 200 ppm for *P. strobus* and 50 to 100 ppm for *P. arundinacea* (Figure 4.20). There is a wider range of values in the simulation for *T. canadensis* than is observed in the calculated values, however the observed values fall within the range of simulated values (Figure 4.20). For *C. americana*, the simulation shows a gradual increase in WUE from days 100 to 200 where is reaches a maximum between 100 and 150. The observed WUE values match the simulated values from day 100 to approximately day 150, before declining to below 100 ppm (Figure 4.20).

Table 4.6 Final input $\delta^{13}C$ (‰) values for Biome-BGC ecophysical modeling of species 1) *P. strobus*, 2) *T. canadensis* sun, 3) *T. canadensis* Shade, 4) *P. arundinacea*, and 5) *C. americana* in Storrs, CT 2013.

| Day | 1 | 2 | 3 | 4 | 5 |
|---|---|---|---|---|---|
| 100 | -26.93 | -36.72 | -37.50 | -32.90 | -34.16 |
| 101 | -27.82 | -36.78 | -37.51 | -32.13 | -34.58 |
| 102 | -26.51 | -37.18 | -37.62 | -32.71 | -35.62 |
| 103 | -31.81 | -37.23 | -37.65 | -34.49 | -36.84 |
| 104 | -28.14 | -37.52 | -37.77 | -36.35 | -36.48 |
| 105 | -28.77 | -37.47 | -37.75 | -35.82 | -36.61 |
| 106 | -26.59 | -37.12 | -37.58 | -36.01 | -35.97 |
| 107 | -25.78 | -35.88 | -37.03 | -35.02 | -35.12 |
| 108 | -25.55 | -29.48 | -34.00 | -33.68 | -34.78 |
| 109 | -28.02 | -21.89 | -21.93 | -33.11 | -35.31 |
| 110 | -26.69 | -22.34 | -22.38 | -33.91 | -34.52 |
| 111 | -26.41 | -37.04 | -37.54 | -32.60 | -36.11 |
| 112 | -27.95 | -36.44 | -37.24 | -35.25 | -36.50 |
| 113 | -27.31 | -34.33 | -36.24 | -35.82 | -36.25 |
| 114 | -31.05 | -29.76 | -34.22 | -35.43 | -36.73 |
| 115 | -26.07 | -20.74 | -28.88 | -36.15 | -34.26 |
| 116 | -26.66 | -21.77 | -21.81 | -32.33 | -35.55 |

| | | | | | |
|---|---|---|---|---|---|
| 117 | -25.74 | -21.91 | -21.95 | -34.32 | -35.30 |
| 118 | -25.93 | -21.93 | -21.98 | -33.92 | -35.21 |
| 119 | -26.26 | -22.23 | -22.27 | -33.77 | -34.65 |
| 120 | -25.37 | -22.13 | -22.17 | -32.83 | -34.84 |
| 121 | -25.76 | -22.23 | -22.27 | -33.16 | -34.66 |
| 122 | -25.62 | -22.39 | -22.43 | -32.85 | -34.38 |
| 123 | -25.17 | -22.83 | -22.86 | -32.38 | -33.19 |
| 124 | -26.60 | -22.03 | -22.07 | -30.90 | -35.03 |
| 125 | -25.25 | -22.08 | -22.12 | -33.43 | -34.92 |
| 126 | -25.81 | -22.23 | -22.27 | -33.27 | -34.65 |
| 127 | -25.94 | -22.49 | -22.53 | -32.82 | -34.23 |
| 128 | -26.89 | -22.89 | -22.95 | -32.11 | -33.74 |
| 129 | -30.85 | -22.32 | -22.49 | -31.25 | -34.85 |
| 130 | -28.99 | -35.97 | -37.25 | -32.76 | -34.40 |
| 131 | -28.04 | -36.30 | -37.40 | -32.16 | -33.85 |
| 132 | -31.84 | -35.99 | -37.38 | -31.30 | -34.97 |
| 133 | -26.56 | -36.23 | -37.25 | -32.81 | -34.59 |
| 134 | -27.76 | -35.69 | -36.92 | -32.65 | -36.05 |
| 135 | -26.33 | -33.42 | -35.82 | -35.08 | -35.77 |
| 136 | -29.31 | -13.94 | -23.88 | -34.64 | -34.66 |
| 137 | -25.62 | -34.69 | -36.67 | -32.60 | -32.87 |
| 138 | -26.07 | -22.34 | -22.38 | -30.36 | -34.44 |
| 139 | -26.29 | -22.41 | -22.45 | -32.44 | -34.32 |
| 140 | -31.59 | -22.24 | -22.44 | -32.24 | -35.05 |
| 141 | -27.05 | -30.05 | -34.90 | -33.04 | -33.31 |
| 142 | -26.44 | -23.46 | -23.60 | -30.64 | -32.36 |
| 143 | -26.10 | -22.83 | -22.86 | -29.64 | -33.60 |
| 144 | -28.66 | -22.68 | -22.80 | -31.21 | -34.19 |
| 145 | -27.04 | -36.43 | -37.36 | -31.80 | -34.41 |
| 146 | -31.78 | -37.03 | -37.60 | -32.33 | -36.32 |
| 147 | -29.52 | -36.96 | -37.56 | -35.47 | -35.73 |
| 148 | -25.96 | -36.06 | -37.17 | -34.53 | -34.15 |
| 149 | -25.88 | -25.71 | -32.56 | -31.98 | -33.25 |
| 150 | -28.22 | -31.64 | -35.78 | -30.87 | -33.61 |
| 151 | -26.73 | -33.36 | -36.42 | -30.91 | -32.35 |
| 152 | -26.42 | -23.82 | -23.95 | -29.58 | -31.94 |
| 153 | -27.34 | -23.70 | -23.86 | -29.16 | -32.70 |
| 154 | -29.36 | -23.51 | -23.76 | -29.80 | -33.77 |

| | | | | | |
|---|---|---|---|---|---|
| 155 | -26.46 | -32.76 | -35.79 | -30.95 | -33.99 |
| 156 | -26.10 | -22.77 | -22.80 | -31.69 | -33.69 |
| 157 | -25.95 | -22.75 | -22.78 | -31.34 | -33.67 |
| 158 | -29.38 | -22.49 | -22.61 | -31.34 | -34.42 |
| 159 | -31.75 | -34.45 | -36.84 | -32.18 | -35.18 |
| 160 | -26.75 | -36.87 | -37.55 | -33.31 | -33.80 |
| 161 | -27.19 | -36.75 | -37.53 | -31.36 | -33.60 |
| 162 | -27.46 | -36.56 | -37.50 | -30.96 | -33.38 |
| 163 | -27.26 | -36.55 | -37.49 | -30.72 | -33.33 |
| 164 | -28.16 | -37.11 | -37.65 | -30.69 | -34.49 |
| 165 | -31.28 | -37.09 | -37.70 | -32.44 | -35.05 |
| 166 | -28.02 | -36.95 | -37.60 | -33.12 | -34.16 |
| 167 | -26.44 | -36.77 | -37.51 | -31.83 | -33.58 |
| 168 | -29.40 | -36.90 | -37.63 | -31.11 | -34.00 |
| 169 | -27.56 | -36.42 | -37.47 | -31.38 | -33.12 |
| 170 | -26.99 | -36.59 | -37.49 | -30.34 | -33.36 |
| 171 | -26.47 | -36.77 | -37.51 | -30.78 | -33.58 |
| 172 | -26.63 | -36.43 | -37.38 | -31.10 | -33.60 |
| 173 | -27.29 | -34.84 | -36.84 | -31.07 | -33.41 |
| 174 | -26.98 | -20.85 | -28.75 | -30.71 | -33.12 |
| 175 | -28.46 | -23.65 | -23.86 | -30.39 | -33.28 |
| 176 | -28.03 | -23.85 | -24.11 | -30.35 | -32.85 |
| 177 | -29.66 | -34.87 | -37.09 | -29.93 | -33.56 |
| 178 | -30.65 | -28.61 | -35.08 | -30.62 | -34.16 |
| 179 | -33.61 | -35.60 | -37.37 | -31.31 | -35.32 |
| 180 | -31.88 | -36.16 | -37.48 | -33.08 | -34.55 |
| 181 | -31.74 | -35.55 | -37.30 | -31.87 | -34.50 |
| 182 | -30.34 | -34.16 | -36.82 | -31.79 | -33.95 |
| 183 | -33.30 | -29.20 | -35.60 | -31.04 | -35.12 |
| 184 | -32.66 | -28.51 | -35.28 | -32.69 | -34.86 |
| 185 | -30.37 | -23.24 | -32.48 | -32.30 | -33.91 |
| 186 | -29.33 | -23.92 | -24.19 | -30.94 | -33.52 |
| 187 | -29.12 | -24.07 | -24.36 | -30.49 | -33.33 |
| 188 | -29.12 | -24.07 | -24.36 | -30.28 | -33.33 |
| 189 | -28.55 | -24.09 | -24.36 | -30.28 | -33.00 |
| 190 | -27.48 | -23.84 | -24.01 | -29.96 | -32.62 |
| 191 | -30.13 | -23.28 | -23.50 | -29.66 | -33.94 |
| 192 | -31.35 | -23.65 | -24.01 | -31.10 | -34.31 |

| | | | | | |
|---|---|---|---|---|---|
| 193 | -30.16 | -35.95 | -37.38 | -31.47 | -33.97 |
| 194 | -28.41 | -35.56 | -37.14 | -31.07 | -33.59 |
| 195 | -29.87 | -31.81 | -35.98 | -30.81 | -33.95 |
| 196 | -29.61 | -21.66 | -30.79 | -31.14 | -33.63 |
| 197 | -28.86 | -23.96 | -24.22 | -30.53 | -33.25 |
| 198 | -27.85 | -24.04 | -24.26 | -30.21 | -32.64 |
| 199 | -29.53 | -24.21 | -24.53 | -29.63 | -33.47 |
| 200 | -28.96 | -24.33 | -24.65 | -30.40 | -33.10 |
| 201 | -28.94 | -24.33 | -24.64 | -30.02 | -33.09 |
| 202 | -28.31 | -23.92 | -24.19 | -30.01 | -32.94 |
| 203 | -27.33 | -23.48 | -23.58 | -29.96 | -32.99 |
| 204 | -30.11 | -23.54 | -23.82 | -30.10 | -33.92 |
| 205 | -29.92 | -35.47 | -37.24 | -30.98 | -33.86 |
| 206 | -26.40 | -35.31 | -36.95 | -30.86 | -33.13 |
| 207 | -33.84 | -12.72 | -30.23 | -30.46 | -35.57 |
| 208 | -28.47 | -36.53 | -37.46 | -33.64 | -33.99 |
| 209 | -27.50 | -35.53 | -37.11 | -31.52 | -33.27 |
| 210 | -28.85 | -31.30 | -35.65 | -30.38 | -33.54 |
| 211 | -26.57 | -19.74 | -26.13 | -30.64 | -32.70 |
| 212 | -27.41 | -23.14 | -23.22 | -29.89 | -33.38 |
| 213 | -27.19 | -23.12 | -23.19 | -30.58 | -33.36 |
| 214 | -30.09 | -23.09 | -23.30 | -30.58 | -34.03 |
| 215 | -27.91 | -31.27 | -35.52 | -31.27 | -33.39 |
| 216 | -28.50 | -22.93 | -23.05 | -30.53 | -33.81 |
| 217 | -27.97 | -29.04 | -34.58 | -31.14 | -33.77 |
| 218 | -26.31 | -18.01 | -23.34 | -31.13 | -33.73 |
| 219 | -26.70 | -22.93 | -22.98 | -31.27 | -33.49 |
| 220 | -29.16 | -22.89 | -23.04 | -30.84 | -33.94 |
| 221 | -31.06 | -23.38 | -23.68 | -31.29 | -34.23 |
| 222 | -30.67 | -23.13 | -23.38 | -31.41 | -34.19 |
| 223 | -26.43 | -36.20 | -37.31 | -31.44 | -33.12 |
| 224 | -27.06 | -34.68 | -36.73 | -30.45 | -33.44 |
| 225 | -27.60 | -22.64 | -30.87 | -30.71 | -33.33 |
| 226 | -28.90 | -22.81 | -22.93 | -30.44 | -33.97 |
| 227 | -27.39 | -22.61 | -22.66 | -31.38 | -33.95 |
| 228 | -26.44 | -22.71 | -22.74 | -31.57 | -33.73 |
| 229 | -26.85 | -22.93 | -22.99 | -31.28 | -33.51 |
| 230 | -27.11 | -23.15 | -23.22 | -30.85 | -33.28 |

| | | | | | |
|---|---|---|---|---|---|
| 231 | -27.74 | -23.06 | -23.15 | -30.53 | -33.50 |
| 232 | -29.16 | -23.08 | -23.23 | -30.75 | -33.76 |
| 233 | -26.96 | -23.33 | -23.41 | -30.98 | -32.93 |
| 234 | -26.88 | -23.39 | -23.48 | -30.11 | -32.79 |
| 235 | -27.01 | -22.93 | -23.02 | -29.96 | -33.38 |
| 236 | -26.68 | -22.97 | -23.02 | -30.80 | -33.40 |
| 237 | -26.86 | -22.91 | -22.97 | -30.80 | -33.54 |
| 238 | -28.21 | -23.21 | -23.34 | -30.91 | -33.51 |
| 239 | -31.63 | -23.12 | -23.43 | -30.66 | -34.54 |
| 240 | -30.53 | -36.39 | -37.52 | -31.91 | -34.13 |
| 241 | -29.38 | -35.65 | -37.26 | -31.27 | -33.82 |
| 242 | -26.68 | -35.24 | -36.88 | -30.96 | -33.85 |
| 243 | -26.63 | -25.12 | -32.30 | -31.48 | -33.16 |
| 244 | -32.51 | -23.36 | -23.79 | -30.53 | -34.81 |
| 245 | -32.29 | -28.76 | -35.30 | -32.25 | -34.69 |
| 246 | -32.47 | -29.11 | -35.44 | -32.04 | -34.80 |
| 247 | -29.26 | -32.64 | -36.18 | -32.23 | -33.98 |
| 248 | -28.12 | -24.17 | -32.24 | -31.35 | -33.59 |
| 249 | -27.22 | -22.51 | -22.57 | -30.87 | -34.12 |
| 250 | -27.04 | -22.24 | -22.27 | -31.88 | -34.45 |
| 251 | -27.20 | -22.79 | -22.85 | -32.51 | -33.72 |
| 252 | -25.86 | -22.57 | -22.60 | -31.24 | -33.82 |
| 253 | -28.35 | -22.15 | -22.22 | -31.65 | -34.66 |
| 254 | -31.51 | -30.07 | -35.50 | -32.79 | -34.75 |
| 255 | -28.06 | -24.82 | -32.80 | -32.47 | -33.00 |
| 256 | -30.01 | -23.56 | -23.86 | -30.09 | -33.96 |
| 257 | -26.67 | -35.42 | -36.99 | -31.15 | -33.64 |
| 258 | -27.21 | -32.16 | -35.48 | -31.26 | -34.61 |
| 259 | -27.51 | -22.61 | -30.82 | -32.82 | -34.27 |
| 260 | -26.06 | -16.92 | -23.41 | -32.23 | -34.79 |
| 261 | -26.79 | -21.87 | -21.91 | -33.17 | -35.16 |
| 262 | -26.75 | -22.47 | -22.51 | -33.76 | -34.10 |
| 263 | -25.98 | -22.66 | -22.70 | -32.00 | -33.59 |
| 264 | -26.31 | -22.83 | -22.88 | -31.42 | -33.37 |
| 265 | -28.90 | -22.67 | -22.80 | -31.05 | -34.15 |
| 266 | -27.94 | -36.71 | -37.49 | -31.83 | -34.57 |
| 267 | -25.61 | -35.23 | -36.88 | -32.74 | -33.22 |
| 268 | -26.74 | -31.43 | -35.17 | -31.04 | -34.41 |

| | | | | | |
|---|---|---|---|---|---|
| 269 | -27.45 | -18.59 | -27.52 | -32.57 | -34.20 |
| 270 | -28.11 | -15.53 | -22.82 | -32.16 | -34.41 |
| 271 | -28.76 | -22.23 | -22.31 | -32.50 | -34.59 |
| 272 | -27.10 | -22.59 | -22.65 | -32.75 | -34.01 |
| 273 | -27.14 | -22.36 | -22.41 | -31.88 | -34.32 |
| 274 | -26.11 | -22.57 | -22.61 | -32.43 | -33.78 |
| 275 | -27.60 | -22.93 | -23.04 | -31.81 | -33.62 |
| 276 | -27.91 | -22.95 | -23.07 | -31.28 | -33.69 |
| 277 | -27.78 | -22.74 | -22.84 | -31.33 | -33.93 |
| 278 | -31.83 | -22.41 | -22.65 | -31.70 | -34.94 |
| 279 | -31.39 | -32.71 | -36.36 | -32.90 | -34.63 |
| 280 | -32.63 | -35.10 | -37.16 | -32.37 | -35.14 |
| 281 | -28.21 | -35.69 | -37.23 | -33.11 | -33.72 |
| 282 | -27.80 | -36.20 | -37.25 | -31.42 | -34.78 |
| 283 | -28.34 | -35.04 | -36.78 | -33.29 | -34.96 |
| 284 | -28.96 | -32.79 | -35.93 | -33.57 | -34.90 |
| 285 | -29.36 | -28.36 | -34.41 | -33.44 | -34.39 |
| 286 | -28.94 | -21.50 | -30.97 | -32.47 | -34.50 |
| 287 | -28.11 | -16.78 | -26.82 | -32.76 | -35.56 |
| 288 | -27.61 | -14.95 | -23.53 | -34.60 | -35.01 |
| 289 | -28.18 | -15.82 | -22.82 | -33.77 | -34.32 |
| 290 | -29.74 | -22.23 | -22.35 | -32.55 | -34.70 |
| 291 | -30.84 | -22.74 | -22.97 | -33.06 | -34.55 |
| 292 | -27.60 | -22.03 | -22.07 | -32.41 | -34.91 |
| 293 | -29.27 | -21.98 | -22.07 | -33.67 | -35.02 |
| 294 | -27.88 | -21.75 | -21.79 | -33.74 | -35.41 |
| 295 | -26.92 | -22.05 | -22.09 | -34.48 | -34.86 |
| 296 | -27.95 | -22.06 | -22.13 | -33.67 | -34.87 |
| 297 | -29.94 | -21.20 | -21.26 | -33.61 | -36.42 |
| 298 | -29.26 | -21.28 | -21.32 | -35.98 | -36.34 |
| 299 | -30.28 | -21.08 | -21.14 | -35.88 | -36.62 |
| 300 | -29.96 | -21.31 | -21.37 | -36.27 | -36.21 |

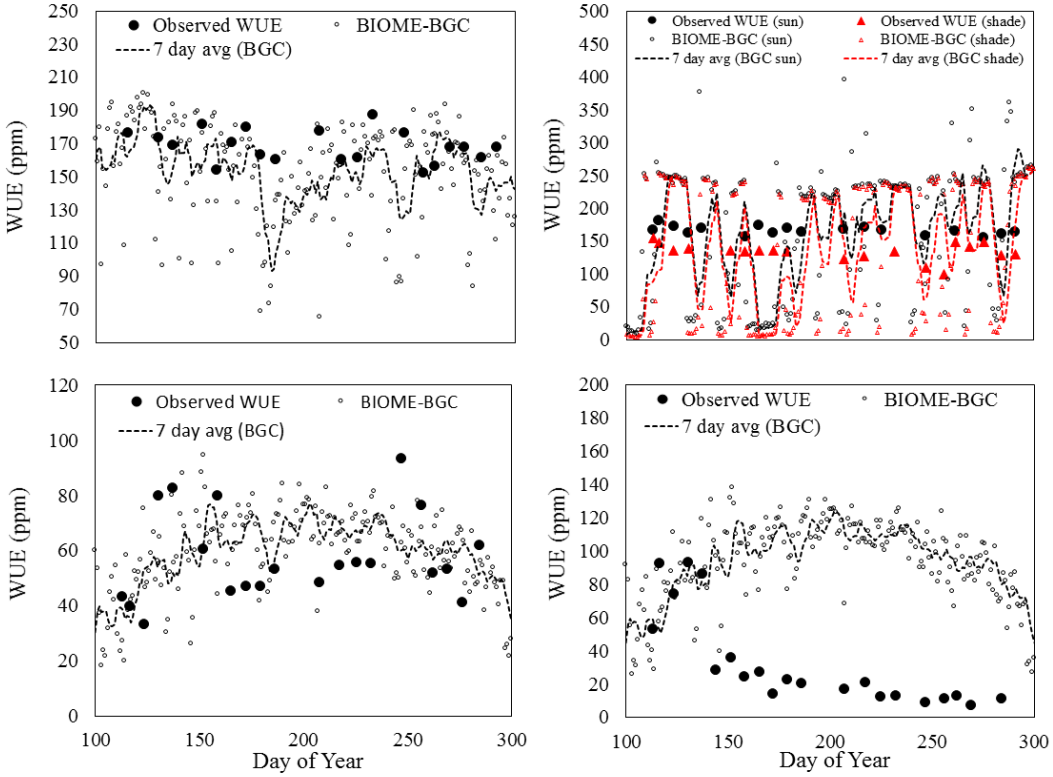


Figure 4.20 BIOME-BGC simulated WUE for a) *P. strobus*, b) *T. canadensis* in the sun and shade, c) *P. arundinacea*, and d) *C. americana*

### *4.4.4 $CO_2$ assimilation rate*

The rate of calculated $CO_2$ assimilation for each plant was relatively stable for the duration of the growing season, with the exception of *C. americana*, which experienced a drop in $A_n$ over the sampling period, coinciding with the period of leaf flush (Figure 4.21). Gymnosperm samples typically showed calculated assimilation rates between 1 and 2.5 with little fluctuation (*P. strobus*, 2.05 ± 0.11 mol*m$^{-2}$s$^{-1}$; *T. canadensis* sun, 1.71 ± 0.17 mol*m$^{-2}$s$^{-1}$; *T. canadensis* shade, 2.14 ± 0.08 mol*m$^{-2}$s$^{-1}$; Figure 4.21). Angiosperms have

rates below 1 mol*m$^{-2}$s$^{-1}$ with slightly more seasonal fluctuation. *C. americana* has a higher $CO_2$ assimilation during leaf flush due to its leaf mass and wax production at that time (Figure 4.21). Carbon assimilation rates for *T. canadensis* leaves in the sun were larger than in the shade (Figure 4.21).

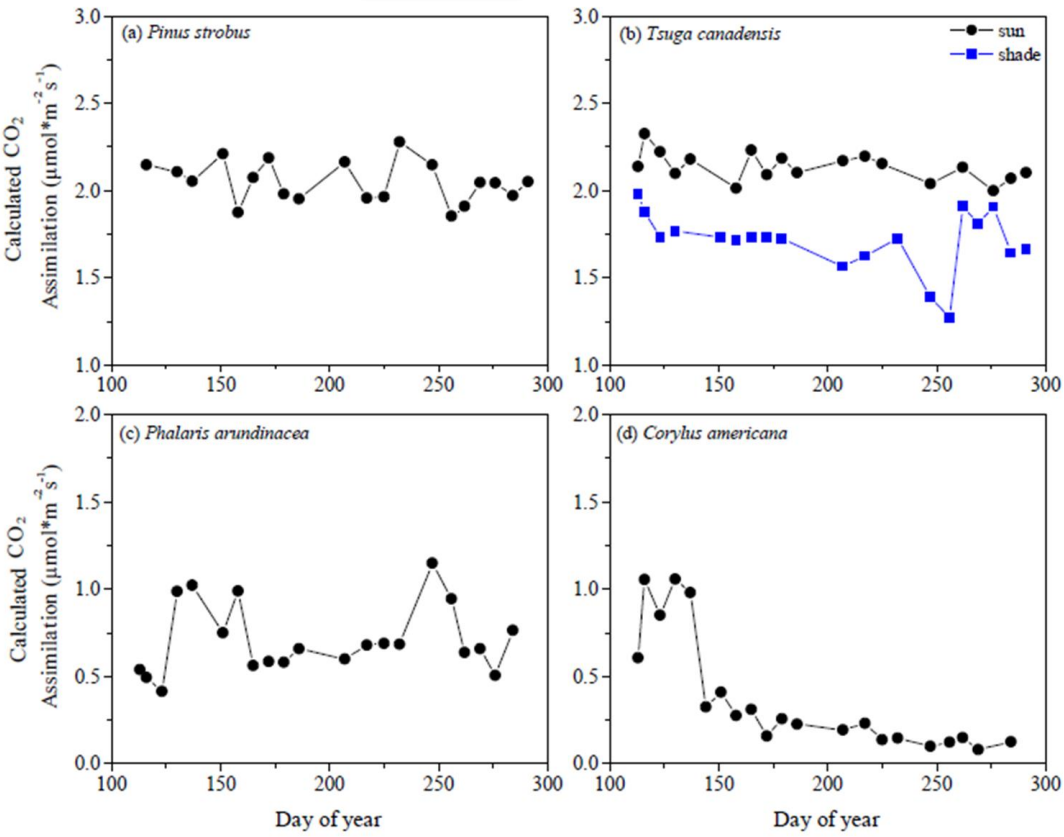


Figure 4.21 Temporal variations in carbon dioxide assimilation rates for a) *P. strobus*, b) *T. canadensis* in the sun and shade, c) *P. arundinacea*, d) *C. americana*

### *4.4.5 WUE in humid and arid environments*

Recent data shows that plants grown in arid conditions generally maintain relatively stable WUEs throughout the growing season (Table 4.7, Figure 4.22). Gymnosperms grown under arid conditions (*Pinus sylvestris, Picea pungens*, Washington) [26] have WUE's

between 200 and 240 ppm, which is significantly higher than the 100 to 200 ppm we report from our gymnosperms growing in moist environments (*P. strobus*, *T. canadensis*, Connecticut; Figure 4.22 and Figure 4.19). The same phenomenon occurs when comparing angiosperms *P. tremuloides* and *S. vulgaris* (150 to 200 ppm) [26] and *P. arundinacea* and *C. americana* (10 to 100 ppm) (Figure 4.22 and Figure 4.19). In both cases, there is a distinct separation in the WUE based on taxonomic class of the plants, with the exception of the angiosperm *Betula pendula* that has WUE values closer to those of *P. sylvestris* and *P. pungens* (Figure 4.22).

Table 4.7 Calculated carbon isotope discrimination and WUE from 5 plant species

| Day of Year | $\delta^{13}C$* | δD* | $\delta D_{H2O}$* | Δleaf (‰) | ci/ca** | An/gc (ppm) | % Humid |
|---|---|---|---|---|---|---|---|
| *Betula pendula* | | | | | | | |
| 147 | -30.9 | -176 | -103 | 17 | 0.50 | 198 | 39 |
| 184 | -26.7 | -177 | -103 | 13 | 0.33 | 266 | 48 |
| 205 | -29.3 | -157 | -102 | 16 | 0.44 | 223 | 41 |
| 236 | -28.1 | -166 | -104 | 14 | 0.39 | 244 | 49 |
| 257 | -28.0 | -171 | -104 | 14 | 0.39 | 245 | 61 |
| 270 | -27.8 | -175 | -103 | 14 | 0.38 | 249 | 79 |
| 296 | -28.2 | -165 | -103 | 14 | 0.39 | 242 | 73 |
| *Syringa vulgaris* | | | | | | | |
| 147 | -32.8 | -189 | -103 | 19 | 0.58 | 167 | 39 |
| 184 | -33.0 | -200 | -103 | 20 | 0.59 | 164 | 48 |
| 205 | -32.9 | -197 | -102 | 19 | 0.59 | 166 | 41 |
| 236 | -33.3 | -196 | -104 | 20 | 0.60 | 160 | 49 |
| 257 | -33.8 | -198 | -104 | 20 | 0.62 | 150 | 61 |
| 270 | -32.8 | -198 | -103 | 19 | 0.58 | 168 | 79 |
| 296 | -33.1 | -194 | -103 | 20 | 0.59 | 163 | 73 |
| *Populus tremuloides* | | | | | | | |
| 147 | -31.9 | -173 | -103 | 18 | 0.54 | 182 | 39 |
| 184 | -32.7 | -179 | -103 | 19 | 0.58 | 169 | 48 |
| 205 | -33.0 | -175 | -102 | 19 | 0.59 | 164 | 41 |
| 236 | -32.7 | -173 | -104 | 19 | 0.58 | 168 | 49 |

| | | | | | | | |
|---|---|---|---|---|---|---|---|
| 257 | -32.3 | -181 | -104 | 19 | 0.56 | 175 | 61 |
| 270 | -32.6 | -184 | -103 | 19 | 0.57 | 170 | 79 |
| 296 | -33.2 | -178 | -103 | 20 | 0.60 | 160 | 73 |
| *Pinus sylvestris* | | | | | | | |
| 147 | -29.0 | -194 | -103 | 15 | 0.43 | 230 | 39 |
| 184 | -30.3 | -196 | -103 | 17 | 0.48 | 208 | 48 |
| 205 | -29.0 | -194 | -102 | 15 | 0.43 | 228 | 41 |
| 236 | -28.9 | -190 | -104 | 15 | 0.42 | 230 | 49 |
| 257 | -29.4 | -194 | -104 | 16 | 0.44 | 223 | 61 |
| 270 | -30.2 | -198 | -103 | 17 | 0.48 | 210 | 79 |
| 296 | -29.2 | -191 | -103 | 16 | 0.43 | 226 | 73 |
| *Picea pungens* | | | | | | | |
| 147 | -30.6 | -201 | -103 | 17 | 0.49 | 203 | 39 |
| 184 | -29.8 | -204 | -103 | 16 | 0.46 | 215 | 48 |
| 205 | -29.1 | -199 | -102 | 15 | 0.43 | 227 | 41 |
| 236 | -29.8 | -195 | -104 | 16 | 0.46 | 216 | 49 |
| 257 | -29.8 | -203 | -104 | 16 | 0.46 | 217 | 61 |
| 270 | -29.7 | -205 | -103 | 16 | 0.45 | 218 | 79 |
| 296 | -29.1 | -198 | -103 | 15 | 0.43 | 227 | 73 |

* Data published in Pedentchouk et al., 2008

** $c_i/c_a$ calculated by $c_i/c_a = (\Delta_{leaf} - a)/(b - a)$

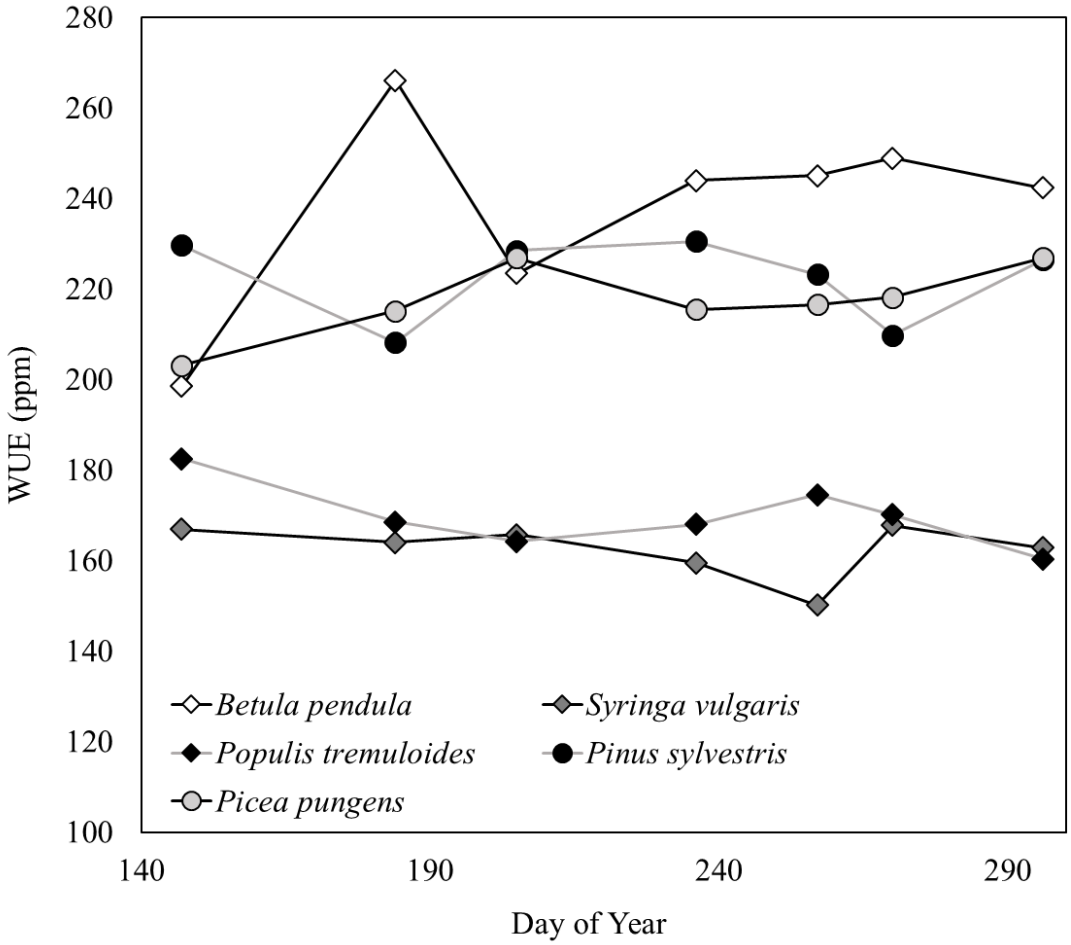


Figure 4.22 Seasonal variability in WUE of angiosperms *Betula pendula* (white diamonds), *Populus tremuloides* (black diamonds), *Syringa vulgaris* (gray diamonds) and gymnosperms *Pinus sylvestris* (black circles) and *Picea pungens* (gray circles) grown during 2005, in central Washington State, USA. WUE values calculated from previously published compound specific *n*-alkane $\delta^{13}C$ values using the method described.[26]

## 4.5.0 DISCUSSION

### *4.5.1 Seasonal trends in $\delta^{13}C$ values*

The carbon incorporated into leaves and leaf biomolecules is ultimately derived from the atmosphere and thus, to first order, biomolecule $\delta^{13}C$ is regulated by the $\delta^{13}CO_2$ of the atmosphere. However, secondary processes that include regulation of stomata and

the diffusion of $CO_2$ to the sites of carboxylation, as well as fractionation between internal carbon pools, play a critical role in determining carbon isotopic compositions of leaf lipids. The offset between original $\delta^{13}CO_2$ and individual biomolecules can reflect, in a sense, the "metabolic distance" [73,74]. Our data show that the carbon isotopic composition of leaf wax *n*-alkanes (e.g. *n*-$C_{27\text{-}33}$) varies significantly within a single species/tree and between plants over the course of the growing season. The magnitude of variation within a single plant can be as large as or larger than the difference in mean values between plants from different functional groups (e.g. angiosperms versus gymnosperms).

*P. arundinacea*, commonly known as reed-canary grass, is an invasive wetland species that is located on a small flood plain in our study area. This plant is characterized by multiple intervals of enriched carbon isotopes within the lipid layer. The first carbon enrichment period (days 130 and 158) occurred during a period of intense rainfall that caused flooding and left the grasses completely submerged under water for several weeks (Figure 4.17). Hydrogen isotope data from *P. arundinacea* suggests continued production of leaf waxes throughout the growing season [28]. With the plants completely submerged in water, they had no access to atmospheric carbon and in response used all available carbon leading to isotopic enrichment. A second period of carbon isotope enrichment occurred as the weekly average temperature began to decrease. Isotopic enrichment at this time may reflect variation in stomatal regulation that biased the internal carbon dioxide partial pressure within a leaf, leading to changes in the magnitude of isotopic fractionation of carbon in the leaf waxes.

The angiosperm *C. americana* (American hazelnut) shows no "plateau" value in $\delta^{13}C_{nC27-33}$ as has been observed in other angiosperm plants in riparian environments [75], but rather a progressive depletion through the growing season (Figure 4.17). This is opposite the pattern observed for hydrogen isotopes in these same leaves, where $\delta D_{nC27-33}$ values are depleted during leaf flush and become enriched for the remainder of the growing season. This trend may be the result of production of *n*-alkanes that occurs during leaf flush [28,75]. As the leaves are forming in the early spring period, the plant undergoes maximum leaf growth and mass gain. This period of leaf flush is associated with a shift to heavier carbon isotope values associated with maximum C assimilation.

There are distinct differences in carbon isotope fractionation between the *T. canadensis* grown in the sun and *T. canadensis* grown in the shade throughout the growing season (Figure 4.17). Carbon isotope discrimination differences within a single species are often correlated to complex climatic gradients such as temperature and precipitation [76] and depend on three main factors: 1) the $\delta^{13}C$ of atmospheric $CO_2$, 2) the concentration of atmospheric $CO_2$, and 3) the ratio of atmospheric $CO_2$ and intercellular leaf $CO_2$ [29]. However, for our sampled plants, there are no climatic differences that can account for the differences in isotopic discrimination. Since the sampled trees were grown under identical atmospheric and environmental conditions, the differences between sun and shade leaves are likely related to intercellular leaf $CO_2$ concentration. Differences in absorbed irradiance, which affects leaf water content and morphological plasticity and changes the amount of internal space within the mesophyll layer of the needles, affects the amount of $CO_2$ allowed into the leaf [77]. This is further demonstrated by the higher inherent

photosynthetic rates of plants with leaves grown in high sunlight. These are characterized by higher rates of photosynthesis (16 to 20 mg of $CO_2$ per $dm^2$ hr) than leaves grown in the shade (2 to 5 mg of $CO_2$ per $dm^2$ hr) [78]. These differences in the intake and photosynthesis of carbon may lead to the observed differences in the isotopic signatures of sun and shade for *T. canadensis* grown in identical environments.

### *4.5.2 Comparison of $\delta^{13}C_{nC27-33}$ and $\delta D_{nC27-33}$ in plants and sediments*

Previous studies show a strong negative correlation between leaf wax *n*-alkyl lipid δD and $\delta^{13}C$ values. This relationship is argued to indicate the importance of WUE on the δD of leaf wax biomarkers [23]. Our data however, show no correlation, whether positive or negative, between the *n*-alkane δD and $\delta^{13}C$ values either between sampled species or within a single tree over time (Figure 4.23). Instead, a bivariate plot of carbon and hydrogen isotope values from our selected species shows little overlap (Figure 4.23), with data from individual plants plotting in discrete groupings. The angiosperms, *C. americana* (blue diamonds) and *P. arundinacea* (orange diamonds), tend to produce *n*-alkanes that are more depleted in $^{13}C$ relative to the gymnosperms *P. strobus* (yellow circles) and *T. canadensis* (green circles). *n*-Alkanes from *C. americana* are more D-enriched than *P. arundinacea*, with overlap occurring only during leaf flush as a result of D-depletion in *n*-alkanes from *C. americana* during that interval. The two gymnosperms show no overlap in $\delta D_{nC27-33}$ values, with *n*-alkanes from *T. canadensis* being approximately 20 ‰ more enriched than *P. strobus* throughout the growing season (Figure 4.23). Although there are no obvious trends between measured *n*-alkane $\delta D_{nC27-33}$ and $\delta^{13}C_{nC27-33}$ values, there is a broad separation between the angiosperms and gymnosperms in terms of $\delta^{13}C_{nC27-33}$.

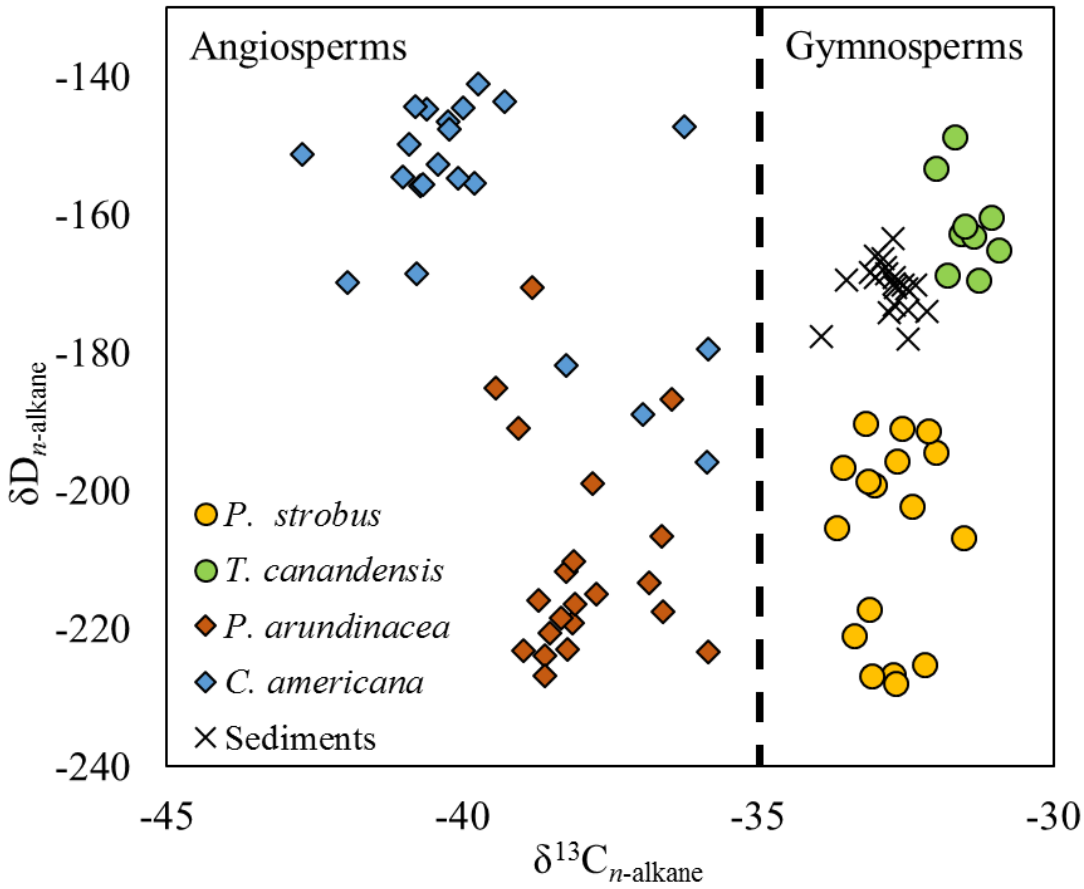


Figure 4.23 Comparison of $\delta D_{nC27\text{-}33}$ and $\delta^{13}C_{nC27\text{-}33}$ of our four sampled plant species and sediments. The angiosperms *P. arundinacea* and *C. americana* are more depleted (orange diamonds and blue diamonds, respectively) while the gymnosperms *P. strobus* and *T. canadensis* are more enriched (green circles and yellow circles, respectively). Sediments are represented with black Xs and are more enriched in $\delta^{13}C$, plotting near *T. canadensis*.

### *4.5.3 Sedimentary δD and δ13C and weighted plant averages*

The carbon and hydrogen isotope values of sedimentary *n*-alkanes are commonly used as a paleoenvironmental proxy because they incorporate geochemical signatures of multiple plants over long periods of time. We calculated a theoretical abundance-weighted $\delta D_{nC27\text{-}33}$ and $\delta^{13}C_{nC27\text{-}33}$ that uses isotopic values of our plant species and the relative compound abundance in each of these to assess how well a simple weighting of these

components might reflect an ecosystem average (i.e. sediment). Simple abundance-weighted averages of the four components produce reasonable agreement between the measured sediment $\delta D_{nC27\text{-}33}$ and calculated $\delta D_{nC27\text{-}33}$ using the four endmember values and abundances. These match reasonably well throughout the growing season. However, sedimentary $\delta^{13}C_{nC27\text{-}33}$ values (mean of ~ –32.8 ‰) are inconsistent with a simple weighted plant average that fluctuated around a value of –38.2 ± 1.6 ‰ (Figure 4.18). Modern vegetation maps [79] show that evergreen plants comprise a small percentage of the overall vegetation in the Fenton catchment today, but are locally abundant in the sample area. Prior to 8,000 years ago, the southern New England region was dominantly evergreen vegetation. Sedimentary cores from the Fenton river show abundant Pine pollen in cores less than 1-2 m deep. Thus, fluvial sediment may contain a mixed modern-inherited signature that is distinct from what would be predicted from modern vegetation.

### *4.5.4 WUE of riparian plants*

Plant stomata are located on the surface of the plant leaves and regulate the diffusion of $CO_2$ to the site of carboxylation and the loss of water through the open pore. Plants regulate the stomatal opening and closing to minimize water loss and maximize $CO_2$ uptake. Water use efficiency (WUE) can be defined in a variety of ways, however for the purpose of this paper we use the definition for intrinsic WUE: the molar ratio of $CO_2$ fixed to the water transpired [23,39,76,80]. This ratio is calculated using carbon isotope discrimination, which provides an integrated measure environmental and physiological properties of a leaf due to the strong negative correlation between isotope discrimination and the internal to external isotope $CO_2$ concentration ratio [76]. Plants undergoing $C_3$

photosynthesis discriminate against $^{13}CO_2$. This discrimination occurs in two steps: 1) carbon isotopic fractionation due to diffusion of $CO_2$ in air (4.4 ‰), and 2) fractionation due to carboxylation with RuBP (30 ‰) [25,39,60,76]. Discrimination increases as the ratio of internal carbon dioxide concentration and atmospheric carbon dioxide concentration decreases [38,39,76].

In previous studies, a negative correlation between δD and $\delta^{13}C$ was observed in leaf samples, indicating WUE was an important control on hydrogen isotope ratios of leaf waxes [23]. We did not observe any correlation between hydrogen and carbon isotopes within the normal alkane pool (Figure 4.23). Likewise, we observed minimal correlation between instantaneous WUE and relative humidity (Figure 4.24).

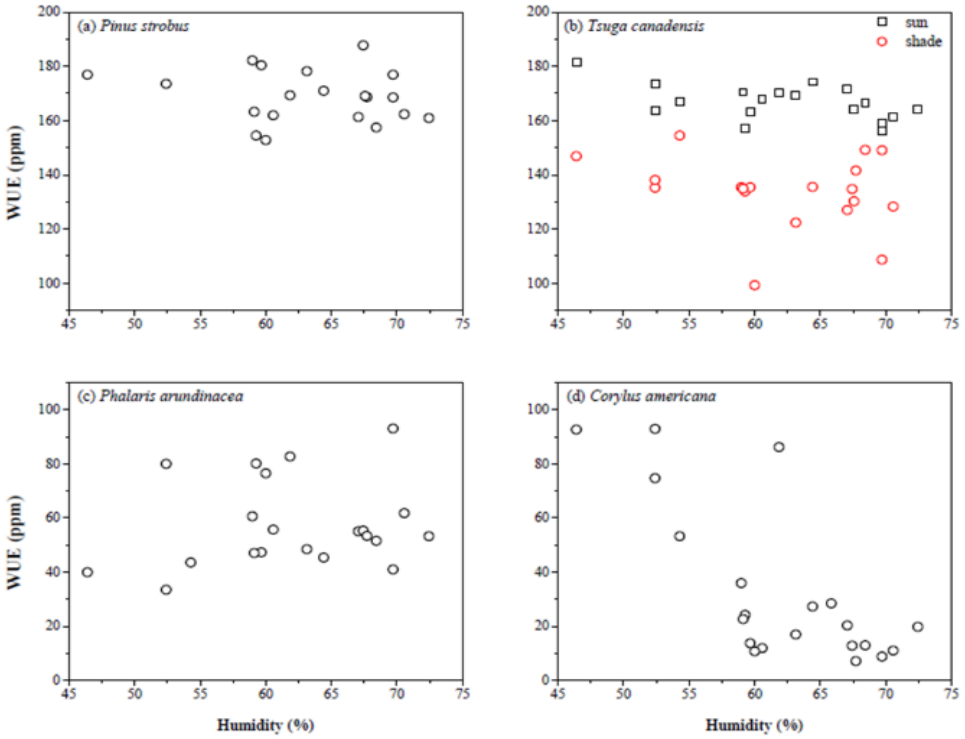


Figure 4.24 The relationship between WUE and humidity for a) *P. strobus*, b) *T. canadensis* in the sun and shade, c) *P. arundinacea*, and d) *C. americana*.

Plants regulate their stomata to minimize water loss while maximizing $CO_2$ assimilation. Short-term controls of stomatal aperture changes include soil water availability, vapor pressure deficit, light, temperature, wind speed, and atmospheric $CO_2$ concentration while long term controls consist of stomatal density, maximum stomatal conductance, light intensity/ quality, and root-to-shoot signals of water availability [81,82]. Long-term controls dictate differences between species, seen in Figure 4.19. If *n*-alkanes are produced throughout a growing season, changes in short term controls may be recorded in the $\delta^{13}C_{nC27\text{-}33}$ and $\delta D_{nC27\text{-}33}$.

Gymnosperms (*P. strobus* and *T. canadensis*) have higher calculated WUE throughout the season (between 100 and 200 ppm) whereas angiosperms (*P. arundinacea* and *C. americana*) have lower calculated WUE (between 5 and 100 ppm) but all vary during the sample interval. BIOME-BGC model results provide a tool for predicting changes to stomatal regulation as a function of ambient environment and improving interpretation of isotopic data. BIOME-BGC model simulations produce distinct temporal patterns of WUE for each of the sampled species. The shape of these curves is dictated by physiological response to the same environmental forcing. For *P. strobus*, *T. canadensis* and *P. arundinacea*, modeled WUE and calculated WUE are generally consistent, with the model predicting a slight decline in WUE over the growing season for *P. strobus*, and a peak in WUE in mid-summer for *P. arundinacea* (Figure 4.20). For *P. strobus*, correspondence between isotope and simulated values necessitated increasing the photosynthetic capacity of this species, higher than the default values set by BIOME-BGC for a typical evergreen needle leafed species (Table 4.6). This included specifically higher values of nitrogen partitioning into the Rubisco enzyme.

The high variability found in BIOME-BGC simulations of daily WUE for *T. canadensis* could not be reduced through changing model parameters, which are a result of the high observed maximum $g_s$ for this species (3.29 mol $m^{-2}$ $s^{-1}$ water vapor). However, observed WUE have mean values of 167 and 133 ppm for sun and shade leaves, respectively, compared to the simulated values of 165 and 138 ppm for sun and shade leaves, respectively (Figure 4.20). The high variance, while plausibly representing the actual gas-exchange in comparison to the low variable isotopic values, may indicate a

slower, more stable integrated path of C inclusion, especially in alkane waxes (Figure 4.20). The high correspondence between WUE derived values for the grass, *P. arundianacea*, likely indicates that cutin is produced continuously through the growing season (Figure 4.20) and physiological responses evidenced in isotopic signatures of leaf *n*-alkanes.

BIOME-BGC simulations of *C. americana* show poor agreement with isotope-calculated WUE values, with the exception of the time interval coincident with leaf flush (Figure 4.20). Hydrogen isotope data for this plant, and published studies [75] show that angiosperm trees achieve stable isotopic composition early in the growing season during the period of leaf flush. Early season physiological activity and conditions may likewise, set the carbon source imprint of waxes in this species. This indicates that, while leaf gas exchange is still occurring throughout the growing season, it is no longer recorded in the leaf waxes post leaf flush (~ day 150). These data confirm evidence for early season setting of hydrogen and carbon isotopes in *n*-alkanes in angiosperm trees/large shrubs within mid-latitude environments [28,75,83]. In contrast, temporal changes in measured hydrogen isotopes, WUE and modeled WUE data suggest continued production of *n*-alkanes within grass leaves and gymnosperm needles throughout the growing season.

Differences in measured and modeled WUE is mirrored in the calculated carbon assimilation rate (Figure 4.21). Importantly, calculated assimilation rates show higher C fixation when a plant species has higher light availability (Figure 4.21), as well as high rates of fixation during the period of maximum leaf expansion and mass accumulation (Figure 4.21).

### *4.5.5 Tsuga canadensis: Sun versus shade analysis*

*T. canadensis* leaves grown in the same environment with varying amounts of sunlight have distinct stomatal densities, WUE, $\delta D_{nC27-33}$, and $\delta^{13}C_{nC27-33}$ (Table 4.8). Likewise, these are characterized by a higher rate of $CO_2$ assimilation (average 2.14 µmol*$m^{-2}s^{-1}$) in sun-leaves versus shade (average 1.71 µmol*$m^{-2}s^{-1}$). Assimilation and WUE differences are related to subtly different $\delta D_{nC27-33}$ (–168 ‰ shade and –161 ‰ sun) [28] and $\delta^{13}C$ (–33 ‰ shade and –31 ‰ sun; Figure 4.17; Table 4.8) values. These differences may result from effects of UV-B [41,84]. In general, the effects of UV-B radiation are often masked by the effects of drought or nutrient deficiency [41]. However, we suspect our plants do not experience these problems due to their proximity to stream water. Several studies suggest UV-B may be responsible for changes in epidermal anatomy or wax deposition [85,86], limitations to carbon assimilation rates [87,88], and changes in stomatal density [41].

Table 4.8 Physical and chemical differences between sun and shade *T. canadensis**

| | D[a] | An[b] | WUE | $\delta^{13}C$ | $\delta D$ | *C* (ng/g)[c] | AHPCL | CPI |
|---|---|---|---|---|---|---|---|---|
| Sun | 8.40*$10^6$ | 2.14 | 167 | -31.3 | -161 | 1.71*$10^4$ | 29.5 | 5 |
| Shade | 5.29*$10^6$ | 1.71 | 134 | -33.4 | -168 | 1.11*$10^4$ | 29.4 | 8 |

* All values are seasonal averages
[a] Stomatal Density
[b] $CO_2$ Assimilation rate
[c] Weighted *n*-alkane concentration

### *4.5.6 WUE differences of plants in arid and humid environments*

Numerous studies have addressed water stress and plant water use strategies [45,76,89-91]. These suggest that plants under moderate water stress have higher

WUEs than plants with little to no water stress. We calculated WUEs for five angiosperm and gymnosperm species grown in central Washington State, USA over the 2005 growing season, using published *n*-alkane isotope data [26]. The central Washington State area is considered an arid environment where the plants are expected to experience elevated water stress [26]. This provides a contrast to the 5 angiosperm and gymnosperm plants sampled as part of our study, as our plants should have reduced levels of water stress due to their proximity to the river and generally humid environment. Comparison of gymnosperms and angiosperms from these two sites show consistent separation of the two groups, with higher WUE for both in the more arid environment as compared to the Fenton River site.

## 4.6.0 CONCLUSIONS

We sampled leaves of five different angiosperm (*C. americana* and *P. arundinacea*) and gymnosperm (*P. strobus, T. candensis* in sun, *T. canadensis* in shade) plants growing alongside the Fenton River in Storrs, CT throughout the 2013 growing season to evaluate the environmental and physical controls on $\delta D_{nC27\text{-}33}$ and $\delta^{13}C_{nC27\text{-}33}$. We focused on closely associated streamside vegetation with roots visibly located in the river water and coupled data with model simulations of WUE for each plant species using real climate information and the BIOME-BGC model. These simulations were used to assess timescales of integration of geochemical signals and how well isotopic data might inform on plant function.

Modeled and measured data show three key results. First, isotope and modeled WUE data suggest three of the four plant species (*T. canadensis, P. strobus,*

*P. arundinacea*) produce *n*-alkanes throughout the growing season and record plant responses to environmental conditions. *n*-Alkane isotopes of an angiosperm tree/large shrub, records a short duration interval during the time of leaf-flush. Model simulations of WUE or assimilation based on *n*-alkane isotopes and stomatal measurements of fossil angiosperm tree leaves are thus likely to record an early season environmental response (in temperate, mid latitude environment). Model simulations of WUE and assimilation based on *n*-alkane isotopes and stomatal measurements of fossil gymnosperms are likely to reflect seasonally integrated conditions, or those close to the time at which the leaf material/needles were integrated into the sedimentary record. Second, our data show distinct water use efficiency (WUE) differences between angiosperms versus gymnosperms, as well as differences in carbon isotopic fractionation and $CO_2$ assimilation between each sampled plant. The difference is evident in measured and calculated WUE. Differences between gymnosperms and angiosperms are also represented by differences in carbon assimilation, where gymnosperms are characterized by higher $CO_2$ assimilation rates. Measurable variations in stomatal density, WUE, $CO_2$ assimilation, and timing of wax synthesis, are all recorded in leaf wax *n*-alkanes. Third, isotopic heterogeneity between *n*-alkanes of plants with different functional types that share a close proximity to the stream edge indicates that constraints on weighted temporal and spatial integration provided by sediments is critical to interpreting paleoenvironmental signatures.

## 4.7.0 ACKNOWLEDGEMENTS

We thank K. Patros and J. White for their support collecting and processing samples. In addition, we thank Robert Capers for assistance with plant identification. The authors thank Steven C. Murphy and Yvette Eley for reviewing our manuscript and giving valuable feedback. Financial support for this project was provided in part, by NSF-EAR-1338256.

## 4.8.0 REFERENCES


(1) Barthlott, W.; Neinhuis, C. *Planta* **1997**, *202* (1), 1–8.

(2) Barbour, M. M.; Schurr, U.; Henry, B. K.; Wong, S. C.; Farquhar, G. D. *Plant Physiol.* **2000**, *123* (2), 671–680.

(3) Barbour, M. M.; Roden, J. S.; Farquhar, G. D.; Ehleringer, J. R. *Oecologia* **2004**, *138* (3), 426–435.

(4) Sachse, D.; Radke, J.; Gleixner, G. *Org. Geochem.* **2006**, *37* (4), 469–483.

(5) Jetter, R.; Kunst, L.; Samuels, A. L. *Annu. Plant Rev.* **2007**, *23*, 145–181.

(6) Nichols, J.; Booth, R. K.; Jackson, S. T.; Pendall, E. G.; Huang, Y. *Geochim. Cosmochim. Acta* **2010**, *74* (4), 1407–1416.

(7) Kolattukudy, P. E. *Lipids* **1970**, *5* (2), 259–275.

(8) Kolattukudy, P. E.; Walton, T. J. *Prog. Chem. Fats Other Lipids* **1973**, *13* (C), 119–175.

(9) Bi, X.; Sheng, G.; Liu, X.; Li, C.; Fu, J. *Org. Geochem.* **2005**, *36* (10), 1405–1417.

(10) Hou, J.; D'Andrea, W. J.; MacDonald, D.; Huang, Y. *Org. Geochem.* **2007**, *38* (6), 977–984.

(11) Ubierna, N.; Farquhar, G. D. *Plant, Cell Environ.* **2014**, *37* (7), 1494–1498.

(12) Eley, Y.; Dawson, L.; Pedentchouk, N. *Org. Geochem.* **2016**, *96*, 28–42.

(13) Tipple, B. J.; Pagani, M. *Earth Planet. Sci. Lett.* **2010**, *299* (1–2), 250–262.

(14) Tipple, B. J.; Pagani, M.; Krishnan, S.; Dirghangi, S. S.; Galeotti, S.; Agnini, C.; Giusberti, L.; Rio, D. *Earth Planet. Sci. Lett.* **2011**, *311* (1–2), 82–92.

(15) Sachse, D.; Billault, I.; Bowen, G. J.; Chikaraishi, Y.; Dawson, T. E.; Feakins, S. J.; Freeman, K. H.; Magill, C. R.; McInerney, F. A.; van der Meer, M. T. J.; Polissar, P.; Robins, R. J.; Sachs, J. P.; Schmidt, H.-L.; Sessions, A. L.; White, J. W. C.; West, J. B.; Kahmen, A. *Annu. Rev. Earth Planet. Sci.* **2012**, *40*, 221–249.

(16) Schimmelmann, A.; Lewan, M. D.; Wintsch, R. P. *Geochim. Cosmochim. Acta* **1999**, *63* (22), 3751–3766.

(17) Zhuang, G.; Brandon, M. T.; Pagani, M.; Krishnan, S. *Earth Planet. Sci. Lett.* **2014**, *390*, 186–198.

(18) Sauer, P. E.; Eglinton, T. I.; Hayes, J. M.; Schimmelmann, A.; Sessions, A. L. *Geochim. Cosmochim. Acta* **2001**, *65* (2), 213–222.

(19) Polissar, P. J.; Freeman, K. H.; Rowley, D. B.; McInerney, F. A.; Currie, B. S. *Earth Planet. Sci. Lett.* **2009**, *287* (1–2), 64–76.

(20) Hren, M. T.; Pagani, M.; Erwin, D. M.; Brandon, M. *Geology* **2010**, *38* (1), 7–10.

(21) Douglas, P. M. J.; Pagani, M.; Brenner, M.; Hodell, D. A.; Curtis, J. H. *Geochim. Cosmochim. Acta* **2012**, *97*, 24–45.

(22) Voelker, S. L.; Meinzer, F. C.; Lachenbruch, B.; Brooks, J. R.; Guyette, R. P. *Plant, Cell Environ.* **2014**, *37* (3), 766–779.

(23) Hou, J.; D'Andrea, W. J.; MacDonald, D.; Huang, Y. *Org. Geochem.* **2007**, *38* (8), 1251–1255.

(24) Hall, S. A.; Penner, W. L. *Palaeogeogr. Palaeoclimatol. Palaeoecol.* **2013**, *369*, 272–281.

(25) Franks, P. J.; Royer, D. L.; Beerling, D. J.; Van de Water, P. K.; Cantrill, D. J.; Barbour, M. M.; Berry, J. A. *Geophys Res Lerr* **2014**, *41*, 4685–4694.

(26) Pedentchouk, N.; Sumner, W.; Tipple, B.; Pagani, M. *Org. Geochem.* **2008**, *39* (8), 1066–1071.

(27) Eley, Y.; Dawson, L.; Black, S.; Andrews, J.; Pedentchouk, N. *Geochim. Cosmochim. Acta* **2014**, *128*, 13–28.

(28) Oakes, A. M.; Hren, M. T. *Org. Geochem.* **2016**, *97*, 122–130.

(29) Lockheart, M. J.; Poole, I.; Van Bergen, P. F.; Evershed, R. P. *Org. Geochem.* **1998**, *29* (4), 1003–1008.

(30) Chikaraishi, Y.; Naraoka, H.; Poulson, S. R. *Phytochemistry* **2004**, *65* (10), 1369–1381.

(31) Chikaraishi, Y.; Naraoka, H. *Phytochemistry* **2003**, *63* (3), 361–371.

(32) Pagani, M.; Pedentchouk, N.; Huber, M.; Sluijs, A.; Schouten, S.; Brinkhuis, H.; Damsté, J. S. S.; Dickens, G. R. *Nature* **2006**, *442* (7103), 671–675.

(33) Hou, J.; D'Andrea, W. J.; Huang, Y. *Geochim. Cosmochim. Acta* **2008**, *72* (14), 3503–3517.

(34) Wang, Y.; Yang, H.; Zhang, J.; Gao, W.; Huang, C.; Xie, B. *Chemosphere* **2015**, *119*, 1346–1352.

(35) Sachse, D.; Kahmen, A.; Gleixner, G. *Org. Geochem.* **2009**, *40* (6), 732–742.

(36) Farquhar, G. D.; Cernusak, L. A.; Barnes, B. **2007**, *143* (1), 11–18.

(37) Ferrio, J. P.; Pou, A.; Florez-Sarasa, I.; Gessler, A.; Kodama, N.; Flexas, J.; Ribas-Carbó, M. *Plant, Cell Environ.* **2012**, *35* (3), 611–625.

(38) Farquhar, G. D.; O'Leary, M. H.; Berry, J. A. *Aust. J. Plant Physiol.* **1982**, *9* (2), 121.

(39) Farquhar, G. D.; Ehleringer, J. R.; Hubick, K. T. *Annu. Rev. Plant Physiol. Plant Mol. Biol.* **1989**, *40* (1), 503–537.

(40) Fessenden, J. E.; Ehleringer, J. R. *Oecologia* **2003**, *136* (1), 129–136.

(41) Gitz, D. C.; Liu-Gitz, L.; Britz, S. J.; Sullivan, J. H. *Environ. Exp. Bot.* **2005**, *53* (3), 343–355.

(42) Grice, K.; Lu, H.; Zhou, Y.; Stuart-Williams, H.; Farquhar, G. D. *Phytochemistry* **2008**, *69* (16), 2807–2814.

(43) Ghashghaie, J.; Badeck, F. W. *New Phytol.* **2014**, *201* (3), 751–769.

(44) Forrester, D. I. *Tree Physiol.* **2015**, *35* (3), 289–304.

(45) Liu, E. K.; Mei, X. R.; Yan, C. R.; Gong, D. Z.; Zhang, Y. Q. *Agric. Water Manag.* **2016**, *167*, 75–85.

(46) Diefendorf, A. F.; Mueller, K. E.; Wing, S. L.; Koch, P. L.; Freeman, K. H. *Proc. Natl. Acad. Sci.* **2010**, *107* (13), 5738–5743.

(47) Tipple, B. J. *Proc. Natl. Acad. Sci.* **2013**, *110* (4), 1144–1145.

(48) Kahmen, A.; Dawson, T. E.; Vieth, A.; Sachse, D. *Plant, Cell Environ.* **2011**, *34* (10), 1639–1651.

(49) Diefendorf, A. F.; Freeman, K. H.; Wing, S. L.; Graham, H. V. *Geochim. Cosmochim. Acta* **2011**, *75* (23), 7472–7485.

(50) Cowan, I. R.; Farquhar, G. D. *Stomatal function in relation to leaf metabolism and environment.*; Jennings, D. H., Ed.; Cambridge Univ. Press: Cambridge, UK, 1977.

(51) Franks, P. J.; Farquhar, G. D. *Plant Physiol.* **2001**, *125* (February), 935–942.

(52) Franks, P. J.; Beerling, D. J. *Proc. Natl. Acad. Sci. U. S. A.* **2009**, *106* (25), 10343–10347.

(53) Flexas, J.; Ribas-Carbó, M.; Diaz-Espejo, A.; Galmés, J.; Medrano, H. *Plant, Cell Environ.* **2008**, *31* (5), 602–621.

(54) Dow, G. J.; Bergmann, D. C.; Berry, J. A. *New Phytol.* **2014**, *210*, 1218–1226.

(55) Dillen, S. Y.; Marron, N.; Koch, B.; Ceulemans, R. *Ann. Bot.* **2008**, *102* (3), 399–407.

(56) Farquhar, G. D.; Sharkey, T. D. *Annu. Rev. Plant Physiol.* **1982**, *33* (1), 317–345.

(57) von Caemmerer, S. *Biochemical models of leaf photosynthesis.*; CSIREO Publishing: Collingwood, Vic., Australia, 2000.

(58) Buckley, T. N.; Mott, K. A.; Farquhar, G. D. *Plant, Cell Environ.* **2003**, *26* (10), 1767–1785.

(59) Franks, P. J. *New Phytol.* **2013**, *197*, 1077–1094.

(60) Roeske, C. A.; O'Leary, M. H. *Biochemistry* **1984**, *23* (1980), 6275–6284.

(61) Conte, M. H.; Weber, J. C.; Carlson, P. J.; Flanagan, L. B. *Oecologia* **2003**, *135* (1), 67–77.

(62) Vivin, P.; Gross, P.; Aussenac, G.; Guehl, J.-M. *Plant Physiol. Biochem.* **1995**, *33* (2), 201–211.

(63) Running, S. W.; Hunt, E. J. R. In *Scaling Physiological processes: leaf to globe*; Ehleringer, J. R., Field, C. B., Eds.; Academic: San Diego, 1993; pp 141–158.

(64) White, M. A.; Running, S. W.; Thornton, P. E. *Int. J. Biometeorol.* **1999**, *42* (3), 139–145.

(65) Wang, W.; Ichii, K.; Hashimoto, H.; Michaelis, A. R.; Thornton, P. E.; Law, B. E.; Nemani, R. R. *Ecol. Modell.* **2009**, *220* (17), 2009–2023.

(66) Cienciala, E.; Tatarinov, F. A. *For. Ecol. Manage.* **2006**, *237* (1–3), 252–266.

(67) Kang, S.; Lee, D.; Lee, J.; Running, S. W. *Ecol. Res.* **2006**, *21* (1), 64–74.

(68) Churkina, G.; Running, S. W. *Ecosystems* **1998**, *1* (2), 206–215.

(69) Schimel, D.; Melillo, J.; Tian, H.; McGuire, A. D.; Kicklighter, D.; Kittel, T.; Rosenbloom, N.; Running, S.; Thornton, P.; Ojima, D.; Parton, W.; Kelly, R.; Sykes, M.; Neilson, R.; Rizzo, B. *Science (80-. ).* **2000**, *287* (5460), 2004–2006.

(70) Churkina, G.; Zaehle, S.; Hughes, J.; Viovy, N.; Chen, Y.; Jung, M.; Heumann, B. W.; Ramankutty, N.; Heimann, M.; Jones, C. *Biogeosciences* **2010**, *7* (9), 2749–2764.

(71) Pietsch, S. A.; Hasenauer, H.; Thornton, P. E. *For. Ecol. Manage.* **2005**, *211* (3), 264–295.

(72) White, M. A.; Thornton, P. E.; Running, S. W.; Nemani, R. R. *Earth Interact.* **2000**, *4* (3), 1–85.

(73) Schmidt, H.-L.; Robins, R. J.; Werner, R. A. *Isotopes Environ. Health Stud.* **2015**, *51* (1), 155–199.

(74) Hayes, J. M. *Rev. Mineral. Geochemistry* **2001**, *43* (March), 225–277.

(75) Tipple, B. J.; Berke, M. A.; Doman, C. E.; Khachaturyan, S.; Ehleringer, J. R. *Proc. Natl. Acad. Sci. U. S. A.* **2013**, *110* (7), 2659–2664.

(76) Zhang, J.; Marshall, J. D. *Can. J. For. Res.* **1994**, *24* (1), 92–99.

(77) Richardson, A. D.; Ashton, P. M. .; Berlyn, G. P.; McGroddy, M. E.; Cameron, I. R. *Ann. Bot.* **2001**, *88* (6), 1007–1015.

(78) Boardman, N. K. *Annu. Rev. Plant Physiol.* **1977**, *28* (1), 355–377.

(79) CLEAR. Connecticut's Changing Landscape.

(80) Bacon, M. A. *Water-use efficiency in plant biology*; Blackwell, 2004.

(81) Haworth, M.; Elliott-Kingston, C.; McElwain, J. C. *J. Exp. Bot.* **2011**, *62* (8), 2419–2423.

(82) Brantley, S.; Ford, C. R.; Vose, J. M. *Ecol. Appl.* **2013**, *23* (4), 777–790.

(83) Tipple, B. J.; Pagani, M. *Geochim. Cosmochim. Acta* **2013**, *111*, 64–77.

(84) Graham, H. V.; Patzkowsky, M. E.; Wing, S. L.; Parker, G. G.; Fogel, M. L.; Freeman, K. H. *Geochim. Cosmochim. Acta* **2014**, *144*, 82–95.

(85) Laakso, K.; Sullivan, J. H.; Huttunen, S. *Plant, Cell Environ.* **2000**, *23* (5), 461–472.

(86) Petropoulou, Y.; Kyparissis, A.; Nikolopoulos, D.; Manetas, Y. *Physiol. Plant.* **1995**, *94*, 37–44.

(87) Allen, D. J.; Nogués, S.; Baker, N. R. *J. Exp. Bot.* **1998**, *49* (328), 1775–1788.

(88) Nogués, S.; Allen, D. J.; Morison, J. I. L.; Baker, N. R. *Plant Physiol.* **1999**, *121* (2), 489–496.

(89) Field, C.; Mooney, H. A. *Oecologia* **1983**, *56* (2), 348–355.

(90) Monneveux, P.; Rekika, D.; Acevedo, E.; Merah, O. *Plant Sci.* **2006**, *170* (4), 867–872.

(91) Abbasi, A. R.; Sarvestani, R.; Mohammadi, B.; Baghery, A. *J. Agric. Sci. Technol.* **2014**, *16* (3), 505–516.

## 4.9.0 SUPPLIMENTARY DATA

Supplementary Table 4.9 Master data sheet of physical and chemical changes of 5 sampled plants and collected sediments

| **Name** | **$\delta D_{H2O}$** | **Day** | **ng/g** | **$\delta D_{27\text{-}33}$** | **$\varepsilon_{27\text{-}33}$** | **$\delta^{13}C_{27\text{-}33}$** | **Humid** | **Δleaf** | **ci/ca** | **WUE** | **$g_{cmax}$** | **$g_{ctot}$** | **An[a]** | **°C[b]** |
|---|---|---|---|---|---|---|---|---|---|---|---|---|---|---|
| ***Pinus strobus*** | | | | | | | | | | | | | | |
| fen-1-a13 | -48.4 | 113 | 25 | - | - | -33.0 | 54.3 | - | - | - | 1.139 | 0.012 | - | 10.4 |
| fen-2-a13 | -49.4 | 116 | - | - | - | -32.2 | 46.4 | 18.7 | 0.56 | 177 | 1.139 | 0.012 | 2.1 | 11.1 |
| fen-3-a13 | -46.3 | 123 | 19 | -187 | -147 | - | - | - | - | - | - | - | - | - |
| fen-4-a13 | -48.1 | 130 | 33 | -202 | -162 | -32.4 | 52.4 | 18.9 | 0.57 | 174 | 1.139 | 0.012 | 2.1 | 13.8 |
| fen-5-a13 | -45.6 | 137 | 497 | -196 | -157 | -32.7 | 61.9 | 19.2 | 0.58 | 169 | 1.139 | 0.012 | 2.1 | 13.3 |
| fen-7-a13 | -47.3 | 151 | 12 | - | - | -31.9 | 59.0 | 18.3 | 0.54 | 182 | 1.139 | 0.012 | 2.2 | 14.4 |
| fen-8-a13 | -46.6 | 158 | 78 | -197 | -157 | -33.6 | 59.3 | 20.1 | 0.61 | 154 | 1.139 | 0.012 | 1.9 | 21.2 |
| fen-9-a13 | -56.7 | 165 | 92 | -191 | -142 | -32.6 | 64.4 | 19.1 | 0.57 | 171 | 1.139 | 0.012 | 2.1 | 18.6 |
| fen-10-a13 | -53.9 | 172 | 88 | -194 | -148 | -32.0 | 59.7 | 18.5 | 0.55 | 180 | 1.139 | 0.012 | 2.2 | 19.4 |
| fen-11-a13 | -53.3 | 179 | 50 | -199 | -154 | -33.0 | 59.1 | 19.6 | 0.59 | 163 | 1.139 | 0.012 | 2.0 | 23.5 |
| fen-12-a13 | -51.0 | 186 | 71 | -190 | -147 | -33.2 | 72.4 | 19.7 | 0.60 | 161 | 1.139 | 0.012 | 2.0 | 24.4 |
| fen-13-a13 | -41.3 | 207 | 451 | -191 | -156 | -32.1 | 63.1 | 18.6 | 0.55 | 178 | 1.139 | 0.012 | 2.2 | 27.7 |
| fen-14-a13 | -46.4 | 217 | 263 | -199 | -160 | -33.1 | 67.1 | 19.7 | 0.60 | 161 | 1.139 | 0.012 | 2.0 | 20.7 |
| fen-15-a13 | -41.7 | 225 | 2192 | -217 | -183 | -33.1 | 60.6 | 19.6 | 0.60 | 162 | 1.139 | 0.012 | 2.0 | 21.2 |
| fen-16-a13 | -46.5 | 232 | 173 | -207 | -168 | -31.5 | 67.4 | 18.0 | 0.53 | 188 | 1.139 | 0.012 | 2.3 | 21.1 |
| fen-17-a13 | -42.9 | 247 | 207 | -225 | -191 | -32.2 | 69.7 | 18.7 | 0.56 | 177 | 1.139 | 0.012 | 2.1 | 22.4 |
| fen-18-a13 | -37.9 | 256 | 564 | -205 | -174 | -33.7 | 60.0 | 20.2 | 0.62 | 153 | 1.139 | 0.012 | 1.9 | 19.8 |
| fen-19-a13 | -43.9 | 262 | 142 | -221 | -185 | -33.4 | 68.4 | 19.9 | 0.61 | 157 | 1.139 | 0.012 | 1.9 | 15.6 |
| fen-20-a13 | -42.1 | 269 | 67 | - | - | -32.7 | 67.7 | 19.2 | 0.58 | 169 | 1.139 | 0.012 | 2.0 | 16.2 |
| fen-21-a13 | -43.0 | 276 | 165 | -227 | -192 | -32.7 | 69.7 | 19.2 | 0.58 | 168 | 1.139 | 0.012 | 2.0 | 15.8 |

| | | | | | | | | | | | | | | |
|---|---|---|---|---|---|---|---|---|---|---|---|---|---|---|
| fen-22-a13 | -39.8 | 284 | 190 | -227 | -195 | -33.1 | 70.6 | 19.6 | 0.59 | 162 | 1.139 | 0.012 | 2.0 | 17.7 |
| fen-23-a13 | -41.9 | 291 | 207 | -228 | -194 | -32.7 | 67.6 | 19.2 | 0.58 | 169 | 1.139 | 0.012 | 2.1 | 13.7 |
| ***Tsuga canadensis* (shade)** | | | | | | | | | | | | | | |
| fen-1-b13 | -48.4 | 113 | 10 | - | - | -31.3 | 54.3 | 19.3 | 0.58 | 167 | 9.79 | 0.013 | 2.1 | 10.4 |
| fen-2-b13 | -49.4 | 116 | 12 | - | - | -30.4 | 46.4 | 18.4 | 0.55 | 182 | 9.79 | 0.013 | 2.3 | 11.1 |
| fen-3-b13 | -46.3 | 123 | 76 | -165 | -125 | -30.9 | 52.4 | 18.9 | 0.57 | 173 | 9.79 | 0.013 | 2.2 | 11.1 |
| fen-4-b13 | -48.1 | 130 | 64 | - | - | -31.5 | 52.4 | 19.5 | 0.59 | 164 | 9.79 | 0.013 | 2.1 | 13.8 |
| fen-5-b13 | -45.6 | 137 | 27 | - | - | -31.1 | 61.9 | 19.1 | 0.57 | 170 | 9.79 | 0.013 | 2.2 | 13.3 |
| fen-8-b13 | -46.6 | 158 | 140 | - | - | -31.9 | 59.3 | 19.9 | 0.61 | 157 | 9.79 | 0.013 | 2.0 | 21.2 |
| fen-9-b13 | -56.7 | 165 | 59 | - | - | -30.9 | 64.4 | 18.9 | 0.56 | 174 | 9.79 | 0.013 | 2.2 | 18.6 |
| fen-10-b13 | -53.9 | 172 | 273 | -163 | -115 | -31.6 | 59.7 | 19.6 | 0.59 | 163 | 9.79 | 0.013 | 2.1 | 19.4 |
| fen-11-b13 | -53.3 | 179 | 29 | - | - | -31.1 | 59.1 | 19.1 | 0.57 | 170 | 9.79 | 0.013 | 2.2 | 23.5 |
| fen-12-b13 | -51.0 | 186 | 36 | - | - | -31.5 | 72.4 | 19.5 | 0.59 | 164 | 9.79 | 0.013 | 2.1 | 24.4 |
| fen-13-b13 | -41.3 | 207 | 252 | - | - | -31.2 | 63.1 | 19.2 | 0.58 | 169 | 9.79 | 0.013 | 2.2 | 27.7 |
| fen-14-b13 | -46.4 | 217 | 298 | -160 | -120 | -31.1 | 67.1 | 19.0 | 0.57 | 171 | 9.79 | 0.013 | 2.2 | 20.7 |
| fen-15-b13 | -41.7 | 225 | 685 | -170 | -133 | -31.3 | 60.6 | 19.2 | 0.58 | 168 | 9.79 | 0.013 | 2.2 | 21.2 |
| fen-16-b13 | -46.5 | 232 | 789 | -148 | -107 | - | - | - | - | - | - | - | - | - |
| fen-17-b13 | -42.9 | 247 | 819 | -169 | -131 | -31.8 | 69.7 | 19.8 | 0.60 | 159 | 9.79 | 0.013 | 2.0 | 22.4 |
| fen-19-b13 | -43.9 | 262 | 496 | -163 | -125 | -31.4 | 68.4 | 19.3 | 0.58 | 166 | 9.79 | 0.013 | 2.1 | 15.6 |
| fen-20-b13 | -42.1 | 269 | 176 | -179 | -143 | - | - | - | - | - | - | - | - | - |
| fen-21-b13 | -43.0 | 276 | 599 | -153 | -115 | -32.0 | 69.7 | 20.0 | 0.61 | 156 | 9.79 | 0.013 | 2.0 | 15.8 |
| fen-22-b13 | -39.8 | 284 | 1680 | -149 | -113 | -31.7 | 70.6 | 19.7 | 0.60 | 161 | 9.79 | 0.013 | 2.1 | 17.7 |
| fen-23-b13 | -41.9 | 291 | 660 | -162 | -125 | -31.5 | 67.6 | 19.50 | 0.59 | 164 | 9.79 | 0.013 | 2.1 | 13.7 |
| ***Tsuga canadensis* (sun)** | | | | | | | | | | | | | | |
| fen-1-c13 | -48.4 | 113 | 12 | - | - | -32.1 | 54.3 | 20.1 | 0.61 | 154 | 7.67 | 0.013 | 2.0 | 10.4 |

| | | | | | | | | | | | | | | |
|---|---|---|---|---|---|---|---|---|---|---|---|---|---|---|
| fen-2-c13 | -49.4 | 116 | 2 | - | - | -32.6 | 46.4 | 20.6 | 0.63 | 147 | 7.67 | 0.013 | 1.9 | 11.1 |
| fen-3-c13 | -46.3 | 123 | 6 | - | - | -33.3 | 52.4 | 21.3 | 0.66 | 135 | 7.67 | 0.013 | 1.7 | 11.1 |
| fen-4-c13 | -48.1 | 130 | 36 | - | - | -33.1 | 52.4 | 21.2 | 0.65 | 138 | 7.67 | 0.013 | 1.8 | 13.8 |
| fen-5-c13 | -45.6 | 137 | 381 | -149 | -106 | - | - | - | - | - | - | - | - | - |
| fen-7-c13 | -47.3 | 151 | 657 | -164 | -110 | -33.3 | 59.0 | 21.3 | 0.66 | 135 | 7.67 | 0.013 | 1.7 | 14.4 |
| fen-8-c13 | -46.6 | 158 | 123 | - | - | -33.3 | 59.3 | 21.4 | 0.67 | 134 | 7.67 | 0.013 | 1.7 | 21.2 |
| fen-9-c13 | -56.7 | 165 | 29 | - | - | -33.2 | 64.4 | 21.3 | 0.66 | 136 | 7.67 | 0.013 | 1.7 | 18.6 |
| fen-10-c13 | -53.9 | 172 | 169 | - | -137 | -33.3 | 59.7 | 21.3 | 0.66 | 135 | 7.67 | 0.013 | 1.7 | 19.4 |
| fen-11-c13 | -53.3 | 179 | 37 | - | - | -33.3 | 59.1 | 21.4 | 0.66 | 135 | 7.67 | 0.013 | 1.7 | 23.5 |
| fen-13-c13 | -41.3 | 207 | 35 | - | - | -34.1 | 63.1 | 22.2 | 0.69 | 122 | 7.67 | 0.013 | 1.6 | 27.7 |
| fen-14-c13 | -46.4 | 217 | 486 | -160 | -113 | -33.8 | 67.1 | 21.9 | 0.68 | 127 | 7.67 | 0.013 | 1.6 | 20.7 |
| fen-16-c13 | -46.5 | 232 | 258 | -168 | -132 | -33.3 | 67.4 | 21.4 | 0.66 | 135 | 7.67 | 0.013 | 1.7 | 21.1 |
| fen-17-c13 | -42.9 | 247 | 279 | -166 | -128 | -34.9 | 69.7 | 23.0 | 0.73 | 109 | 7.67 | 0.013 | 1.4 | 22.4 |
| fen-18-c13 | -37.9 | 256 | 12 | - | - | -35.5 | 60.0 | 23.7 | 0.75 | 99 | 7.67 | 0.013 | 1.3 | 19.8 |
| fen-19-c13 | -43.9 | 262 | 16 | - | - | -32.4 | 68.4 | 20.5 | 0.63 | 149 | 7.67 | 0.013 | 1.9 | 15.6 |
| fen-20-c13 | -42.1 | 269 | 12 | - | - | -32.9 | 67.7 | 20.9 | 0.65 | 142 | 7.67 | 0.013 | 1.8 | 16.2 |
| fen-21-c13 | -43.0 | 276 | 3 | - | - | -32.4 | 69.7 | 20.5 | 0.63 | 149 | 7.67 | 0.013 | 1.9 | 15.8 |
| fen-22-c13 | -39.8 | 284 | 26 | - | - | -33.7 | 70.6 | 21.8 | 0.68 | 128 | 7.67 | 0.013 | 1.6 | 17.7 |
| fen-23-c13 | -41.9 | 291 | 19 | - | - | -33.6 | 67.6 | 21.7 | 0.67 | 130 | 7.67 | 0.013 | 1.7 | 13.7 |
| ***Phalaris arundinacea*** | | | | | | | | | | | | | | |
| fen-1-d13 | -48.4 | 113 | 122 | -170 | -128 | -38.8 | 54.3 | 27.2 | 0.89 | 44 | 1.58 | 0.012 | 0.5 | 10.4 |
| fen-2-d13 | -49.4 | 116 | 3805 | -191 | -149 | -39.0 | 46.4 | 27.5 | 0.90 | 40 | 1.58 | 0.012 | 0.5 | 11.1 |
| fen-3-d13 | -46.3 | 123 | 163 | -185 | -146 | -39.4 | 52.4 | 27.9 | 0.92 | 33 | 1.58 | 0.012 | 0.4 | 11.1 |
| fen-4-d13 | -48.1 | 130 | 938 | -207 | -167 | -36.6 | 52.4 | 24.9 | 0.80 | 80 | 1.58 | 0.012 | 1.0 | 13.8 |
| fen-5-d13 | -45.6 | 137 | 743 | -187 | -148 | -36.5 | 61.9 | 24.7 | 0.79 | 83 | 1.58 | 0.012 | 1.0 | 13.3 |

| | | | | | | | | | | | | | | |
|---|---|---|---|---|---|---|---|---|---|---|---|---|---|---|
| fen-7-d13 | -47.3 | 151 | 892 | -199 | -159 | -37.8 | 59.0 | 26.1 | 0.85 | 61 | 1.58 | 0.012 | 0.7 | 14.4 |
| fen-8-d13 | -46.6 | 158 | 1196 | -218 | -179 | -36.6 | 59.3 | 24.9 | 0.80 | 80 | 1.58 | 0.012 | 1.0 | 21.2 |
| fen-9-d13 | -56.7 | 165 | 874 | -216 | -169 | -38.7 | 64.4 | 27.1 | 0.89 | 45 | 1.58 | 0.012 | 0.6 | 18.6 |
| fen-10-d13 | -53.9 | 172 | 338 | -224 | -180 | -38.6 | 59.7 | 27.0 | 0.88 | 47 | 1.58 | 0.012 | 0.6 | 19.4 |
| fen-11-d13 | -53.3 | 179 | 223 | -227 | -183 | -38.6 | 59.1 | 27.0 | 0.88 | 47 | 1.58 | 0.012 | 0.6 | 23.5 |
| fen-12-d13 | -51.0 | 186 | 199 | -212 | -169 | -38.2 | 72.4 | 26.6 | 0.87 | 53 | 1.58 | 0.012 | 0.7 | 24.4 |
| fen-13-d13 | -41.3 | 207 | 387 | -221 | -187 | -38.5 | 63.1 | 26.9 | 0.88 | 48 | 1.58 | 0.012 | 0.6 | 27.7 |
| fen-14-d13 | -46.4 | 217 | 843 | -219 | -181 | -38.1 | 67.1 | 26.5 | 0.86 | 55 | 1.58 | 0.012 | 0.7 | 20.7 |
| fen-15-d13 | -41.7 | 225 | 1067 | -216 | -182 | -38.1 | 60.6 | 26.4 | 0.86 | 56 | 1.58 | 0.012 | 0.7 | 21.2 |
| fen-16-d13 | -46.5 | 232 | 239 | -210 | -172 | -38.1 | 67.4 | 26.5 | 0.86 | 55 | 1.58 | 0.012 | 0.7 | 21.1 |
| fen-17-d13 | -42.9 | 247 | 822 | -223 | -189 | -35.8 | 69.7 | 24.1 | 0.77 | 93 | 1.58 | 0.012 | 1.1 | 22.4 |
| fen-18-d13 | -37.9 | 256 | 560 | -213 | -182 | -36.8 | 60.0 | 25.1 | 0.81 | 76 | 1.58 | 0.012 | 0.9 | 19.8 |
| fen-19-d13 | -43.9 | 262 | 432 | -218 | -182 | -38.3 | 68.4 | 26.7 | 0.87 | 52 | 1.58 | 0.012 | 0.6 | 15.6 |
| fen-20-d13 | -42.1 | 269 | 366 | -223 | -189 | -38.2 | 67.7 | 26.6 | 0.87 | 53 | 1.58 | 0.012 | 0.7 | 16.2 |
| fen-21-d13 | -43.0 | 276 | 456 | -223 | -188 | -39.0 | 69.7 | 27.4 | 0.90 | 41 | 1.58 | 0.012 | 0.5 | 15.8 |
| fen-22-d13 | -39.8 | 284 | 69 | -215 | -182 | -37.7 | 70.6 | 26.0 | 0.85 | 62 | 1.58 | 0.012 | 0.8 | 17.7 |
| ***Corylus americana*** | | | | | | | | | | | | | | |
| fen-1-f13 | -48.4 | 113 | 7152 | -182 | -140 | -38.2 | 54.3 | 26.6 | 0.87 | 53 | 0.53 | 0.011 | 0.6 | 10.4 |
| fen-2-f13 | -49.4 | 116 | 8528 | -196 | -154 | -35.9 | 46.4 | 24.1 | 0.77 | 93 | 0.53 | 0.011 | 1.1 | 11.1 |
| fen-3-f13 | -46.3 | 123 | 4517 | -189 | -149 | -36.9 | 52.4 | 25.2 | 0.81 | 75 | 0.53 | 0.011 | 0.8 | 11.1 |
| fen-4-f13 | -48.1 | 130 | 7208 | -179 | -138 | -35.8 | 52.4 | 24.1 | 0.77 | 93 | 0.53 | 0.011 | 1.1 | 13.8 |
| fen-5-f13 | -45.6 | 137 | 792 | -147 | -106 | -36.3 | 61.9 | 24.5 | 0.78 | 86 | 0.53 | 0.011 | 1.0 | 13.3 |
| fen-6-f13 | -46.5 | 144 | 947 | -141 | -99 | -39.7 | 65.9 | 28.2 | 0.93 | 28 | 0.53 | 0.011 | 0.3 | 18.2 |
| fen-7-f13 | -47.3 | 151 | 539 | -144 | -101 | -39.3 | 59.0 | 27.7 | 0.91 | 36 | 0.53 | 0.011 | 0.4 | 14.4 |
| fen-8-f13 | -46.6 | 158 | 1423 | -144 | -103 | -40.0 | 59.3 | 28.5 | 0.94 | 24 | 0.53 | 0.011 | 0.3 | 21.2 |

| | | | | | | | | | | | | | | |
|---|---|---|---|---|---|---|---|---|---|---|---|---|---|---|
| fen-9-f13 | -56.7 | 165 | 240 | -155 | -105 | -39.8 | 64.4 | 28.3 | 0.93 | 27 | 0.53 | 0.011 | 0.3 | 18.6 |
| fen-10-f13 | -53.9 | 172 | 1207 | -145 | -96 | -40.6 | 59.7 | 29.1 | 0.97 | 14 | 0.53 | 0.011 | 0.2 | 19.4 |
| fen-11-f13 | -53.3 | 179 | 2524 | -155 | -107 | -40.1 | 59.1 | 28.6 | 0.94 | 23 | 0.53 | 0.011 | 0.3 | 23.5 |
| fen-12-f13 | -51.0 | 186 | 1469 | -146 | -101 | -40.3 | 72.4 | 28.7 | 0.95 | 20 | 0.53 | 0.011 | 0.2 | 24.4 |
| fen-13-f13 | -41.3 | 207 | 617 | -153 | -116 | -40.4 | 63.1 | 28.9 | 0.96 | 17 | 0.53 | 0.011 | 0.2 | 27.7 |
| fen-14-f13 | -46.4 | 217 | 2395 | -148 | -106 | -40.2 | 67.1 | 28.7 | 0.95 | 20 | 0.53 | 0.011 | 0.2 | 20.7 |
| fen-15-f13 | -41.7 | 225 | 348 | -156 | -119 | -40.7 | 60.6 | 29.2 | 0.97 | 12 | 0.53 | 0.011 | 0.1 | 21.2 |
| fen-16-f13 | -46.5 | 232 | 218 | - | - | -40.7 | 67.4 | 29.2 | 0.97 | 13 | 0.53 | 0.011 | 0.1 | 21.1 |
| fen-17-f13 | -42.9 | 247 | 521 | -150 | -112 | -40.9 | 69.7 | 29.4 | 0.98 | 9 | 0.53 | 0.011 | 0.1 | 22.4 |
| fen-18-f13 | -37.9 | 256 | 332 | -144 | -111 | -40.8 | 60.0 | 29.3 | 0.97 | 11 | 0.53 | 0.011 | 0.1 | 19.8 |
| fen-19-f13 | -43.9 | 262 | 2067 | -156 | -117 | -40.7 | 68.4 | 29.2 | 0.97 | 13 | 0.53 | 0.011 | 0.1 | 15.6 |
| fen-20-f13 | -42.1 | 269 | 410 | -154 | -117 | -41.0 | 67.7 | 29.5 | 0.98 | 7 | 0.53 | 0.011 | 0.1 | 16.2 |
| fen-21-f13 | -43.0 | 276 | 593 | -170 | -133 | -41.9 | 69.7 | 30.5 | 1.02 | - | - | - | - | - |
| fen-22-f13 | -39.8 | 284 | 510 | -169 | -134 | -40.8 | 70.6 | 29.3 | 0.97 | 11 | 0.53 | 0.011 | 0.1 | 17.7 |
| fen-23-f13 | -41.9 | 291 | 852 | -151 | -114 | -42.7 | 67.6 | 31.37 | 1.05 | - | - | - | - | - |
| **Sediments** | | | | | | | | | | | | | | |
| Fen-2 | -49.4 | 116 | 25201 | -170 | -127 | -32.7 | 46.4 | 20.7 | 0.64 | 145 | - | - | - | 11.1 |
| Fen-3 | -46.3 | 123 | - | -174 | -134 | -32.8 | 52.4 | 20.8 | 0.64 | 143 | - | - | - | 11.1 |
| Fen-4 | -48.1 | 130 | - | -178 | -131 | -32.5 | 52.4 | 20.5 | 0.63 | 148 | - | - | - | 13.8 |
| Fen-5 | -45.6 | 137 | 1479 | -174 | -130 | -32.4 | 61.9 | 20.5 | 0.63 | 149 | - | - | - | 13.3 |
| Fen-7 | -47.3 | 151 | 52707 | -168 | -126 | -32.8 | 59.0 | 20.9 | 0.64 | 142 | - | - | - | 14.4 |
| Fen-8 | -46.6 | 158 | 12988 | -174 | -126 | -32.1 | 59.3 | 20.2 | 0.62 | 154 | - | - | - | 21.2 |
| Fen-9 | -56.7 | 165 | 9502 | -168 | -116 | -32.8 | 64.4 | 20.9 | 0.64 | 142 | - | - | - | 18.6 |
| Fen-10 | -53.9 | 172 | 4413 | -166 | -111 | -33.0 | 59.7 | 21.1 | 0.65 | 139 | - | - | - | 19.4 |
| Fen-11 | -53.3 | 179 | 12421 | -171 | -118 | -32.5 | 59.1 | 20.5 | 0.63 | 148 | - | - | - | 23.5 |

| | | | | | | | | | | | | | | |
|---|---|---|---|---|---|---|---|---|---|---|---|---|---|---|
| Fen-12 | -51.0 | 186 | 16454 | -168 | -119 | -33.1 | 72.4 | 21.2 | 0.65 | 138 | - | - | - | 24.4 |
| Fen-13 | -41.3 | 207 | 4094 | -165 | -128 | - | - | - | - | - | - | - | - | 27.7 |
| Fen-14 | -46.4 | 217 | 4247 | -169 | -130 | -33.0 | 67.1 | 21.1 | 0.65 | 139 | - | - | - | 20.7 |
| Fen-15 | -41.7 | 225 | 2354 | -166 | -124 | -32.9 | 60.6 | 21.0 | 0.65 | 141 | - | - | - | 21.2 |
| Fen-16 | -46.5 | 232 | 4113 | -163 | -124 | -32.7 | 67.4 | 20.8 | 0.64 | 144 | - | - | - | 21.1 |
| Fen-17 | -42.9 | 247 | 3824 | -170 | -134 | -32.3 | 69.7 | 20.4 | 0.62 | 150 | - | - | - | 22.4 |
| Fen-18 | -37.9 | 256 | 1701 | -169 | -134 | -33.5 | 60.0 | 21.6 | 0.67 | 131 | - | - | - | 19.8 |
| Fen-19 | -43.9 | 262 | 5074 | -169 | -128 | -32.7 | 68.4 | 20.8 | 0.64 | 145 | - | - | - | 15.6 |
| Fen-20 | -42.1 | 269 | 4289 | -170 | -127 | -32.5 | 67.7 | 20.6 | 0.63 | 147 | - | - | - | 16.2 |
| Fen-21 | -43.0 | 276 | 5963 | -173 | -136 | -32.7 | 69.7 | 20.8 | 0.64 | 144 | - | - | - | 15.8 |
| Fen-22 | -39.8 | 284 | 4242 | -178 | -144 | -33.9 | 70.6 | 22.1 | 0.69 | 124 | - | - | - | 17.7 |
| Fen-23 | -41.9 | 291 | 477 | -170 | -134 | -32.7 | 67.6 | 20.7 | 0.64 | 145 | - | - | - | ### |

* " - " indicates no data

[a] An = CO2 Assimilation rate

[b] °C = Mean Daily Temperature

# CHAPTER FIVE

# A multivariate approach to polycyclic aromatic hydrocarbon (PAH) source apportionment in sediments and soils in the New England (USA) region using compound specific hydrogen and carbon isotopes

**Abigail M. Oakes**[a],

Gregory M. Harris[b], Chad E. Fagan[b], Michael T. Hren[ab]

[a] *Department of Chemistry, 55 N. Eagleville Rd., University of Connecticut, Storrs CT 06269, USA*

[b] *Center for Integrative Geosciences, 345 Mansfield Rd., University of Connecticut, Storrs CT 06269, USA*

## 5.1.0 ABSTRACT

Polycyclic aromatic hydrocarbons (PAHs) are ubiquitous environmental pollutants of particular concern due to their mutagenic and carcinogenic properties. Identifying the source and movement of these compounds in the environment poses a significant challenge. Molecular distributions and stable isotopic compositions of PAHs vary as a function of both source and production/degradation processes and therefore provide an opportunity for delineating origin and transport through the natural system. Here we utilize a multivariate approach to identify spatial variations in source materials, transport/degradation, and determine if there are differences in molecular and isotopic distributions of PAHs between sites dominated by aerial and aquatic modes of transport. We measured the concentration, $\delta^{13}C$, and $\delta D$ of 16 EPA priority PAHs in over 100 soil and sediment samples collected across Connecticut and Rhode Island, USA. Our data show that despite large variations in industrial activities and land use, the distribution of PAHs with different numbers of ring units remains fairly stable at all sites with percent distributions at 9.4 % 2-3 ring, 47.9 % 4 ring, and 42.8 % 5-6 ring compounds. The distribution of PAH compounds in the sediments indicate a mixture of pyrogenic and petrogenic sources with a majority of PAHs produced through pyrogenic means. While all sites are dominated by pyrogenic sources, carbon and hydrogen isotopes are highly variable, ranging from –29.6 to –20.6 ‰ and –131 to –33 ‰ respectively. Based on established endmember isotopic compositions the PAHs collected from Connecticut and Rhode Island are made up of a complex mixture of three main source materials: Liquid fossil fuels, low temperature coal combustion, and industrial contaminants.

## 5.2.0 INTRODUCTION

Polycyclic aromatic hydrocarbons (PAHs) are persistent organic pollutants that are comprised of two or more fused aromatic rings and are ubiquitous in the environment [1]. PAHs are a concern for both human and environmental health because they possess toxic characteristics, are environmentally persistent, bioaccumulate, and are prone to long-range transboundary atmospheric transport and deposition [2]. Although PAHs are naturally formed in un-combusted petroleum (petrogenic), the majority of PAHs in the environment are by-products of incomplete combustion of biomass (pyrogenic), such as wood and fossil fuels, including petroleum and coal [1,3,4]. Relative PAH abundances are generally indicative of PAH source, with pyrogenic sources in urban atmospheric dust depleted in lower molecular weight (2-3 ring) PAHs and petrogenic sources dominated by low molecular weight PAHs [5].

Recently there has been a surge of interest in measuring the spatial distribution of PAHs as a means of tracing environmental pollution from anthropogenic and natural sources [2,6–8]. PAHs are extensively used as molecular tracers of combustion-related airborne particles [4,9] because they are a major cause for numerous human health problems [10,11]. PAHs account for most of the total mutagenic activity of airborne particles (approx. 35-82% [12]) and are known to cause problems such as lung cancer, respiratory disease, and heart disease [10–12]. Due to these factors, a reduction of PAH emissions is necessary to improve overall air quality.

Atmospheric PAHs come from a multitude of sources (e.g. vehicle exhaust, power generation, cooking, asphalt surfaces, and industrial processes) however, identifying the sources of these compounds in the natural environment can be complicated due to the

variety of sources. A number of techniques are used to determine source or origin, however the majority use diagnostic ratios of PAHs [4,6,13]. Diagnostic ratios are a "fingerprinting" technique that differentiates pyrogenic and petrogenic sources by using molecular indices based on ratios of structural isomers [5,14,15]. These indices rely on the fact that low temperature production of PAHs (petrogenic) is governed by thermodynamic processes, whereas high temperature production (pyrogenic) is governed by kinetic processes [15]. Hence, PAH distribution and, more specifically, structural isomer distribution is temperature dependent and thus these indices can be used to determine the origin of PAHs in the environment [15]. These isomeric ratios, while useful in determining the PAH production methods (pyrogenic versus petrogenic), are not source specific, have considerable intra-source variability, and are limited to these bulk characterizations [13]. Diagnostic ratios discriminate between petroleum (petrogenic) or fire (pyrogenic) derived sources, however the diagnostic ratios are inconclusive with regards to identifying specific petrogenic or pyrogenic sources.

While there is an extensive body of literature regarding diagnostic ratios as a tool for determining PAH source, the carbon isotopic composition ($\delta^{13}C$) of an individual PAH molecule is a better tracer of PAH source [1]. The $\delta^{13}C$ composition of PAHs is determined solely from source materials and evaporation, photodecomposition, and microbial degradation have minimal effect on intrinsic carbon isotope composition of a PAH molecule relative to source materials [1,16–18]. Carbon isotopes provide a key tool for discriminating between PAH source [1,8,19], however , variations in $\delta^{13}C$ of PAHs produced from different sources have a small range and typically differ by only a few ‰ [20]. Compound specific hydrogen ($\delta D$) isotopes of PAHs in tandem with $\delta^{13}C$ can greatly

improve constraints on source apportionment of PAHs [1,20,21]. δD has a relatively large range in ‰ (sometimes greater than 100 ‰) and, used in combination with $\delta^{13}C$ and concentration data, represents a promising approach to PAH source determination.

Here we use a multivariate (δD, $\delta^{13}C$, and concentration) approach to examine the spatial variability in PAH source in areas with distinct land use, industrial activity, and potential mode of transport (airborne versus aquatic). The sites are located in both highly urbanized and mostly rural areas, to account for the varied land use strategies of the Connecticut-Rhode Island region. A duel compound specific isotope approach corroborated with general source appointment from diagnostic ratios provides a novel method to elucidate contributors from specific source materials.

## 5.3.0 SAMPLE COLLECTION AND METHODS

### *5.3.1 Study area*

We collected soils from 55 sites in Connecticut and Rhode Island, USA during Spring and Summer of 2015. The sampling area covered approximately 14,000 $km^2$ and is dominated by temperate broadleaf and mixed deciduous/coniferous forests containing oaks, beech, hickories, maple, and various conifer species. Coastal salt marshes have distinct zones of vegetation, with tall saltmarsh cordgrass grown along the water's edge, salt-meadow cordgrass and spike grass in the high marsh, and glasswort in the salt pannes. Sample sites span a range of land uses and land use histories and are characterized by large regional variabilities in urbanization [22]. In general, samples sites range from 1.10 km from the city center to 27.04 km from the city center.

Hartford CT has a humid continental climate with cold winter and warm humid summers with average rainfall of approximately 112 cm/year. The Greater Hartford

Metropolitan is the largest metro in the state and spans approximately 110 $km^2$ and 3 cities: East Hartford, Hartford, and West Hartford. The temperatures in Hartford and the majority of inland sampling sites range from an average of –9 °C in January to 17 °C in July [23]. New London has a southern coastal climate which is similar to the continental climate of Hartford, however seasonal extremes are tempered by proximity to the Atlantic Ocean leading to slightly warmer winters and a longer frost-free season. The region receives approximately 190 cm/yr precipitation and the temperature ranges from a mean of –5 °C in January to 18 °C in July [23].

### *5.3.2 Study design and sample collection*

Sample locations were chosen to examine spatial variations in molecular distributions and isotopic differences in a variety of urban and rural areas in both inland and coastal environments. Furthermore, these sites were chosen to specifically differentiate between sites that are affected only by atmospheric or local production and deposition, and those that are biased by both airborne and aquatic transport. We collected samples of modern soil and sediment samples from 55 urban and rural sites (Table 5.10). All sites were located in state or city parks, a minimum of 35 meters away from roadways, parking areas, and walking paths in locations where routine maintenance does not occur to minimize any localized contamination. At each site, a minimum of two samples were taken within 4.5 m of each other to characterize site heterogeneity. PAHs in Connecticut are transported through two main pathways: airborne depositions and aquatic transport. Our samples are separated into three distinct categories based on the types of transport possible at that site. First is airborne, for sites that are only subject to deposition from the atmosphere. Second is riverine, for samples collected from fluvial sediments and subject

to transport and mobilization by freshwater. Lastly is marine, for samples located in saltmarshes where sediments are subject to transport and mobilization by salt water.

Sediments and soils were collected from the top 1 to 5 cm depth after any loose brush, wood chips, etc. associated with the O horizon were removed. Approximately 200 to 400 g of sample was placed in a 0.25 L polyethylene bag and transported in a cool, dry container until they returned to the University of Connecticut where these were frozen at –20 °C prior to sample preparation.

Table 5.10 Sampling Locations, abbreviations, latitudes and longitudes, and mass sediment/soil extracted

| **Sampling Site** | **Abb.** | **Lat (N)** | **Long (W)** | **Mass Extracted** |
|---|---|---|---|---|
| Aslop A | ASA | 41.80417 | -72.81889 | 115.8 |
| Aslop B | ASB | 41.80417 | -72.81889 | 181.2 |
| Batterson A | BAA | 41.71583 | -72.78750 | 107.7 |
| Batterson B | BAB | 41.71583 | -72.78750 | 136.8 |
| Bluff Point A | BPA | 41.33361 | -72.03222 | 109.7 |
| Bluff Point B | BPB | 41.33361 | -72.03222 | 109.1 |
| C. Mount A | CMA | 41.76583 | -72.48250 | 68.7 |
| C. Mount B | CMB | 41.76583 | -72.48250 | 101.9 |
| C.M. Park A | CPA | 41.78667 | -72.62556 | 174.4 |
| C.M. Park B | CPB | 41.78667 | -72.62556 | 164.2 |
| Camp O. A | COA | 41.47667 | -72.15278 | 87.5 |
| Camp O. B | COB | 41.47667 | -72.15278 | 81.9 |
| Charlestown D. | CHD | 41.35111 | -71.71917 | 94.1 |
| Charlestown S. | CHS | 41.35111 | -71.71917 | 30.6 |
| Clark A | CLA | 41.64139 | -72.55917 | 74.4 |
| Clark B | CLB | 41.64139 | -72.55917 | 48.9 |
| Deadmans D. | DMD | 41.61160 | -72.62310 | 125.0 |
| Deadmans S. | DMS | 41.61160 | -72.62310 | 50.1 |
| Drake A | DKA | 41.87250 | -72.80028 | 95.7 |
| Drake B | DKB | 41.87250 | -72.80028 | 22.8 |
| Elys Ferry D. | EFD | 41.60944 | -72.62389 | 33.9 |
| Elys FerryS. | EFS | 41.60944 | -72.62389 | 24.2 |
| Fort T. A | FTA | 41.34361 | -72.09472 | 168.9 |
| Fort T. B | FTB | 41.34361 | -72.09472 | 163.8 |

| | | | | |
|---|---|---|---|---|
| Gay City A | GCA | 41.73167 | -72.44028 | 98.1 |
| Gay City B | GCB | 41.73167 | -72.44028 | 79.9 |
| Goodwin A | GWA | 41.69361 | -72.69028 | 121.9 |
| Goodwin B | GWB | 41.69361 | -72.69028 | 97.5 |
| Gorman A | GMA | 41.73611 | -72.59500 | 98.1 |
| Gorman B | GMB | 41.73611 | -72.59500 | 135.1 |
| Great Oak A | GOA | 41.39750 | -72.00700 | 163.8 |
| Great Oak B | GOB | 41.39750 | -72.00700 | 71.2 |
| Great River A | GRA | 41.75833 | -72.65889 | 126.5 |
| Great River B | GRB | 41.75833 | -72.65889 | 166.1 |
| Hains Park A | HPA | 41.36167 | -72.29500 | 61.0 |
| Hains Park B | HPB | 41.36167 | -72.29500 | 187.0 |
| Haley Woods A | HWA | 41.39556 | -72.00694 | 22.0 |
| Haley Woods B | HWB | 41.39556 | -72.00694 | 30.1 |
| Hammock Point | HP | 41.25889 | -72.51778 | 38.2 |
| Island Ave. D. | IAD | 41.31690 | -72.01830 | 49.8 |
| Island Ave. S. | IAS | 41.31690 | -72.01830 | 70.3 |
| Lyman Allen A | LAA | 41.42083 | -72.13167 | 116.5 |
| Lyman Allen B | LAB | 41.42083 | -72.13167 | 106.7 |
| Manchester A | MCA | 41.77667 | -72.52778 | 134.9 |
| Manchester B | MCB | 41.77667 | -72.52778 | 110.3 |
| Mills Wood A | MWA | 41.69028 | -72.80389 | 94.6 |
| Mills Wood B | MWB | 41.69028 | -72.80389 | 114.7 |
| Morea A | MRA | 41.71833 | -72.88861 | 79.5 |
| Morea B | MRB | 41.71833 | -72.88861 | 60.6 |
| Municipal A | MPA | 41.57250 | -72.56111 | 155.5 |
| Municipal B | MPB | 41.57250 | -72.56111 | 132.2 |
| Nassahegon A | NSA | 41.75528 | -72.93972 | 53.9 |
| Nassahegon B | NAB | 41.75528 | -72.93972 | 97.0 |
| Nehantic A | NHA | 41.41667 | -72.26528 | 89.5 |
| Nehantic B | NHB | 41.41667 | -72.26528 | 74.9 |
| Nepaug A | NPA | 41.85167 | -72.95778 | 114.4 |
| Nepaug B | NPB | 41.85167 | -72.95778 | 96.2 |
| Northwest A | NWA | 41.94750 | -72.70194 | 140.6 |
| Northwest B | NWB | 41.94750 | -72.70194 | 158.4 |
| Ocean Beach A | OBA | 41.30111 | -72.10139 | 110.1 |
| Ocean Beach B | OBB | 41.30111 | -72.10139 | 133.6 |
| Old Lyme | OL | 41.31389 | -72.33750 | 64.2 |
| Old Saybrook | OS | 41.27889 | -72.39306 | - |

| | | | | |
|---|---|---|---|---|
| Parkway A | PWA | 41.37333 | -72.18167 | 141.8 |
| Parkway B | PWB | 41.37333 | -72.18167 | 131.9 |
| Peace Nature A | PNA | 41.36694 | -71.97389 | 133.0 |
| Peace Nature B | PNB | 41.36694 | -71.97389 | 149.9 |
| Plainville A | PVA | 41.71694 | -72.88194 | 40.4 |
| Plainville B | PVB | 41.71694 | -72.88194 | 91.9 |
| Pope Park A | PPA | 41.75833 | -72.69806 | 109.1 |
| Pope Park B | PPB | 41.75833 | -72.69806 | 143.6 |
| Poquetanck A | PQA | 41.46850 | -72.06610 | 170.0 |
| Poquetanck B | PQB | 41.46850 | -72.06610 | 141.3 |
| Ragged A | RGA | 41.62806 | -72.80389 | 94.3 |
| Ragged B | RGB | 41.62806 | -72.80389 | 82.6 |
| Riverside Hart A | RHA | 41.77528 | -72.66667 | 108.8 |
| Riverside Hart B | RHB | 41.77528 | -72.66667 | 98.7 |
| Riverside Park A | RPA | 41.36750 | -72.09694 | 88.3 |
| Riverside Park B | RPB | 41.36750 | -72.09694 | 63.3 |
| Rocky Neck | RN | 41.30250 | -72.24500 | 101.3 |
| Salmon Brook A | SBA | 41.94778 | -72.79722 | 152.2 |
| Salmon Brook B | SBB | 41.94778 | -72.79722 | 160.7 |
| Salmon River A | SRA | 41.62222 | -72.42278 | 159.4 |
| Salmon River B | SRB | 41.62222 | -72.42278 | 212.4 |
| Sand Hill A | SHA | 41.84111 | -72.55056 | 54.5 |
| Sand Hill B | SHB | 41.84111 | -72.55056 | 72.7 |
| Sand Hill Rd. A | SNA | 41.57328 | -72.61085 | 165.2 |
| Sand Hill Rd. B | SNB | 41.57328 | -72.61085 | 115.5 |
| Scantic A | SCA | 41.83833 | -72.54667 | 164.1 |
| Scantic B | SCB | 41.83833 | -72.54667 | 153.3 |
| Spice A | SIA | 41.75833 | -72.76389 | 179.2 |
| Spice B | SIB | 41.75833 | -72.76389 | 122.1 |
| Spring Park A | SPA | 41.93611 | -72.65444 | 164.3 |
| Spring Park B | SPB | 41.93611 | -72.65444 | 178.5 |
| Stanley A | STA | 41.69167 | -72.77472 | 205.1 |
| Stanley B | STB | 41.69167 | -72.77472 | 181.0 |
| Talcott Mtn A | TMA | 41.83944 | -72.79278 | 68.9 |
| Talcott Mtn B | TMB | 41.83944 | -72.79278 | 179.0 |
| Valley Falls A | VFA | 41.82278 | -72.44417 | 114.1 |
| Valley Falls B | VFB | 41.82278 | -72.44417 | 64.6 |
| Westerly D. | WD | 41.32683 | -71.78624 | 44.3 |
| Westerly S. | WS | 41.32683 | -71.78624 | 23.7 |

| | | | | |
|---|---|---|---|---|
| Williams A | WLA | 41.70333 | -72.55889 | 73.3 |
| Williams B | WLB | 41.70333 | -72.55889 | 64.2 |
| Windsor A | WDA | 41.81222 | -72.64722 | 125.5 |
| Windsor B | WDB | 41.81222 | -72.64722 | 109.8 |

### *5.3.3 Sample preparation*

Sediments and soils were freeze-dried (Labconco Freezone 4.5) prior to extraction. A minimum of 22 g of sediment or soil was extracted for 24 hours via Soxhlet extraction with approximately 300 mL of dichloromethane (DCM). The total lipid extract (TLE) was saponified with approximately 5 mL of 1M KOH in methanol (MeOH) and heated for 2 h at 85 °C. The reaction was cooled to room temperature, then quenched with 5 mL of 5 % sodium chloride. The neutral fraction was separated using liquid/liquid extraction for PAH separation.

The neutral fraction was then separated into three fractions based on molecular polarity using column chromatography. Silica gel columns were built using approximately 15-20 grams of silica in an ashed borosilicate pipette. The sample was added to the column and run through with 60 mL of hexanes to ensure complete removal of the abundant *n*-alkanes. The second fraction is slightly more polar and is collected using a 70:30 hexanes:DCM mixture. Approximately 60 to 90 mL of the second fraction is collected, depending on sample richness. The final fraction is the polar fraction where 30 mL of MeOH clears the remainder of the sample from the column.

### *5.3.4 PAH determination*

PAHs were dried at ~45 °C under a continuous flow of nitrogen and concentrated down to 2 mL and dissolved in toluene. PAH content in sediments and soils was determined by Thermo-Scientific Trace GC Ultra filter with a split-splitless (SSL) injector and flame ionization detector (FID) using a DB-5 column (60 m × 0.25 mm i.d., 0.25 µm) with He as the carrier (1.5 mL/min). The initial GC oven temperature was held at 70 °C for 3.80 minutes then warmed to 180 °C at 15 °C/min, followed by a ramp to 290 °C at 4.2 °C/min, ramp to 310 °C at 5.2 °C/min and held at 310 °C for 19.20 min.

A standard mix containing the EPA priority PAHs naphthalene (NAP), acenaphthene (ACE), acenaphthylene (ACY), fluorene (FLR), phenanthrene (PHE), anthracene (ANT), fluoranthene (FTN), pyrene (PYR), benzo (a) anthracene (BaA), chrysene (CHY), benzo (b) fluoranthene (BbF), benzo (k) fluoranthene (BkF), benzo (a) pyrene (BaP), dibenzo (a,h) anthracene (DahA), indeno (1,2,3-c,d) pyrene (IcdP), and benzo (g,h,i) perylene (BahiP) at 200 µg/mL in toluene was used for calibration (Restek SV Calibration Mix #5/610 PAH mix, Bellefonte PA, USA). All solvents were HPLC grade: Toluene, DCM, solvent extracted water, and hexanes were provided by Sigma Aldrich (Natick MA, USA).

### *5.3.5 Isotopic measurements*

Hydrogen and carbon isotopes of individual PAHs were measured using a Thermo GC-Isolink attached to a Thermo Scientific MAT 253 isotope ratio mass spectrometer (IRMS) with a 60 m × 0.25 µm ID, 0.25 nm film thickness BP-5 fused silica column with a helium carrier at a flow of 1.5 ml/min. The initial GC temperature was held at 90 °C for 1 min then warmed to 180 °C at 10 °C/min, followed by a ramp to 310 °C at 2 °C/min and

held for 19 minutes. The separated molecules were thermally decomposed to $H_2$ and $CO_2$ and isotopic ratios of compound specific hydrogen or carbon, respectively, were measured. We measured the $H_3^+$ factor daily prior to standard calibration and sample analysis and averaged 6.8 over the duration of analysis.

The isotopic compositions of individual PAHs were determined using in-house laboratory gas references and a suite of *n*-alkanes of known composition that were measured multiple times are at a range of concentrations (Mix A5 prepared by A. Schimmelmann). Typical standard deviation for hydrogen isotopes for repeated analysis of A. Schimmelmann's Mix A5 *n*-alkane isotope standard was less than 4 ‰ for a range of concentrations. Standard deviation for carbon isotope measurements for standards is less than 0.3 ‰ (1 σ).

## 5.4.0 RESULTS AND DISCUSSION

### *5.4.1 PAH Concentrations and Composition*

Sample locations vary from heavily wooded areas with mostly deciduous plant life to coastal salt marshes on the Long Island Sound. In addition, sample sites can be characterized by those sites that are subject to surface flooding by fresh or marine waters (and thus subject to potential marine transport of PAHs) and those outside the reach of fluvial transport and subject only to local or airborne deposition of PAHs. All locations were rich in organic matter, which favor PAH accumulation [1]. The content of PAHs (sum of 16 EPA PAHs) in Connecticut and Rhode Island sediments and soils range from 17.0 ng/g to 5452 ng/g dry material (Table 5.11). The site with the highest concentration is located 22.5 km south-east of the city of Hartford on the banks of the Connecticut River, while the lowest concentration of PAHs is located 24.5 km northwest of Hartford.

Table 5.11 Concentration and diagnostic ratios of sampling locations

| Sample | PAH ng/g | $PAH_{heavy}$ ng/g* | %O.M. ** | FLT/ (FLT+PYR) | BaA/ (BaA+CHR) | LMW/ HMW |
|---|---|---|---|---|---|---|
| ASA | - | - | 23.55 | - | - | - |
| ASB | 2697 | 1244.83 | 2.40 | 0.52 | 0.32 | 0.10 |
| BAA | 208.3 | 189.75 | 11.59 | 0.66 | 0.26 | 0.03 |
| BAB | 4315 | 1552.85 | 8.16 | 0.50 | 0.33 | 0.22 |
| BPA | 150.4 | 107.52 | 9.68 | 0.58 | 0.27 | 0.11 |
| BPB | 168.4 | 152.63 | 12.84 | 0.75 | 0.30 | 0.06 |
| CMA | - | 182.22 | 15.73 | - | - | - |
| CMB | 174.6 | 106.91 | 8.94 | 0.54 | 0.35 | 0.12 |
| CPA | 115.1 | 58.60 | 3.81 | 0.55 | 0.40 | 1.05 |
| CPB | 81.8 | 84.59 | 4.65 | 0.58 | 0.37 | 0.05 |
| COA | 37.7 | 38.39 | 12.38 | 0.53 | 0.32 | 0.00 |
| COB | 103.7 | 91.39 | 22.27 | 0.53 | 0.33 | 0.05 |
| CHD | 355.0 | 352.35 | 37.36 | - | - | 0.16 |
| CHS | 726.2 | 275.62 | 30.61 | - | 0.61 | 0.22 |
| CLA | 528.8 | 236.35 | 18.17 | 0.57 | 0.32 | 0.18 |
| CLB | 4870 | 1841.68 | 42.45 | 0.51 | 0.34 | 0.19 |
| DMD | - | 405.51 | - | - | - | - |
| DMS | - | 693.78 | 17.38 | - | - | - |
| DKA | - | 76.76 | 13.79 | - | - | - |
| DKB | 1852 | 1444.01 | 50.64 | 0.55 | 0.33 | 0.02 |
| EFD | 1812 | 1288.02 | 33.91 | - | 0.43 | 0.34 |
| EFS | 2053 | 1078.08 | 24.22 | - | 0.42 | 0.31 |
| FTA | 99.8 | 74.59 | 2.20 | 0.56 | 0.33 | 0.00 |
| FTB | 244.0 | 162.99 | 4.49 | 0.52 | 0.38 | 0.08 |
| GCA | - | 39.33 | 12.73 | - | - | - |
| GCB | - | 41.38 | 16.62 | - | - | - |
| GWA | 1289 | 586.10 | 9.37 | 0.58 | 0.31 | 0.20 |
| GWB | 1660 | 842.28 | 19.93 | 0.53 | 0.30 | 0.16 |
| GMA | 104.1 | 74.03 | 26.70 | 0.59 | 0.33 | 0.09 |
| GMB | 66.2 | 70.26 | 7.08 | 0.53 | 0.40 | 0.04 |
| GOA | 30.9 | 30.97 | 0.00 | 0.57 | 0.35 | 0.09 |
| GOB | 385.9 | 220.28 | 26.87 | 0.59 | 0.28 | 0.12 |
| GRA | 169.2 | 121.48 | 4.67 | 0.56 | 0.43 | 0.08 |
| GRB | 99.3 | 83.04 | 1.83 | 0.55 | 0.28 | 0.08 |
| HPA | 490.8 | 298.89 | 40.35 | 0.55 | 0.29 | 0.06 |
| HPB | 385.7 | 226.96 | 0.99 | 0.54 | 0.36 | 0.10 |
| HWA | 651.0 | 523.62 | 60.95 | 0.45 | 0.33 | 0.15 |

| | | | | | | |
|---|---|---|---|---|---|---|
| HWB | 969.7 | 439.97 | 30.58 | 0.54 | - | 0.25 |
| HP | 383.5 | 357.97 | 20.26 | 0.46 | 0.37 | - |
| IAD | 28.2 | 205.57 | - | 0.53 | - | - |
| IAS | 353.5 | 837.56 | 15.18 | 0.54 | 0.36 | 0.11 |
| LAA | 394.0 | 201.27 | 9.58 | 0.55 | 0.29 | 0.14 |
| LAB | 1042 | 515.23 | 9.06 | 0.55 | 0.29 | 0.12 |
| MCA | 55.0 | 55.15 | 5.48 | 0.66 | 0.30 | 0.08 |
| MCB | 106.1 | 83.75 | 7.05 | 0.62 | 0.30 | 0.11 |
| MWA | 105.5 | 129.28 | 12.16 | 0.72 | 0.30 | 0.03 |
| MWB | 947.2 | 573.33 | 10.61 | 0.56 | 0.34 | 0.06 |
| MRA | 288.1 | 164.86 | 15.64 | 0.59 | 0.32 | 0.12 |
| MRB | 675.7 | 380.35 | 33.88 | 0.56 | 0.22 | 0.12 |
| MPA | 79.0 | 64.29 | 5.36 | 0.62 | 0.40 | 0.08 |
| MPB | 3399 | 957.21 | 10.59 | 0.50 | 0.39 | 0.29 |
| NSA | 613.0 | 468.26 | 34.35 | 0.56 | 0.34 | 0.07 |
| NAB | 142.7 | 142.04 | 15.57 | 0.66 | - | - |
| NHA | 73.5 | 81.22 | 18.30 | 0.60 | 0.35 | 0.01 |
| NHB | - | - | 19.83 | - | - | - |
| NPA | 117.3 | 44.60 | 12.24 | 0.57 | 0.35 | 1.65 |
| NPB | 17.0 | 47.09 | 9.44 | - | - | - |
| NWA | 30.7 | 40.51 | 7.27 | 0.68 | 0.36 | 0.11 |
| NWB | 72.7 | 57.86 | 2.98 | 0.48 | 0.25 | 0.06 |
| OBA | 886.6 | 394.51 | 13.54 | 0.52 | 0.23 | 0.15 |
| OBB | 67.8 | 49.31 | 7.21 | 0.55 | 0.40 | 0.27 |
| OL | 869.7 | 388.77 | - | 0.41 | 0.41 | 0.42 |
| OS | 987.5 | 744.76 | 21.37 | - | - | - |
| PWA | 135.6 | 63.70 | 5.88 | - | - | - |
| PWB | 956.3 | 464.08 | 1.37 | 0.50 | 0.41 | 0.12 |
| PNA | 361.7 | 185.80 | 6.24 | 0.57 | 0.32 | 0.17 |
| PNB | 32.1 | - | 5.24 | - | - | - |
| PVA | 4027 | 1948.07 | 41.67 | 0.50 | 0.23 | 0.13 |
| PVB | 1556 | 933.79 | 13.22 | 0.55 | 0.29 | 0.12 |
| PPA | 138.5 | 102.68 | 7.28 | 0.82 | 0.30 | 0.20 |
| PPB | 95.6 | 71.04 | 7.68 | 0.88 | 0.28 | 0.19 |
| PQA | 873.0 | 300.02 | 32.06 | 0.51 | 0.37 | 0.23 |
| PQB | 1344 | 476.37 | 6.54 | 0.47 | 0.39 | 0.18 |
| RGA | 217.4 | 208.57 | 14.34 | - | 0.20 | 0.08 |
| RGB | - | - | 15.26 | - | - | - |
| RHA | 86.7 | 74.78 | 7.16 | 0.51 | 0.26 | 0.04 |
| RHB | 163.7 | 118.38 | 6.48 | 0.58 | 0.32 | 0.06 |
| RPA | 306.3 | 203.09 | 14.69 | 0.56 | 0.39 | 0.13 |

| | | | | | | |
|---|---|---|---|---|---|---|
| RPB | 819.1 | 494.70 | 30.53 | 0.58 | 0.32 | 0.08 |
| RN | 1842 | 1223.22 | 22.00 | 0.48 | 0.40 | 0.05 |
| SBA | 121.2 | 100.58 | 1.82 | 0.59 | 0.29 | 0.09 |
| SBB | 1779 | 638.12 | 5.79 | 0.52 | 0.36 | 0.23 |
| SRA | 2037 | 703.09 | 4.19 | 0.53 | 0.32 | 0.22 |
| SRB | 2440 | 618.57 | 9.27 | 0.53 | 0.43 | 0.31 |
| SHA | 239.2 | 164.04 | 39.72 | 0.54 | 0.23 | 0.04 |
| SHB | 174.7 | 125.86 | 27.04 | 0.58 | 0.34 | 0.09 |
| SNA | 5452 | 1528.49 | 3.71 | 0.51 | 0.43 | 0.30 |
| SNB | 4477 | 1766.04 | 7.58 | 0.52 | 0.31 | 0.15 |
| SCA | 128.7 | 93.90 | 1.44 | 0.77 | 0.30 | 0.04 |
| SCB | - | 31.12 | 2.22 | - | - | - |
| SIA | 877.8 | 398.91 | 3.69 | 0.58 | 0.31 | 0.20 |
| SIB | 147.6 | 140.55 | 11.21 | - | 0.22 | 0.07 |
| SPA | 188.0 | 110.76 | 3.78 | 0.63 | 0.27 | 0.09 |
| SPB | 158.3 | 116.35 | 4.67 | 0.60 | 0.32 | 0.06 |
| STA | 416.3 | 215.19 | 1.77 | 0.60 | 0.39 | 0.11 |
| STB | 334.0 | 174.88 | 3.25 | 0.69 | 0.33 | 0.14 |
| TMA | 131.0 | 92.74 | 24.55 | 0.66 | 0.34 | 0.13 |
| TMB | 96.4 | 80.03 | 2.52 | 0.64 | 0.36 | 0.12 |
| VFA | - | 207.33 | 12.45 | - | - | - |
| VFB | 608.5 | 340.03 | 32.30 | 0.55 | 0.38 | 0.10 |
| WD | 3426 | 2314.64 | 13.40 | 0.50 | 0.34 | 0.06 |
| WS | 849.8 | 582.02 | 58.21 | 0.50 | 0.38 | 0.03 |
| WLA | - | 80.63 | 26.05 | - | - | - |
| WLB | 279.8 | 174.98 | 30.29 | 0.60 | 0.25 | 0.08 |
| WDA | 180.5 | 106.08 | 6.93 | 0.55 | 0.23 | 0.07 |
| WDB | 238.9 | 167.82 | 6.64 | 0.71 | 0.27 | 0.06 |

"-" indicates below detection limit
*Heavy PAHs include 4-6 ring compounds
** O.M. = Organic Material

Previous data shows that most frequently, sites with extremely high PAH concentrations are commonly located in highly urbanized areas [1,2,5,24]. Contrary to these studies, sampling sites located within city limits have lower PAH concentrations than sites located in more rural areas (Figure 5.25). We find that sampling sites that have above 2000

ng/g of PAHs are located in areas that have less than 40 % urbanization, while the site with the highest concentration (5452.2 ng/g) was less than 20 % urbanized (Figure 5.26). Since all sampling locations were a minimum of 35 meters from roadways, industrial sites, parking lots, and other direct sources of PAH input, PAHs collected at all sites are most likely the result of transportation (atmospheric or aquatic) and deposition, rather than direct dumping of pollution onto a particular site. In general, vehicle exhaust is believed to be the main source of PAHs in urban atmospheres [25–29]. PAHs are mostly emitted in the gas phase where they are adsorbed onto preexisting small particles (< 2 μm) [29,30]. While adsorbed to particulates in the atmosphere, PAHs are subject to long range transport to remote and rural areas [31]. Since the wind in Connecticut travels from north to south over the city of Hartford [32], it is possible that PAHs emitted to the atmosphere in urban areas are transported outside the city center before accumulating in the sediments and soils, leading to the high concentrations of PAHs in the sediments and soils south of the city.

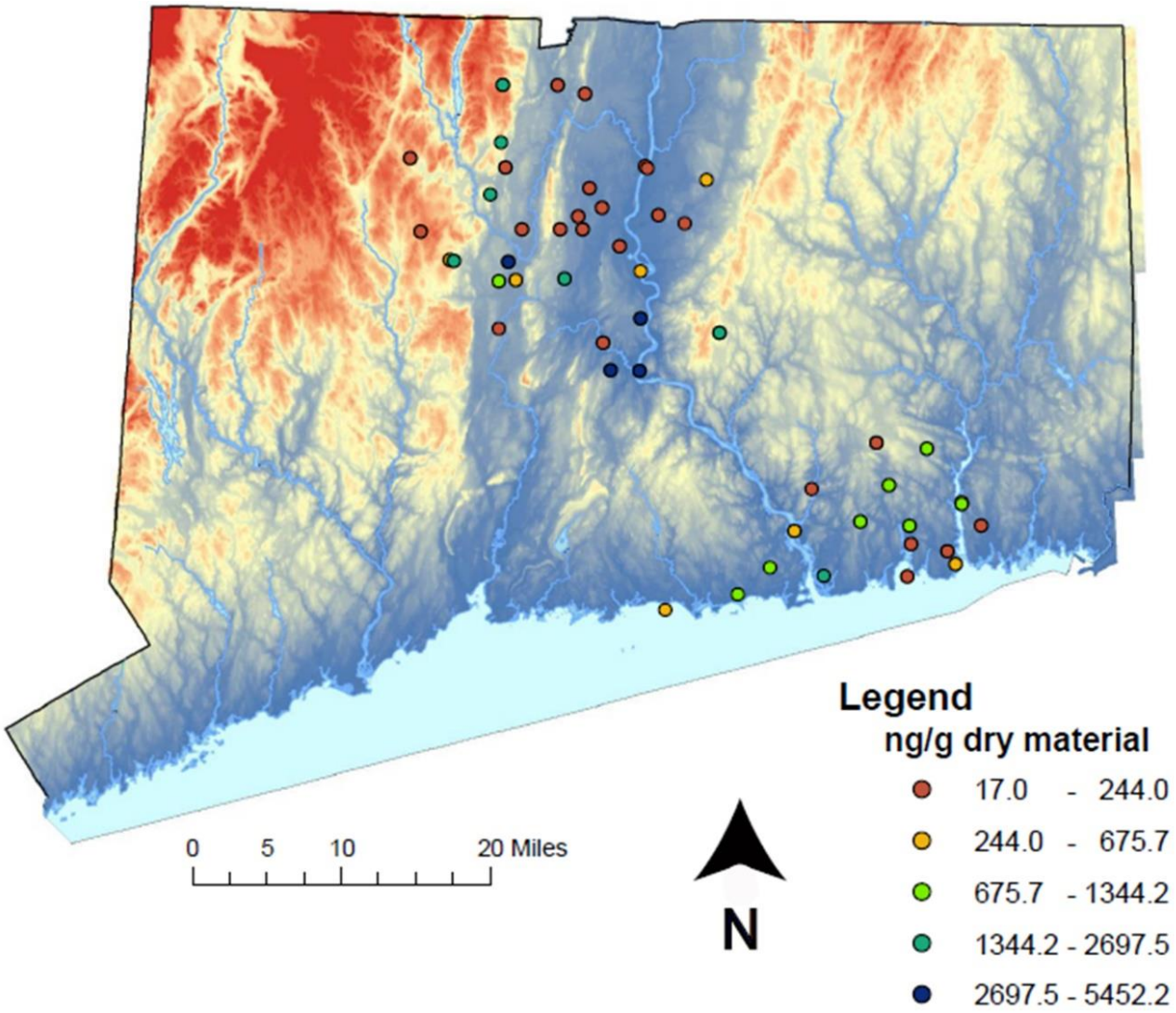


Figure 5.25 Positions of sampling sites and PAH concentrations throughout Connecticut, USA

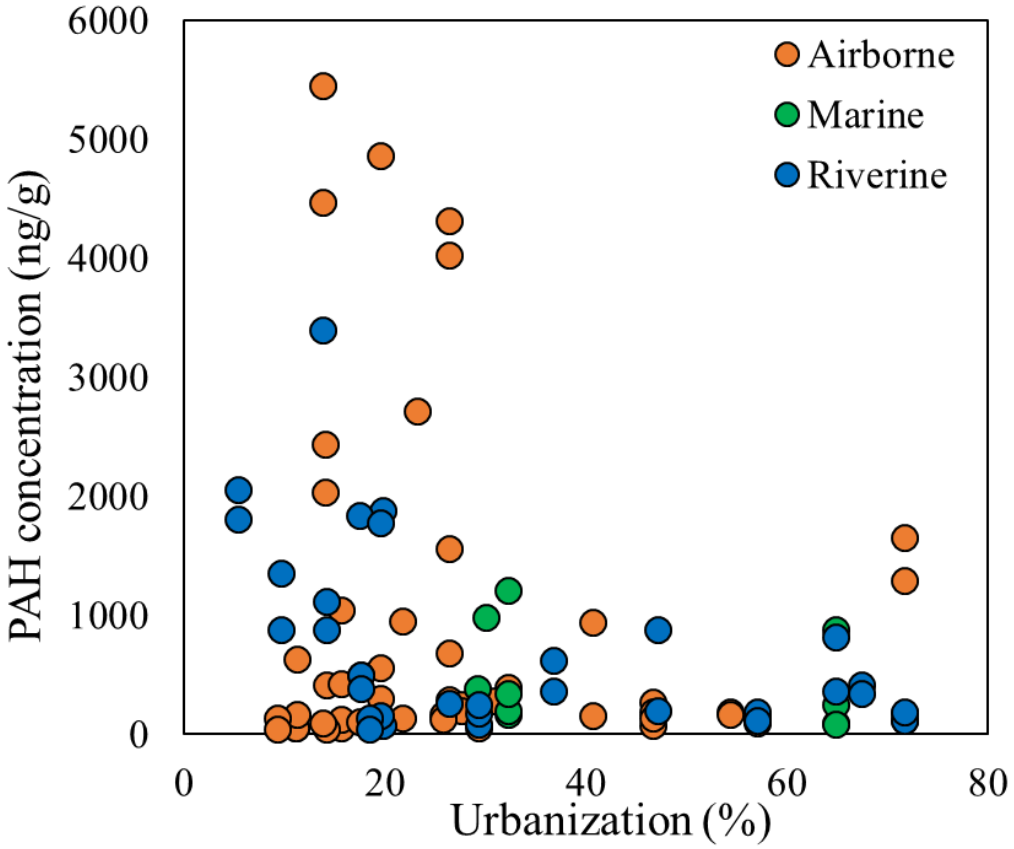


Figure 5.26 Percent urbanization and PAH concentration of sampling sites. Orange circles indicate areas that are only affected through air deposition, blue circles are samples affected by fluvial transport, and green circles represent coastal sampling sites affected by tidal shifts.

The relative abundances of PAHs are characteristic of PAH source [33,34]. Despite the large variations in concentrations throughout the sampling area, the molecular distributions of PAHs with varying ring numbers remain relatively identical (Supplementary Figure 5.32). Pyrogenic sources, such as those most often found in urban areas, tend to be depleted in (2-3 rings) PAHs and enriched in high molecular weight (4-6 ring) PAHs while petrogenic PAHs are enriched in low molecular weight PAHs [35,36]. The average percent by mass of petrogenic PAHs was 9.4 %, whereas 42.8 % (on average) of the overall PAHs contained in the soils and sediments consisted of pyrogenic PAHs. The majority of PAHs extracted from our soil and sediment samples were four ring compounds (47.9 %), which

indicates some mixing of petrogenic and pyrogenic PAHs (4 ring PAHs), with a significantly larger input of pyrogenic PAHs than petrogenic [5,37,38].

### *5.4.2 Diagnostic ratios and bulk source identification*

Diagnostic ratios (DR) are ratios of structural isomers of PAHs that are formed at various temperatures. Low temperatures produce thermodynamically stable PAHs whereas high temperatures form kinetically stable PAHs, thus PAH distribution is indicative of the temperature at which PAHs are formed [15]. These ratios are particularly helpful for bulk characterization of samples (pyrogenic versus petrogenic; Table 5.12). The BaA/ (BaA + CHR) and FLT/ (FLT + PYR) ratios ranged from 0.20 to 0.61 and 0.41 to 0.88 respectively (Table 5.11). The ratio of BaA/(BaA + CHR) separates samples into three distinct categories: values less than 0.2 indicate petroleum sources, between 0.2 and 0.35 indicate a mixed origin (petroleum and combustion sources), and above 0.35 indicates combustion sources (Table 5.12) [14]. Figure 5.27a shows the spatial distribution of BaA/ (BaA + CHR) at each sampling site. We found that the majority of inland samples (33 sites, 66 samples) had ratios between 0.2 and 0.35 (41 samples, approximately 20 sites) indicating mixed combustion and petroleum sources while the coastal samples separate into 15 mixed source and 15 pure combustion samples (Table 5.11).

Table 5.12 Diagnostic ratios for the determination of general PAH source

| **Ratios** | **Values/Source** | **Reference** |
|---|---|---|
| Fluoranthene/ (Fluoranthene +Pyrene) | < 0.4 petroleum source | Bakhtiari et al., 2009 |
| | 0.4-0.5 petroleum combustion | |
| | > 0.5 Combustion of coal, grass, wood | |
| Benzo(a)anthracene/ (Benzo(a)anthracene + Chrysene) | < 0.2 petroleum source | Bakhtiari et al., 2009 |
| | 0.2-0.35 mixed source | |
| | > 0.35 combustion source | |

While there are equal numbers of mixed and combustion related sources, all sites located in coastal salt marshes and exposed to tidal movement are dominated by combustion sources (Figure 5.27). This dominance may be the result of PAH removal and redistribution during tidal and flooding events or through biodegradation that occurs in these salt marshes that are not present in the inland samples [39,40]. Tidal mobilization preferentially removes the petrogenic PAHs since the heavier pyrogenic PAHs are more likely to be adsorbed to sediments and thus immobile [39]. This constant removal of the lighters PAHs could create an apparent dominance of pyrogenic PAHs in coastal sediments.

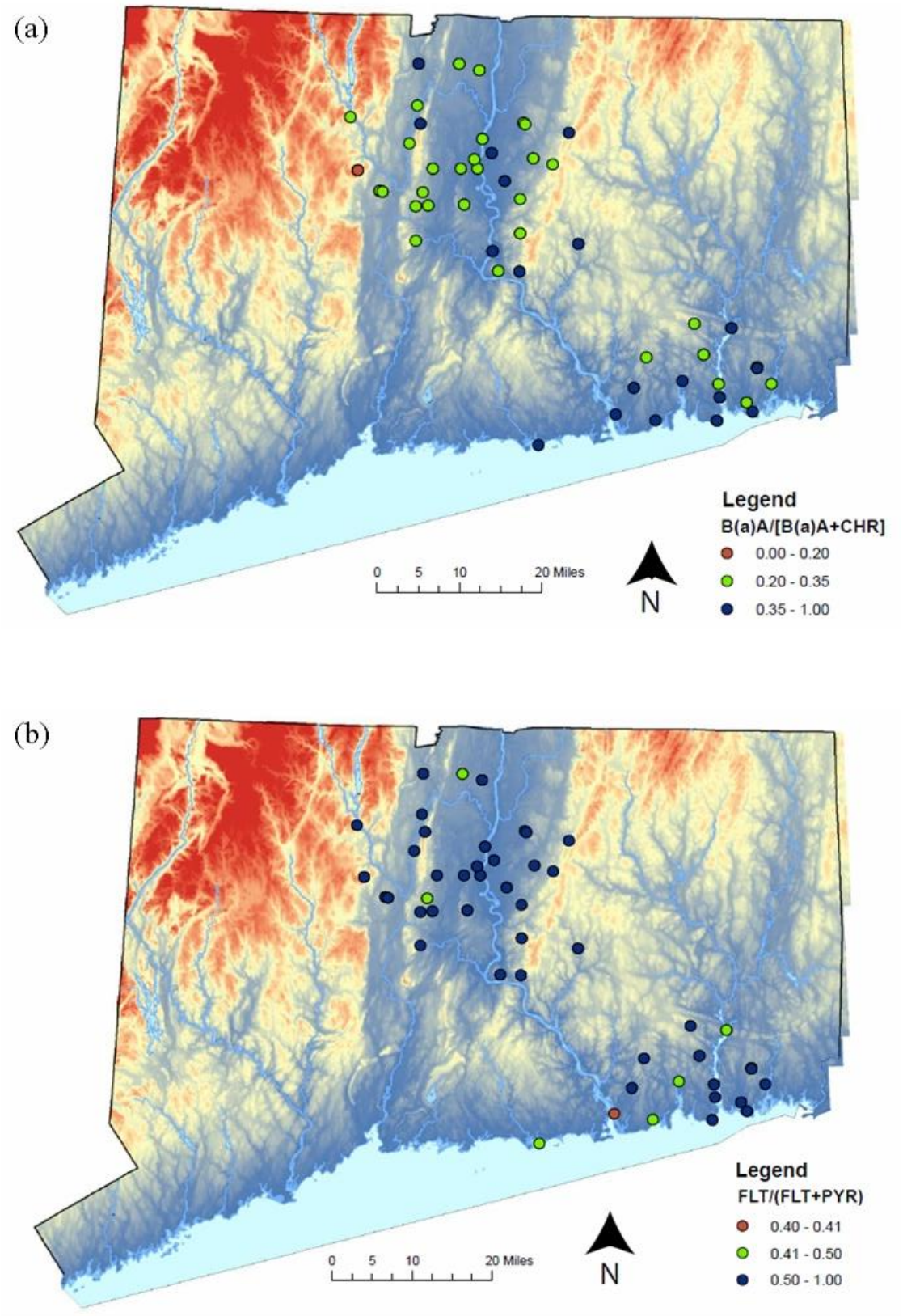


Figure 5.27 Spatial variations in diagnostic ratios a) Benzo (a) anthracene/ (BaA + chrysene) and b) Fluoranthene/ (FLT + pyrene).

Furthermore, it is possible that coastal samples undergo biodegradation of PAHs to a larger degree than inland samples. Biodegradation transforms PAHs from one form to another through a series of biotransformations of organic compounds into less complex, non-PAH, metabolites. This occurs through mineralization into inorganic compounds such as water, carbon dioxide (aerobic) or methane (anaerobic) [40–43]. In wetlands, including coastal salt marshes, there are more bacteria, fungi, and algae that are capable of degrading PAHs, typically the low molecular weight PAHs [40]. Bacteria isolated from coastal sediments located in brackish water were found to degrade phenanthrene up to 58 % in 6 days, while a mixed microbial culture of bacteria reduced the concentration of LMW PAHs by 99.5 % and HMW PAHs by 97 % over 6 months [40,44]. Certain algae have been reported to enhance the degradation of fluoranthene and pyrene when present with bacteria [45]. Increased degradation and mobilization of smaller PAHs in coastal salt marshes may skew diagnostic ratios, thus leading to the appearance of more pyrogenic PAHs along the coast.

Examination of FLT/(FLT + PYR) ratios do not show a similar pattern of combustion PAHs only along the coast, however we do see a higher amount of combustion dominated sites overall in both inland and coastal sites (Figure 5.27). This is unusual, as we would expect these diagnostic ratios to be relatively similar, however studies indicate that different microbial bacteria degrade different PAHs [40]. It is possible that microbial degradation of individual PAHs occurs at different rates, thus causing the differences in DR between the two sets of structural isomers. We can establish reasonable consistency identifying formation process through comparative analysis of BaA/(BaA +CHY) and FLT/(FLT + PYR). The diagnostic ratios indicate that the majority of our sites are dominated by mixed petroleum and combustion sources (Figure 5.28). While the majority

of sites are dominated by a mix of petroleum and combustion sources, we find several sites with diagnostic ratios that suggest strictly combustion related sources.

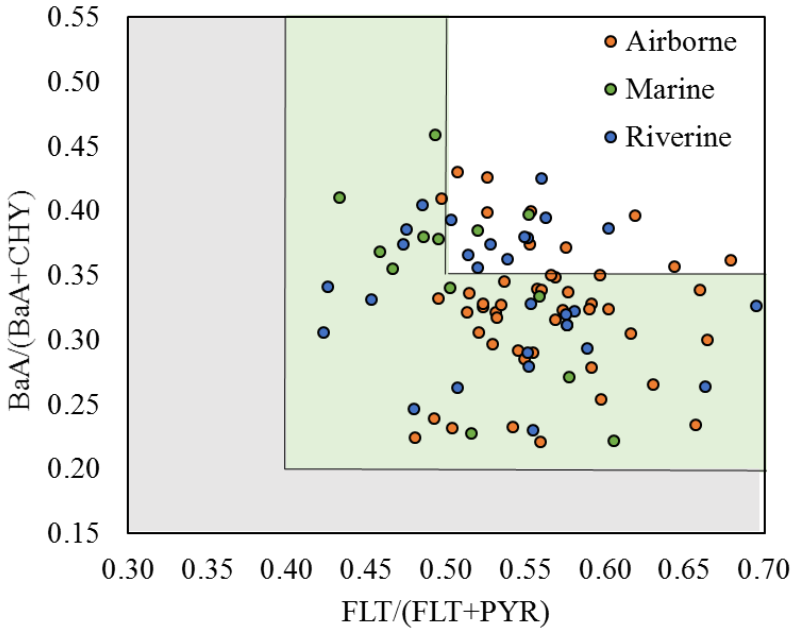


Figure 5.28 Comparative analysis of PAH diagnostic ratios. The gray shaded area represents petroleum dominated source materials, the green shaded area consists of mixed source materials, and white area represents combustion dominated source materials

*5.4.3 Carbon and Hydrogen Isotope Composition of PAHs in Sediments and Soils.*

While diagnostic ratios of PAHs are informative about the bulk characterization of PAH methods of production (pyrogenic versus petrogenic) compound specific stable carbon isotope measurements are used to further corroborate PAH source materials. PAH extracts from all samples were analyzed for their carbon isotopic composition ($\delta^{13}C$). The $\delta^{13}C$ values for the sampling locations ranged between –29.6 and –20.6 ‰ (–24.1 ± 1.6 ‰, $\mu \pm \sigma$; Table 5.13). While there is significant variation between sampling locations, there is no substantial relationship to this variation (Figure 5.29). Overall, the $\delta^{13}C$ values of all PAHs in the present study can be separated into five categories: $C_3$ plants (–27.3 to –30.1 ‰), liquid fossil fuels (–23.7 to –26.9 ‰), low temperature (~650 °C) coal (–22.1 to

–24.3 ‰), high temperature (~900 °C) coal (–25.5 to –28.1 ‰), and industrial emissions (–22.3 to –22.9 ‰). The majority of our samples exhibited $\delta^{13}C$ values that indicate there are multiple sources of PAHs in the environment. Environmental PAHs originate from a complex mixture of liquid fossil fuels, low temperature coal burning, and industrial emissions.

Table 5.13 δD and δ13C of FLT, PYR, and total PAHs

| Abb. | $\delta D_{FLT}$ | $\delta D_{PYR}$ | $\delta D_{PAH}$* | $\delta^{13}C_{FLT}$ | $\delta^{13}C_{PYR}$ | $\delta^{13}C_{PAH}$* |
|---|---|---|---|---|---|---|
| ASB | -78 | -71 | -77 | -23.0 | -24.6 | -23.6 |
| BAB | -52 | -40 | -48 | -24.0 | -24.9 | -23.4 |
| BPA | -43 | -35 | -52 | -23.9 | -23.8 | -24.5 |
| BPB | -91 | -95 | -86 | -24.1 | -24.8 | -26.9 |
| CMB | -47 | -39 | -44 | -24.3 | -25.1 | -25.0 |
| CPB | -57 | -50 | -56 | -23.3 | -24.1 | -23.7 |
| COA | - | - | - | -22.8 | -24.0 | -24.0 |
| COB | - | - | - | -22.2 | -23.2 | -23.0 |
| CHD | -81 | -116 | -132 | -23.6 | -22.7 | -20.6 |
| CLB | -53 | -40 | -51 | -22.7 | -24.6 | -22.7 |
| DKA | -59 | -59 | -60 | - | - | - |
| DKB | - | - | - | -23.5 | -27.1 | |
| EFD | - | - | - | -27.4 | -24.9 | -26.4 |
| EFS | -99 | -52 | -90 | -33.1 | -26.2 | -29.5 |
| FTA | -71 | -63 | -79 | -23.0 | -24.1 | -24.0 |
| FTB | -58 | -50 | -66 | -23.3 | -24.1 | -24.1 |
| GWB | -57 | - | -47 | -24.3 | -25.1 | -23.3 |
| GMA | -44 | -34 | -53 | - | - | -29.6 |
| GRA | -77 | -59 | -62 | -24.4 | -24.8 | -24.4 |
| HPA | - | - | - | -22.1 | -23.7 | - |
| HPB | - | - | - | -21.5 | -22.8 | - |
| HWA | - | - | - | -23.9 | -24.6 | -23.8 |
| HP | -65 | -67 | -101 | -24.6 | -24.3 | -24.2 |
| IAD | -62 | -58 | -68 | -23.1 | -23.5 | -23.3 |
| IAS | -33 | -50 | - | -24.2 | -24.8 | -24.7 |
| LAA | - | - | - | -20.3 | -22.2 | - |
| LAB | - | - | - | -19.4 | -21.3 | - |
| MCB | -73 | -57 | -63 | -24.5 | -24.8 | -25.4 |
| MWB | - | - | - | -23.8 | -23.6 | -24.5 |
| MRA | -43 | -37 | -47 | -22.6 | -24.0 | -23.5 |

| | | | | | | |
|---|---|---|---|---|---|---|
| MRB | -45 | -34 | -41 | -23.0 | -24.4 | -22.9 |
| MPB | - | - | - | -23.9 | -24.9 | -23.0 |
| NSA | - | - | - | -21.8 | -23.4 | -22.5 |
| NPA | - | - | - | -28.5 | -25.1 | -26.3 |
| NWB | -60 | -38 | -43 | -23.3 | -24.8 | -24.1 |
| OBA | -57 | -48 | -54 | -23.6 | -24.9 | -24.2 |
| OBB | - | - | - | -24.0 | -24.2 | -25.2 |
| OL | -96 | -120 | -111 | -25.9 | -24.6 | -25.5 |
| OS | -89 | -78 | - | -22.9 | -23.4 | -22.0 |
| PWA | - | - | - | -23.2 | -24.0 | -23.6 |
| PWB | - | - | - | -23.1 | -23.9 | -25.4 |
| PNA | -72 | -58 | -94 | -23.0 | -24.1 | -23.6 |
| PVA | - | - | - | -23.5 | -24.2 | - |
| PVB | -64 | - | -54 | - | - | -23.9 |
| PPA | -48 | -30 | -48 | -23.1 | -24.8 | -23.1 |
| PQA | - | - | - | -23.6 | -24.9 | -23.1 |
| PQB | - | - | - | -24.1 | -25.5 | -23.8 |
| RGA | - | - | - | -21.6 | -22.9 | -22.4 |
| RHB | - | - | - | -24.9 | -25.6 | -25.1 |
| RPA | -66 | -52 | -63 | -23.8 | -24.8 | -24.1 |
| RPB | - | - | - | -24.5 | -24.8 | -25.1 |
| RN | - | - | - | -24.3 | -25.3 | -24.9 |
| SBB | - | - | - | -22.9 | -24.7 | -22.8 |
| SRA | -63 | -53 | -59 | -22.1 | -23.9 | -22.0 |
| SRB | -74 | -74 | - | -22.3 | -24.0 | -23.0 |
| SHA | -44 | -29 | -37 | -24.1 | -24.9 | -25.6 |
| SHB | -40 | -16 | -42 | -24.4 | -25.2 | -24.5 |
| SNA | -37 | -27 | -33 | -23.3 | -24.9 | -23.2 |
| SNB | - | - | - | -22.9 | -24.6 | - |
| SIA | -66 | -57 | -65 | -22.1 | -23.4 | -22.6 |
| SIB | -54 | - | -54 | -23.7 | -24.2 | -24.0 |
| SPA | -58 | -52 | -59 | -25.3 | -23.7 | -23.5 |
| STA | -39 | -34 | -45 | -21.6 | -23.4 | -21.8 |
| STB | -56 | -52 | -58 | -21.5 | -23.9 | -22.1 |
| TMA | -56 | - | -66 | -24.4 | -25.4 | -24.3 |
| VFA | -31 | -35 | -33 | -27.0 | -29.3 | -27.4 |
| WD | -59 | -54 | -64 | -24.0 | -25.0 | -24.6 |
| WS | - | - | - | -23.2 | -23.6 | -23.8 |
| WDB | - | - | - | -22.4 | -24.1 | -22.6 |

* Weighted average of all detected PAH isotope values

"-" indicates below detection limit

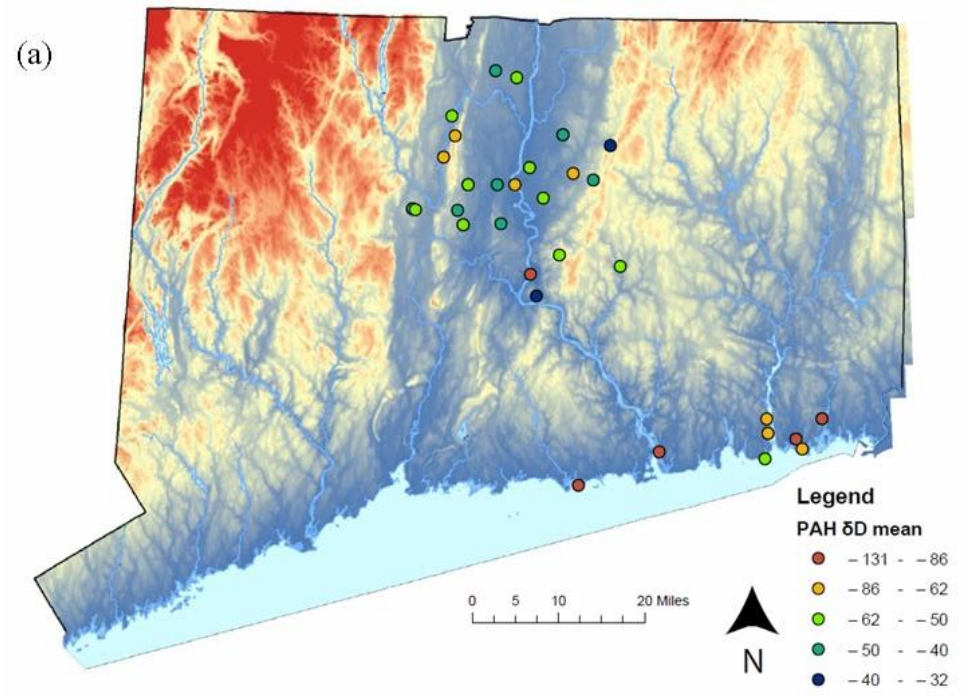


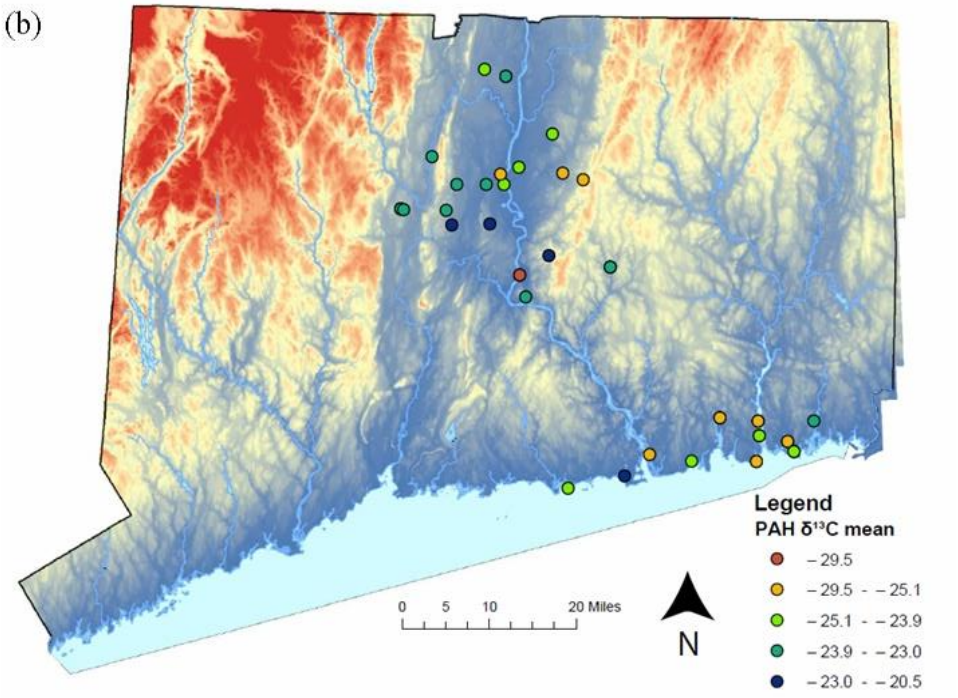


Figure 5.29 Spatial variations of a) hydrogen (δD) and b) carbon ($\delta^{13}C$) isotopic values of PAHs in Connecticut, USA

The use of compound specific stable carbon isotope analysis for source-apportionment of PAHs located in environmental samples has been well established [8,19,20,46,47]. However, differences in carbon isotopic composition from various sources typically only range by a few ‰. Moreover, numerous studies have evaluated the hydrogen compound specific isotopes of *n*-alkanes preserved in sediments and soils and found that there are vast differences in isotopic differences between starting materials [48] often on the magnitude of 100 ‰ or greater. Therefore, hydrogen isotope compositions can be further used to differentiate between sources. PAH extracts were analyzed for their compound specific hydrogen isotope composition (δD) and found large variations between sites. Hydrogen isotopic values ranged from –131 to –33 ‰ (Figure 5.29; Table 5.13) with the majority of the depleted isotope values located in tidal salt marshes and areas affected by tides and flooding (average of –81.4 ± 25 ‰). Studies have shown that PAHs do not readily exchange their hydrogens unless exposed to high temperatures (above 170 °C) and low pH (below 2) [49]. This indicates that the differences in δD between our coastal and inland samples are likely not a result of hydrogen isotope exchange with water, but rather differences in starting materials.

Previous literature [1,20] found that PAHs formed from non-petroleum sources tended to have more isotopically depleted hydrogen and carbon values, with the exception of low temperature coal which has more enriched carbon values. The state of Connecticut currently has a single active coal burning plant in the city of Bridgeport, a coastal city located approximately 106 km west of New London and 85 km south of Hartford [50]. The wind and water currents move from west to east along the northern shore of the Long Island Sound [51] and provide an opportunity for PAH mobility away from the coal burning facility

toward the sampling locations. There is also the possibility of PAH remobilization from sediments near the former AES Thames Generation Plant, a defunct coal burning facility located in Uncasville, CT (8.69 km north of New London on the Thames River). Operations at the Uncasville facility ceased in February 2011 however, due to a lack of environmental safety regulations regarding safe disposal of coal combustion waste (CCW), this facility was responsible for ongoing contamination of the Thames River and surrounding ground water with toxic metals and other pollutants [52]. Over the 52 years in operation where the Thames Generation Plant was burning coal, the harmful byproducts coal ash and slurry were disposed of on site in a variety of unsuitable locations. Since the groundwater from the Thames plant discharges directly into the Thames River [52], seepage from these disposal sites have the potential of mobilizing not only volatile and semi-volatile organic compounds such as PAHs, but heavy metals and other toxins that are associated with coal ash.

### *5.4.4 Duel-isotope approach to PAH Source determination*

There are several studies that measure the δD and $\delta^{13}C$ of PAHs that are formed from different starting materials [19–21,53–55]. We created a bivariate plot of the δD and $\delta^{13}C$ average values of five categories of common environmental PAH sources ($C_3$ plants, liquid fossil fuels, high temperature coal, low temperature coal [1], and industrial emissions [21]) to compare these endmembers to the most common PAHs found in our sampled, FLT and PYR. We find that the majority of FLT and PYR from our samples have carbon isotope values within the range associated with the burning of liquid fossil fuels or low temperature coal (Figure 5.30). There are some outlier points that may indicate source mixing or different sources altogether.

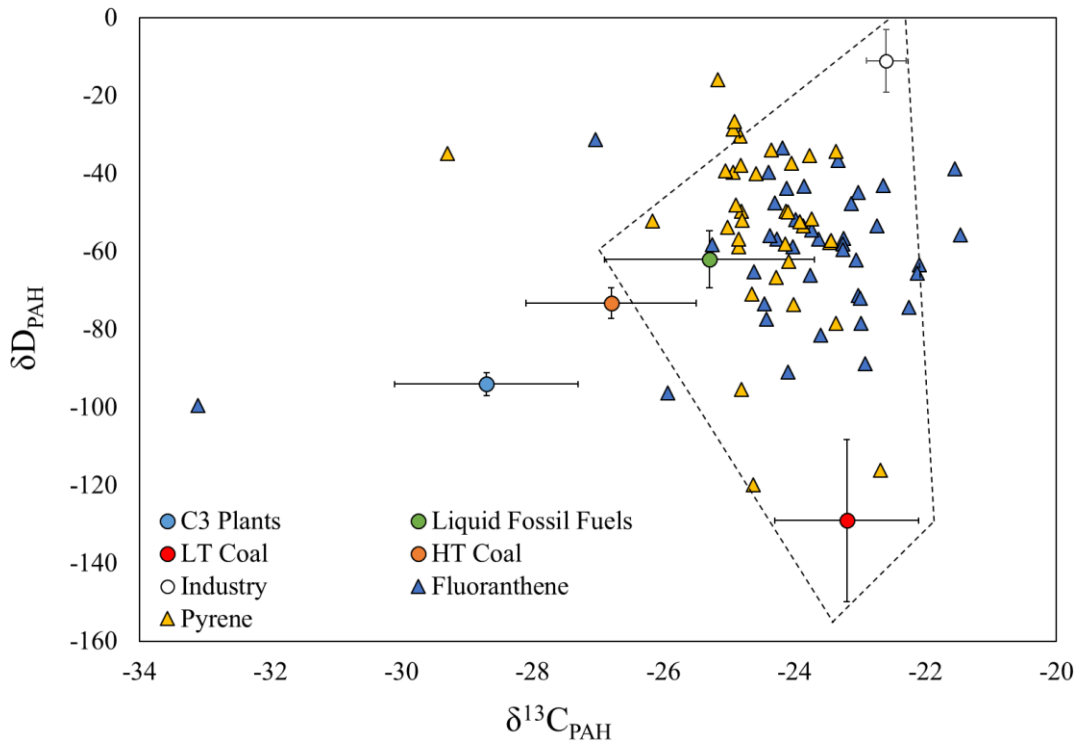


Figure 5.30 Carbon and hydrogen isotopic ranges of PAHs formed from the combustion of $C_3$ plants (blue circle), liquid fossil fuels (orange circle), low temperature (> 600 ℃) coal (green circle), high temperature (< 900 ℃) coal (yellow circle), and industrial emissions (white circle) and their relationship with fluoranthene (blue triangles) and pyrene (yellow triangles) extracted from soil and sediment samples

While our PAHs have carbon isotope values well within the range for vehicle emissions or coal burning, a significant number of samples have unusually isotopically enriched δD values (between –50 and –16 ‰). These heavy PAHs may be derived from industrial smoke stacks, which have produced volatile aromatic compounds, including naphthalene, with δD values of – 11 ± 10 ‰ [21]. PAHs are generally emitted as gases into the atmosphere [29,30] from a range of sources including vehicle exhaust, home heating emissions, and industrial emissions. While car exhaust is still considered the main source of PAHs in the environment, over the past 10-20 years the amount of volatile organic

compounds (VOCs) emitted from cars has decreased and industrial emissions now make up approximately 46 % of VOC emissions [21].

While some PAH δD values are within the accepted ranges for natural sources [1,56], many samples are significantly enriched in deuterium. Since δD of liquid aromatics becomes depleted during progressive evaporation (80 % loss of liquid) [57,58], it has been theorized that isotopic fractionation associated with water condensation (such as a rain cloud formation) may occur [21]. This fractionation occurs because intermolecular van der Waals forces decreases with an increasing number of deuterium atoms. This theory assumes that condensation is the exact opposite of evaporation and will, therefore, have the opposite effect on isotopic fractionation [21]. Given this, our samples are still some of the heaviest PAHs recorded in literature [20,53,59] and are most similar to industrial emissions.

### *5.4.5 Concentration and stable isotopes of fluoranthene and pyrene*

Previous studies indicated that there are two pathways for PAH formation: pentagonal ring (fluoranthene series) and non-pentagonal (pyrene series) [56,48]. Similar to previous studies [2], FLT and PYR concentrations in our samples have a strong linear relationship (Figure 5.31). Sites that are only subject to airborne deposition tend to have higher concentrations of PYR and FLT than sites associated with marine and riverine mobilization. The linear relationship suggests that these structural isomers are produced simultaneously or through similar reactions, while the differences in concentration between sites suggest that the majority of PAHs in the environment are deposited from the atmosphere rather than through aquatic transport.

Hydrogen isotopes of PAHs showed that there is a distinctive isotopic difference between FLT and PYR, with FLT being more depleted in deuterium than PYR [60].

Concentration data for FLT and PYR suggest that these PAHs are produced through similar processes, however it gives little insight into the source materials. Comparison of the δD and $\delta^{13}C$ of FLT and PYR can be used to determine whether these PAHs came from the same source material. The $\delta^{13}C$ of airborne deposited FLT and PYR show a weak liner relationship (Figure 5.31) however, the relationship is stronger than those experienced in sites subject to marine and riverine transport. Similarly, δD values show a slightly stronger relationship than the carbon isotopes (Figure 5.31), particularly for airborne and marine samples however there are still significant outliers, particularly in riverine samples. Since there is no isotopic enrichment or depletion associated with biodegradation [61,62], these outliers may indicate the FLT and PYR in those samples originate from different source materials [15]. Studies of these reaction pathways suggest that low temperature formation occurs under a kinetic control [63,64] while high temperature PAH formation is better explained using a thermodynamic control [56,48]. The higher thermal energy associated with production of PAHs in cylinders and gasoline engines affect isotopic behavior, leading to more enriched $\delta^{13}C$ and δD values and eliminating low temperature processes such as wood burning as likely sources of PAHs [48]

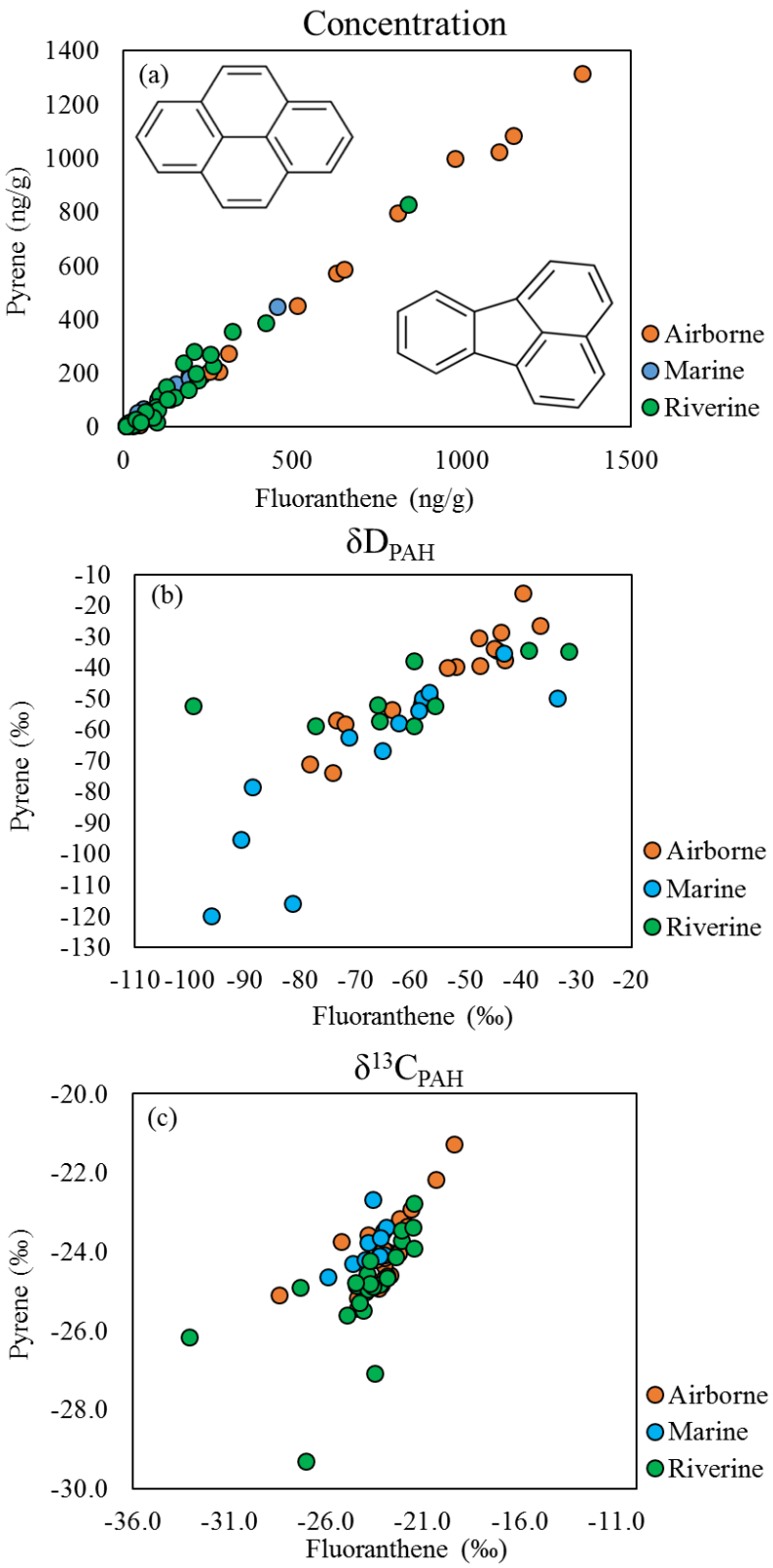


Figure 5.31 Comparative analysis of the linear relationship of a) concentration, b) δD, and c) $\delta^{13}C$ of fluoranthene and pyrene extracted from soil and sediment sample for the determination of single or multi-source origin

## 5.5.0 CONCLUSIONS

In this study, we collected over 100 samples from 55 locations in the states of Connecticut and Rhode Island to determine the source materials for polycyclic aromatic hydrocarbons (PAHs) extracted from environmental soils and sediments. We specifically selected locations to measure differences in PAH concentrations and isotopic values over the wide regional variations in landscapes. Our data show there is a persistent background of PAHs in environmental samples, regardless of the proximity to urban centers. Contrary to most contemporary studies, we found a higher concentration of PAHs in less urbanized areas. This is indicative of highly mobilized contaminants prior to deposition. There are clear differences in the diagnostic ratios between coastal and inland sites as well as differences in hydrogen and carbon isotopic ratios, both of which are indicative of differences in sources materials and methods of PAH production.

While the total concentration of PAHs varied widely from site to site, the percentages of each type of PAH (2-3 rings, 4 rings, 5 rings, and 6 rings) remained fairly stable throughout all sampling locations. These data indicate that there are mixed sources of PAHs, but a large quantity of PAHs in the environment are introduced through pyrogenic means. This is supported by a comparative analysis of the diagnostic ratios of FLT/ (FLT + PYR) and BaA/ (BaA + CHR) that shows the all samples have either mixed sources or solely combustion sources. Observed differences in the diagnostic ratios between coastal and inland sites may indicate there is increased biodegradation or mobilization of PAHs in coastal sediments leading to fewer petrogenic PAHs and skewing the diagnostic ratios to favor pyrogenic sources.

Since there is no hydrogen isotopic exchange with water, the differences in δD values between coastal and inland sites is most likely the result of a difference in source rather than hydrogen isotope exchange between water and individual PAHs. While studies indicate hydrogen exchange is possible at high temperatures and low pH, there is little chance of hydrogen exchange at ambient conditions [49]. While concentration data concluded that the majority of samples were of mixed pyrogenic and petrogenic sources, the δD and $\delta^{13}C$ of FLT and PYR indicate that the majority of PAHs in the environment result from a complex mixing of three main sources: burning of liquid fossil fuels, low temperature coal burning, and industrial emissions.

## 5.6.0 ACKNOWLEDGMENTS

We thank Katherine Truong for her support collecting samples and maintaining field notes as we collected samples. In addition, we thank Yvette Eley for reviewing our manuscript and giving valuable feedback and Chaoran Wang for her thoughtful conversations throughout the writing process.

## 5.7.0 REFERENCES


(1) Bosch, C.; Andersson, A.; Kruså, M.; Bandh, C.; Hovorková, I.; Klánová, J.; Knowles, T. D. J.; Pancost, R. D.; Evershed, R. P.; Gustafsson, Ö. *Environ. Sci. Technol.* **2015**, *49* (13), 7657–7665.

(2) Foan, L.; Leblond, S.; Thöni, L.; Raynaud, C.; Santamaría, J. M.; Sebilo, M.; Simon, V. *Environ. Pollut.* **2014**, *184*, 113–122.

(3) Gustafsson, O.; Gschwend, P. M.; Buesseler, K. O. *Mar. Chem.* **1997**, *57* (1–2), 11–23.

(4) Lima, A. L. C.; Farrington, J. W.; Reddy, C. M. *Environ. Forensics* **2005**, *6* (2), 109–131.

(5) Brown, J. N.; Peake, B. M. *Sci. Total Environ.* **2006**, *359* (1–3), 145–155.

(6) Nam, J. J.; Thomas, G. O.; Jaward, F. M.; Steinnes, E.; Gustafsson, O.; Jones, K. C. *Chemosphere* **2008**, *70* (9), 1596–1602.

(7) Dvorská, A.; Lammel, G.; Klánová, J. *Atmos. Environ.* **2011**, *45* (2), 420–427.

(8) O'Malley, V. P.; Abrajano, T. A. J.; Hellou, J. *Org. Geochem.* **1994**, *21* (6–7), 809–822.

(9) Ravindra, K.; Sokhi, R. S.; Van Grieken, R. *Atmos. Environ.* **2008**, *42*, 2895–2921.

(10) Beelen, R.; Hoek, G.; Raaschou-Nielsen, O.; Stafoggia, M.; Andersen, Z. J.; Weinmayr, G.; Hoffmann, B.; Wolf, K.; Samoli, E.; Fischer, P. H.; Nieuwenhuijsen, M. J.; Xun, W. W.; Katsouyanni, K.; Dimakopoulou, K.; Marcon, A.; Vartiainen, E.; Lanki, T.; Yli-Tuomi, T.; Oftedal, B.; Schwarze, P. E.; Nafstad, P.; de Faire, U.; Pedersen, N. L.; Östenson, C. G.; Fratiglioni, L.; Penell, J.; Korek, M.; Pershagen, G.; Eriksen, K. T.; Overvad, K.; Sørensen, M.; Eeftens, M.; Peeters, P. H.; Meliefste, K.; Wang, M.; Bas Bueno-De-Mesquita, H.; Sugiri, D.; Krämer, U.; Heinrich, J.; De Hoogh, K.; Key, T.; Peters, A.; Hampel, R.; Concin, H.; Nagel, G.; Jaensch, A.; Ineichen, A.; Tsai, M. Y.; Schaffner, E.; Probst-Hensch, N. M.; Schindler, C.; Ragettli, M. S.; Vilier, A.; Clavel-Chapelon, F.; Declercq, C.; Ricceri, F.; Sacerdote, C.; Galassi, C.; Migliore, E.; Ranzi, A.; Cesaroni, G.; Badaloni, C.; Forastiere, F.; Katsoulis, M.; Trichopoulou, A.; Keuken, M.; Jedynska, A.; Kooter, I. M.; Kukkonen, J.; Sokhi, R. S.; Vineis, P.; Brunekreef, B. *Environ. Health Perspect.* **2015**, *123* (November 2012), 525–534.

(11) World Health Organization. Public health, environmental and social determinants of health (PHE) http://www.who.int/phe/health_topics/outdoorair/databases/en/ (accessed Jan 1, 2016).

(12) Pedersen, D. U.; Durant, J. L.; Penman, B. W.; Crespi, C. L.; Hemond, H. F.; Lafleur, A. L.; Cass, G. R. *Environ. Sci. Technol.* **2004**, *38* (3), 682–689.

(13) Galarneau, E. *Atmos. Environ.* **2008**, *42* (35), 8139–8149.

(14) Bakhtiari, A. R.; Zakaria, M. P.; Yaziz, M. I.; Lajia, M. N. H.; Bi, X. *Environ. Asia* **2009**, *2*, 1–10.

(15) Baumard, P.; Budzinski, H.; Michon, Q.; Garrigues, P.; Burgeot, T.; Bellocq, J. *Estuar. Coast. Shelf Sci.* **1998**, *47*, 77–90.

(16) Reddy, C. M.; Pearson, A.; Xu, L.; McNichol, A. P.; Benner, B. A.; Wise, S. A.; Klouda, G. A.; Currie, L. A.; Eglinton, T. I. *Environ. Sci. Technol.* **2002**, *36* (8), 1774–1782.

(17) Mandalakis, M.; Gustafsson, Örjan; Reddy, C. M.; Xu, L. *Environ. Sci. Technol.* **2004**, *38* (20), 5344–5349.

(18) Sheesley, R. J.; Krusa, M.; Krecl, P.; Johansson, C.; Gustafsson, Ö. *Atmos. Chem. Phys. Discuss.* **2008**, *8* (6), 20901–20924.

(19) McRae, C.; Snape, C. E.; Sun, C. G.; Fabbri, D.; Tartari, D.; Trombini, C.; Fallick, A. E. *Environ. Sci. Technol.* **2000**, *34* (22), 4684–4686.

(20) Sun, C.; Cooper, M.; Snape, C. E. *Prepr. Pap-Am. Chem. Soc., Div Fuel Chem* **2003**, *48* (2), 760–761.

(21) Vitzthum von Eckstaedt, C.; Grice, K.; Ioppolo-Armanios, M.; Jones, M. *Atmos. Environ.* **2011**, *45* (31), 5477–5483.

(22) Olson, D. M.; Dinerstein, E.; Wikramanayake, E. D.; Burgess, N. D.; Powell, G. V. N.; Underwood, E. C.; D'amico, J. A.; Itoua, I.; Strand, H. E.; Morrison, J. C.; Loucks, C. J.; Allnutt, T. F.; Ricketts, T. H.; Kura, Y.; Lamoreux, J. F.; Wettengel, W. W.; Hedao, P.; Kassem, K. R. *Bioscience* **2001**, *51* (11), 933.

(23) National Oceanic and Atmospheric Adminstration. NowData-NOAA Online Weather Data http://www.noaa.gov/ (accessed Jan 1, 2016).

(24) Yan, W.; Chi, J.; Wang, Z.; Huang, W.; Zhang, G. *Environ. Pollut.* **2009**, *157* (6), 1823–1830.

(25) Cecinato, A.; Marino, F.; Di Filippo, P.; Lepore, L.; Possanzini, M. *J. Chromatogr. A* **1999**, *846* (1–2), 255–264.

(26) Papageorgopoulou, A.; Manoli, E.; Touloumi, E.; Samara, C. *Chemosphere* **1999**, *39* (13), 2183–2199.

(27) Junker, M.; Kasper, M.; Röösli, M.; Camenzind, M.; Künzli, N.; Monn, C.; Theis, G.; Braun-Fahrländer, C. *Atmos. Environ.* **2000**, *34* (19), 3171–3181.

(28) Zhiqiang, Q.; Siegmann, K.; Keller, A.; Matter, U.; Scherrer, L.; Siegmann, H. C. *Atmos. Environ.* **2000**, *34* (3), 443–451.

(29) Gerdol, R.; Bragazza, L.; Marchesini, R.; Medici, A.; Pedrini, P.; Benedetti, S.; Bovolenta, A.; Coppi, S. *Atmos. Environ.* **2002**, *36* (25), 4069–4075.

(30) Chen, S.; Liao, S.; Jian, W.; Chiu, S.; Fang, G. *J. Environ. Sci. Heal. . Part A Environ. Sci. Eng. Toxicol.* **1997**, *32* (3), 585–604.

(31) Fernández, P.; Vilanova, R. M.; Martínez, C.; Appleby, P.; Grimalt, J. O. *Environ. Sci. Technol.* **2000**, *34* (10), 1906–1913.

(32) Intellicast. WINDcast http://www.intellicast.com/National/Wind/WINDcast.aspx?location=usct0094.

(33) Gonzalez, A.; Moilleron, R.; Chebbo, G.; Thevenot, D. R. *Polycycl. Aromat. Compd.* **2000**, *20*, 1–19.

(34) McCready, S.; Slee, D. J.; Birch, G. F.; Taylor, S. E. *Mar. Pollut. Bull.* **2000**, *40*, 999–1006.

(35) Soclo, H. H.; Garrigues, P.; Ewald, M. *Mar. Pollut. Bull.* **2000**, *40*, 387–396.

(36) Rocher, V.; Azimi, S.; Moilleron, R.; Chebbo, G. *Sci. Total Environ.* **2004**, *323*, 107–122.

(37) Takada, H.; Onda, T.; Harada, M.; Ogura, N. *Sci. Total Environ.* **1991**, *107*, 45–69.

(38) Ngabe, B.; Bidleman, T. F.; Scott, G. I. *Sci. Total Environ.* **2000**, *255*, 1–9.

(39) Abdel-Shafy, H. I.; Mansour, M. S. M. *Egypt. J. Pet.* **2015**, *25* (1), 107–123.

(40) Haritash, A. K.; Kaushik, C. P. *J. Hazard. Mater.* **2009**, *169* (1–3), 1–15.

(41) Yuan, S. Y.; Chang, J. S.; Yen, J. H.; Chang, B. V. *Chemosphere* **2001**, *43* (3), 273–278.

(42) Bumpus, J. *Appl. Environ. Microbiol.* **1989**, *55* (1), 154–158.

(43) Dua, M.; Singh, A.; Sethunathan, N.; Johri, A. *Appl. Microbiol. Biotechnol.* **2002**, *59* (2–3), 143–152.

(44) Tam, N. F. Y.; Guo, C. L.; Yau, W. Y.; Wong, Y. S. *Mar. Pollut. Bull.* **2002**, *45* (1–12), 316–324.

(45) Borde, X.; Guieysse, B.; Delgado, O.; Muoz, R.; Hatti-Kaul, R.; Nugier-Chauvin, C.; Patin, H.; Mattiasson, B. *Bioresour. Technol.* **2003**, *86* (3), 293–300.

(46) O'Malley, V. P.; Burke, R. A.; Schlotzhauer, W. S. *Org. Geochem.* **1997**, *27* (7–8), 567–581.

(47) Lichtfouse, E.; Budzinski, H.; Garrigues, P.; Eglinton, T. I. *Org. Geochem.* **1997**, *25* (5), 353–359.

(48) Oakes, A. M.; Hren, M. T. *Org. Geochem.* **2016**, *97*, 122–130.

(49) Oba, Y.; Naraoka, H. *Org. Geochem.* **2003**, *18*, 29–35.

(50) U.S. Energy Information Adminstration Connecticut: State Profiles and Energy Estimates https://www.eia.gov/state/analysis.cfm?sid=CT (accessed Jan 1, 2017).

(51) Signell, R. P.; Knebel, H. J.; List, J. H.; Farris, A. S. In *5th International Conference on Estuarine and Coastal Modeling*; Spaulding, M. L., Blumberg, A. F., Eds.; ASCE Press, 1997.

(52) Stant, J. **2010**, 1–270.

(53) Vitzthum von Eckstaedt, C. D.; Grice, K.; Ioppolo-Armanios, M.; Kelly, D.; Gibberd, M. *Chemosphere* **2012**, *89* (11), 1407–1413.

(54) Jautzy, J. J.; Ahad, J. M. E.; Gobeil, C.; Smirnoff, A.; Barst, B. D.; Savard, M. M. *Environ. Sci. Technol.* **2015**, *49* (20), 12062–12070.

(55) Okuda, T.; Takada, H.; Naraoka, H. *Polycycl. Aromat. Compd.* **2003**, *6638* (October 2002), 219–236.

(56) Grice, K.; Brocks, J. J. In *Encyclopedia of Geobiology*; Reitner, J., Thiel, V., Eds.; Springer, New York, U.S., 2011; pp 147–167.

(57) Wang, Y.; Huang, Y. S. *Org. Geochem.* **2001**, *32* (8), 991–998.

(58) Wang, Y.; Huang, Y. S. *Appl. Geochemistry* **2003**, *18* (10), 1641–1651.

(59) Hunkeler, D.; Anderson, N.; Aravena, R.; Bernasconi, S. M.; Butler, B. J. *Environ. Sci. Technol.* **2001**, *35* (17), 3462–3467.

(60) Gilmour, I.; Pillinger, C. T. *Mon. Not. R. Astron. Soc.* **1994**, *269* (2), 235–240.

(61) Naraoka, H.; Shimoyama, A.; Harada, K. *Earth Planet. Sci. Lett.* **2000**, *184* (1), 1–7.

(62) Naraoka, H.; Mita, H.; Komiya, M.; Shimoyama, A. *Geochim. Cosmochim. Acta* **2002**, *Spec. Supp*, A546.

(63) Meckenstock, R. U.; Morasch, B.; Griebler, C.; Richnow, H. H. *J. Contam. Hydrol.* **2004**, *75* (3–4), 215–255.

(64) Mazeas, L.; Budzinski, H.; Raymond, K. *Org. Geochem.* **2002**, *33*, 1259–1272.

## 5.8.0 SUPPLIMENTARY DATA

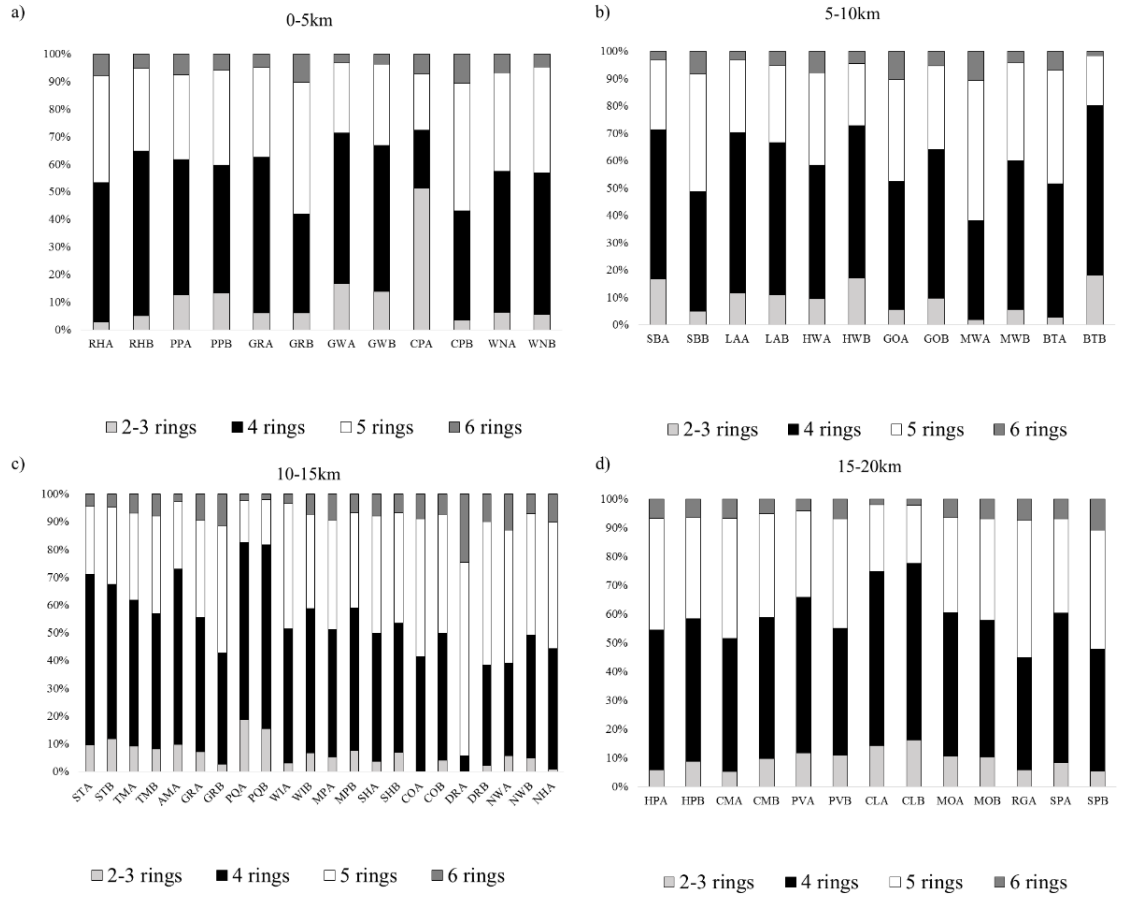


Supplementary Figure 5.32 PAH distribution by number of rings for sites a) 0 to 5 km, b) 5 to 10 km, c) 10 to 15 km, and d) 15 to 20 km from the city center.

# CHAPTER SIX

# Overall conclusions and further research

Abigail M. Oakes

University of Connecticut
Department of Chemistry
Division of Analytical Chemistry

### 6.1.0 BROAD THESIS GOALS

This thesis focused on three key questions relating to processes controlling the production and movement of organically bound carbon through the earth surface environment:

1. How the heterogeneity within stable hydrogen and carbon isotopic compositions of organic biomarkers produced by individual plants in forest ecosystems are preserved in fluvial sediments.
2. How isotopic heterogeneity in organic biomarkers are associated with biological processes and molecular formation, and how informative it is as a proxy for understanding ancient environments or ecosystems.
3. Does the isotopic composition of PAHs provide a tool for tracing movement of these organic pollutants through the environment and identifying potential sources of contamination?

The following sections summarize the key findings and conclusions presented here, in light of these research questions. By demonstrating the value of a multiple method approach throughout - whether investigating temporal changes in biological fractionation of leaf waxes or the use of compound specific stable isotope measurements to identify the source of PAHs - these projects provide new detailed methodologies for future studies spanning a range of disciplines that utilize the tools of analytical environmental chemistry.

### 6.2.0 FENTON RIVER PROJECT

The Fenton River project investigated the temporal heterogeneity in carbon and hydrogen isotopic compositions of leaf wax biomarkers produced in a riparian ecosystem, across the course of a growing season. Chapter 3 considers how differences in plant

seasonal growth patterns and the timing of leaf wax synthesis influences the hydrogen isotope signatures recorded by leaf wax *n*-alkanes from four plants of differing taxonomic class. This is key area of active research, as many disciplines (e.g., food authenticity [1], paleoclimate reconstruction [2–4]) seek to use *n*-alkane δD as an environmental, hydrological or geographical tracer [4–6]. Numerous studies have established that $\delta D_{n\text{-alkane}}$ in terrestrial plants reflects the isotopic composition of source water, with varying degrees of modification due to a range of environmental factors (e.g. relative humidity, evapotranspiration, metabolic distance) [1–8]. By measuring plants with roots visibly in the stream of the Fenton River, however, this project was able to isolate the extent that physiological differences between plants were recorded in $\delta D_{n\text{-alkane}}$ as water availability remained constant throughout sampling.

Chapter 3 concludes that the Fenton River plants from different taxonomic classes (gymnosperm versus angiosperm) show greater fractionation between source water and *n*-alkane δD than previously reported [9,10]. Further, the $\delta D_{n\text{-alkane}}$ values displayed much larger temporal shifts (~60 ‰) in isotope composition throughout the growing season than source water (~15 ‰). Thus, plant specific factors have significant effects on the hydrogen isotope composition of leaf wax biomarkers and must be accounted for when seeking to understand the extent that $\delta D_{n\text{-alkane}}$ values record an environmental water hydrogen isotope signal.

Chapter 4 focuses on the $\delta^{13}C$ of plant wax *n*-alkanes. Key findings show that differentiation between taxonomic classes is possible through carbon isotopic analysis of *n*-alkanes of various plants from the Fenton River ecosystem. Gymnosperms are classified by more positive $\delta^{13}C$ values (> −35.0 ‰) whereas angiosperms have more negative $\delta^{13}C$

values (< −35 ‰). Further, *n*-alkanes preserved in the fluvial sediments have isotopic values near to that of the sampled gymnosperms. This Chapter posits two theories to account for this: 1) ancient sediments from a time when the area was dominated by gymnosperms are being remobilized and deposited in the sampling area, or 2) there is a localized dominance of gymnosperms along the Fenton River leading to higher concentrations of gymnosperm-produced *n*-alkanes in the sediments. Regardless, Chapter 4 concludes that $\delta^{13}C$ of *n*-alkanes preserved in sediments can be used to determine general trends in vegetation inputs in a specific region.

There have been numerous studies that use $\delta^{13}C_{bulk}$ to calculate the intrinsic WUE (mole ratio of $CO_2$ fixed to $H_2O$ transpired) of various plant species [11–14]. In this study $\delta^{13}C_{n\text{-alkane}}$ was used to calculate WUE, correcting for the relative depletion in *n*-alkane isotopic values compared to bulk leaf wax $\delta^{13}C$. Using the corrected $\delta^{13}C$ values, it was possible to determine the temporal variation in WUE of for all of the studied plants throughout the growing season. A distinct separation is observed between taxonomic classes; angiosperms tend to have consistently lower WUE (< 100 ppm) than gymnosperms (100-200 ppm) throughout the growing season. The fidelity of these calculated WUE results was confirmed using a BIOME-BGC ecophysical modeling scenario to simulate WUE and non-alkane $\delta^{13}C_{leaf}$ for the plant species measured [15–17]. Comparison of modeled WUE and calculated WUE were in agreement for all but the angiosperm *C. americana*. This suggests that *C. americana* only produces leaf waxes during leaf flush, and thus only records environmental response in early season.

Once the method for calculating WUE from *n*-alkane $\delta^{13}C$ values was confirmed with empirical data from the Fenton River, Chapter 4 then uses isotopic data from

Pedentchouk et al. (2008) [18] to determine whether the differences in WUE observed between different taxonomic classes would be preserved in plants growing in more arid environments. Regardless of the growth habitat, gymnosperms again tend to have higher WUE (200-280 ppm) relative to angiosperms (> 180 ppm). The fact that the discrimination in WUE persists among angiosperms and gymnosperms in both humid and arid climates shows that $\delta^{13}C$ analysis of biomarkers can be a valuable tool for investigating plant ecology in a variety of different biomes. In addition, as plants growing in an arid climate have much higher WUE that those in a humid climate, leaf wax biomarker $\delta^{13}C$ values could also help identify the type of environment that plants were growing in when their lipids were produced. Furthermore, these data underpin the application of biomarker isotopes to trace the movement of carbon through the earth system.

### 6.3.0 PAH TRACING PROJECT

PAHs are ubiquitous environmental pollutants of concern for human health and are found throughout Connecticut as a result of a prolonged history of natural and anthropogenic fires and industrial activity. In Chapter 5, the concentrations, $\delta^{13}C$, and $\delta D$ values of the 16 EPA priority PAHs extracted from sediments collected from 55 locations across Connecticut and Rhode Island were measured. These values were used to evaluate the application of molecular ratios and stable isotopes as a tool for delineating the source materials of these organic pollutants. These sites were specifically chosen as they are all non-industrial locations, and therefore as close to pristine as possible. Moreover, any PAHs in these environments are dominantly transported by two mechanisms: atmospheric deposition or aqueous transport. The goal of this work was to determine if there was a

distinct isotopic and/or molecular difference between sites with distinct modes of PAH transport, deposition, and potentially secondary degradation.

In previous studies, PAH concentrations have been shown to be highest in urban areas [19–22]. Intuitively one would predict that areas with greater industrial and vehicular activity would be characterized by a higher PAH burden. However, data collected for this project show no consistent relationship between PAH concentration and regional urbanization. In addition to being located in less urban areas, the sampling locations with the highest concentration of PAHs were also subject purely to atmospheric deposition, with no contributions from rivers or marine systems. These results suggest that in Connecticut and Rhode Island, PAHs formed in heavily urbanized are readily transported through the atmosphere, and can ultimately accumulate in sediments and soils considerable distances from their point of origin.

The overall goal of this experiment was to use a multivariate approach to determine the source materials responsible for PAH pollution in the Connecticut and Rhode Island sediments. These samples proved to contain a complex mixture of organic materials, making individual source identification difficult. However, through the use of concentration data and diagnostic ratios, combined with compound specific $\delta^{13}C$ and $\delta D$ measurements, it was possible to establish a likely mixing scenario for the majority of PAHs found across the sampling locations. Diagnostic ratios indicated that the majority of the sample sites contain PAHs from mixed pyrogenic and petrogenic sources, and the remainder were attributed to purely combustion source. Once bulk characterizations were established, comparative analysis of $\delta D$ and $\delta^{13}C$ of the two most common PAHs, fluoranthene and pyrene, indicated that these contaminants were predominantly products

of several key anthropogenic activities: the use of liquid fossil fuels, low temperature coal burning, and industrial emissions. A key finding is that, despite sample location, or dominant depositional mode, diagnostic ratios show a relatively small range, indicative of a generally consistent, if mixed, source. In contrast, stable isotope data show a higher degree of heterogeneity, that exceeds what would be expected from previous isotope data and estimates of petrogenic and pyrogenic sources.

A key output from this project is the contribution of a significant body of novel molecular and compound specific stable isotope data, which has significant value to studies seeking to trace the origin of PAHs in modern and ancient environment. As a result, findings presented in Chapter 5 will be of interest to environmental forensic practitioners investigating the causes of pollution events, those seeking to trace the impact of human activity and landscape change in the archaeological record, and even studies seeking to identify the prevalence of fires and biomass burning deep in Earth's geological history.

## 6.4.0 FURTHER WORK

### *6.4.1 Expanding collection area to include more data points*

This thesis provides a number of avenues for future studies seeking to build on the conclusions presented here, particularly in respect of the tracing and source apportionment of organic contaminants. The conclusions in Chapter 5 are based on PAHs collected from 55 sampling locations in eastern Connecticut and southwest Rhode Island. However, in order to establish a robust PAH profile of the entire state of Connecticut, a much broader sampling regime will be required. For example, although samples collected cover a variety of land use strategies, the western portion of the state is largely unrepresented. This region of Connecticut is particularly important because it has a significant history of charcoal

hearths, particularly in the Litchfield Hills to the northwest [23]. Through geospatial and remote sensing LiDAR (Light Detection and Ranging), over 20,000 relic charcoal hearths have been identified in a 1,170 $km^2$ region [24]. The presence of these charcoal hearths offers multiple opportunities to develop projects to investigate remobilization of previously deposited PAHs from earlier human activity. Such investigations would contribute to our understanding of human-driven environmental changes occurring in this region through the Holocene era [25].

### *6.4.2 Collection and analysis of atmospheric PAHs*

Results presented in Chapter 5 show that the highest concentration of PAHs from sampled locations often occurred in in less urbanized areas, contrary to most previously published literature [26]. This is potentially a result of excess emissions in urban areas, with pollutants undergoing long-range airborne transport prior to deposition. Anthropogenically produced PAHs occur in the atmosphere in complex mixtures [26]. Many of the lower molecular weight PAHs (2-3 ring compounds) exist in the completely in the vapor phase, while higher molecular weight compounds are almost all adsorbed to fine particulates that can remain airborne for days before deposition occurs in remote areas [27–29]. In order to trace the precise transport vectors controlling how PAHs are transported and deposited, a series of atmospheric PAH collection sites can be established throughout the state of Connecticut. By measuring the atmospheric composition of PAHs throughout the sampling area, future research can determine the origin of these ‘rural’ pollutants and plot the partitioning of organic contaminants between the atmosphere, sediments and soils. This will advance understanding of the range, magnitude, and environmental impact of atmospherically-

transported PAHs, and provide new data to further future environmental health and safety policies and practices.

## 6.5.0 REFERENCES


(1) Lockheart, M. J.; Poole, I.; Van Bergen, P. F.; Evershed, R. P. *Org. Geochem.* **1998**, *29* (4), 1003–1008.

(2) Chikaraishi, Y.; Naraoka, H. *Phytochemistry* **2003**, *63* (3), 361–371.

(3) Chikaraishi, Y.; Naraoka, H.; Poulson, S. R. *Phytochemistry* **2004**, *65* (10), 1369–1381.

(4) Pagani, M.; Pedentchouk, N.; Huber, M.; Sluijs, A.; Schouten, S.; Brinkhuis, H.; Damsté, J. S. S.; Dickens, G. R. *Nature* **2006**, *442* (7103), 671–675.

(5) Hou, J.; D'Andrea, W. J.; Huang, Y. *Geochim. Cosmochim. Acta* **2008**, *72* (14), 3503–3517.

(6) Tipple, B. J.; Pagani, M. *Earth Planet. Sci. Lett.* **2010**, *299* (1–2), 250–262.

(7) Tipple, B. J.; Pagani, M.; Krishnan, S.; Dirghangi, S. S.; Galeotti, S.; Agnini, C.; Giusberti, L.; Rio, D. *Earth Planet. Sci. Lett.* **2011**, *311* (1–2), 82–92.

(8) Sachse, D.; Billault, I.; Bowen, G. J.; Chikaraishi, Y.; Dawson, T. E.; Feakins, S. J.; Freeman, K. H.; Magill, C. R.; McInerney, F. A.; van der Meer, M. T. J.; Polissar, P.; Robins, R. J.; Sachs, J. P.; Schmidt, H.-L.; Sessions, A. L.; White, J. W. C.; West, J. B.; Kahmen, A. *Annu. Rev. Earth Planet. Sci.* **2012**, *40*, 221–249.

(9) Bi, X.; Sheng, G.; Liu, X.; Li, C.; Fu, J. *Org. Geochem.* **2005**, *36* (10), 1405–1417.

(10) Tipple, B. J.; Berke, M. A.; Doman, C. E.; Khachaturyan, S.; Ehleringer, J. R. *Proc. Natl. Acad. Sci. U. S. A.* **2013**, *110* (7), 2659–2664.

(11) Bacon, M. A. *Water-use efficiency in plant biology*; Blackwell, 2004.

(12) Zhang, J.; Marshall, J. D. *Can. J. For. Res.* **1994**, *24* (1), 92–99.

(13) Farquhar, G. D.; Ehleringer, J. R.; Hubick, K. T. *Annu. Rev. Plant Physiol. Plant Mol. Biol.* **1989**, *40* (1), 503–537.

(14) Hou, J.; D'Andrea, W. J.; MacDonald, D.; Huang, Y. *Org. Geochem.* **2007**, *38* (8), 1251–1255.

(15) Running, S. W.; Hunt, E. J. R. In *Scaling Physiological processes: leaf to globe*; Ehleringer, J. R., Field, C. B., Eds.; Academic: San Diego, 1993; pp 141–158.

(16) White, M. A.; Running, S. W.; Thornton, P. E. *Int. J. Biometeorol.* **1999**, *42* (3), 139–145.

(17) Wang, W.; Ichii, K.; Hashimoto, H.; Michaelis, A. R.; Thornton, P. E.; Law, B. E.; Nemani, R. R. *Ecol. Modell.* **2009**, *220* (17), 2009–2023.

(18) Pedentchouk, N.; Sumner, W.; Tipple, B.; Pagani, M. *Org. Geochem.* **2008**, *39* (8), 1066–1071.

(19) Bosch, C.; Andersson, A.; Kruså, M.; Bandh, C.; Hovorková, I.; Klánová, J.; Knowles, T. D. J.; Pancost, R. D.; Evershed, R. P.; Gustafsson, Ö. *Environ. Sci. Technol.* **2015**, *49* (13), 7657–7665.

(20) Foan, L.; Leblond, S.; Thöni, L.; Raynaud, C.; Santamaría, J. M.; Sebilo, M.; Simon, V. *Environ. Pollut.* **2014**, *184*, 113–122.

(21) Brown, J. N.; Peake, B. M. *Sci. Total Environ.* **2006**, *359* (1–3), 145–155.

(22) Yan, W.; Chi, J.; Wang, Z.; Huang, W.; Zhang, G. *Environ. Pollut.* **2009**, *157* (6), 1823–1830.

(23) Raab, T.; Hirsch, F.; Ouimet, W.; Johnson, K. M.; Dethier, D.; Raab, A. *Geoarchaeology* **2017**.

(24) Johnson, K. M.; Ouimet, W.; Raslan, Z. In *Bretton Woods, New Hampshire: Geological Society of America*; 2015.

(25) McManimon, C. **2016**, *23*, 1–7.

(26) Manoli, E.; Kouras, A.; Karagkiozidou, O.; Argyropoulos, G.; Voutsa, D.; Samara, C. *Environ. Sci. Pollut. Res.* **2016**, *23* (4), 3556–3568.

(27) Ravindra, K.; Sokhi, R. S.; Van Grieken, R. *Atmos. Environ.* **2008**, *42* (13), 2895–2921.

(28) Chrysikou, L. P.; Samara, C. A. *Atmos. Environ.* **2009**, *43* (30), 4557–4569.

(29) Terzi, S.; Samara, C. A. *Environ. Sci. Technol*. **2004**, *38*, 4973–4978.